Modeling of Heat Treating Processes for Transmission Gears

by

Isaiah Paul Janzen

A Thesis

Submitted to the Faculty

of the

WORCESTER POLYTECHNIC INSTITUTE

in partial fulfillment of the requirements for the

Degree of Master of Science

in

Materials Science and Engineering

December 2009

APPROVED:

Richard D. Sisson, Jr., Advisor

George F. Fuller Professor

Director of Manufacturing and Materials Engineering

Abstract:

The effects of heat treating process parameters on the microstructure, residual stress, and distortion of a vacuum carburized, quenched and cold treated ring gear made of Pyrowear 53 has been determined using Abaqus and DANTE software. The data from these finite element method simulations was compared to measured values from physical testing. It was found that the heat treating process of the ring gear could be simulated and provide similar results to the measured and specified values for hardness, carbon content, and distortion.

The simulations and distortion in this paper provide a detailed view of the mass transfer, heat transfer, and stress that occur during heat treating. These simulations suggest nonuniform cooling of a ring gear leads to greater distortion than uniform cooling. Simulations compared the retained austenite and hardness in ring gears that were oil quenched and high pressure gas quenched.

Acknowledgements

This paper is possible through the efforts of people. I would like to thank my advisor Dr. Richard D. Sisson Jr. for teaching me so many things from metallurgy to business. I would like to thank Sikorsky Aircraft Company, specifically Dr. Soraya Benitez and Jonathan Frost, for supporting this project as well as taking the time to explain the details of aerospace gear processing. I would like to thank the faculty of the materials science and engineering department at WPI as well as the aerospace engineering department for giving me the background knowledge and experience to complete this project. I would like to thank my friends and extended family for taking an interest in my work and encouraging me to work harder. Finally I would like to thank my parents because they taught me more values, ethics and love than any other people. I am also grateful to God for having this entire opportunity.

Table of Contents

Introduction

The heat treating of gears is a critical aspect of gear production. The processes of carburizing for surface hardening, quenching for through hardness, and cryotreating for martensite formation and retained austenite reduction in the carburized layer are important parts of the heat treating process (Rakhit, 18).

While unalloyed low carbon steel has properties that are appropriate for many applications, some aerospace applications require very specific properties that make alloy choice complex. Often the requirements for a part change necessitating a new heat treating process. At that point the process needs to be evaluated to optimize the properties of the part and the processing. In this paper the gear being investigated is composed of Pyrowear 53 steel.

Element	C	Mo	Cu	Ni	Cr	Si	Mn	V
Weight Percent	.10	3.25	2.00	2.00	1.00	1.00	.35	.10

Table 1: Alloy Composition of Pyrowear 53 (Freborg)

Computer simulation has been developed to predict distortion, residual stress, hardness, and fatigue life in recent years (Freborg). Finite element analysis of complex problems that would be virtually impossible using traditional pen and paper methods has supported dramatic increases in understanding and visualizing heat treating processes as well as providing complex stress analysis of the heat treated parts. Modeling current heat treating processes and proposed heat treating processes allows companies to compare methods and optimize parameters at a minimum of cost compared to buying new equipment, staff training, and many full scale test parts (Ferguson).

Therefore the goal of this project is to understand the source of distortion in the heat treating process of an aerospace gear by simulation and measurement of distortion in the current process and to simulate alternative methods of heat treating which mitigate distortion and require no post process machining.

Background

Carburizing

Carburizing is the process of diffusing carbon into a steel so that the surface will become harder. The origins of carburizing go back hundreds of years to the Katana or Samurai sword. The sword was finished by coating the back non cutting edge in a ceramic paste and leaving the front cutting edge exposed. Then the sword was heated up and carbon diffused into the front edge of the sword from the furnace (World's Sharpest, 2008). When the fire in the furnace burns coal there is a large carbon potential.

Carburizing has progressed so that there are a number of different methods of carburizing that can have similar outcomes. One of the simplest is pack carburizing. All that is done is the steel is surrounded with some form of graphite and a high temperature and pressure are generally added to the system so that the carbon can diffuse into the steel. This method is limited by contact between the steel and the carbon so it often has problems with the continuity of the case depth.

Carburizing also takes place in gas atmospheres at or near standard atmospheric pressure. This method is attractive because a vacuum is not required so some cost can be saved. However, the gas interactions do not allow an even case depth. While the gas can easily strike exposed areas such as the top-land of a gear tooth the gas has problems distributing enough carbon to the root of the tooth. This happens because the carbon rich gas will initially strike the tooth root and the carbon will diffuse into the steel. Then the gas immediately next to the root has less carbon. The carbon deficient gas must then move away from the steel and carbon rich gas must move next to the root of the tooth so more carbon can diffuse into the steel. These gas interactions limit the effectiveness of gas carburizing in small spaces.

In the last several decades vacuum carburizing was created. This occurs by creating a weak vacuum (10-25 Pascals) around the part to be carburized and then a small amount of carbon rich gas is introduced into the atmosphere. This gas increases the pressure to about 80,000 Pascals in vacuum carburizing and 450 to 1700 Pascals for low

pressure carburizing (Benitez). The gas will move very rapidly and because physics dictates that atoms and molecules move from areas of high concentration to areas of low concentration the carbon rich gas will be attracted to the carbon deficient steel. When the carbon is on the surface of the steel some will diffuse into the steel. The carbon deficient gas will then be replaced by the carbon rich gas fairly quickly because of the speed the molecules move in the vacuum. This is an efficient process because the vacuum required is relatively low and the composition of the gas can be well controlled (Davis, 2002).

Vacuum carburizing is also attractive because of the low amount of oxygen in the carburizing atmosphere. One of the problems with processing of steels is the oxidizing of the steel at higher temperatures. One of the most important reasons that steels are alloyed is for corrosion, mostly oxidation, resistance. A number of different elements have high oxygen potentials than iron. Specifically, titanium, chromium, manganese, and silicon have higher oxygen potentials than iron (Kozlovskii, 1967). However, it is important to understand that because there is less oxygen in the carburizing atmosphere there is less chance for any oxidation and thus less alloying elements designed to prevent oxidation are needed. Vacuum carburizing also provides a more even carburizing case than atmosphere carburizing because of the fewer gas interactions than during atmosphere carburizing (Parrish 1999). The total number of benefits that vacuum carburizing has make it very popular for precision carburizing applications.

The reason carburizing is such an attractive surface hardening treatment is that is consistently delivers the same results. The physical mechanism that hardens the surface after carburizing is also well understood. As the steel is heated up the iron lattice expands. As the lattice expands the interstitial sites become larger. When the carbon diffuses into the iron it diffuses mostly interstitially and not necessarily through vacancies like larger elements because of its small size compared to the iron. When the lattice is still hot the carbon can diffuse through the iron at relatively high rates. When the lattice is cooled to a lower temperature, generally room temperature, the interstitial spaces have become much smaller and the carbon can not diffuse as easily as it did at high temperature. Now that the lattice has a smaller size or smaller d-space, the distance between adjacent atoms in two different planes is smaller, therefore a force is exerted on the carbon atoms because the carbon atoms are too big to fit comfortably in the interstitial

lattice sites. This produces a compressive stress in all directions away from each carbon atom. When an entire surface is carburized it can be understood that there is a compressive stress that exists close to the surface of the part that does not extend all the way to the core of the part due to the large amount of carbon atoms near the surface and relatively low amount of carbon atoms near the core.

Quenching

The heat treatment of any metal alloy contributes greatly to the properties the part exhibits. Steels in particular respond well to heat treatment. The unique phases that steels have over a range of compositions and temperatures allows for useful phase transformations. To harden a steel one of the most common methods is to heat the steel into the austenite region then rapidly cool it to near room temperature. This transforms the austenite to martensite. The crystal structure of the steel changes from face centered cubic austenite to body centered tetragonal martensite significantly fast that the carbon and other elements are not permitted to diffuse to a yet untransformed part of the steel. There is also a volume increase that occurs with this transformation of about four percent (Sisson). This volume increase creates residual stresses in the steel (Easterling, 2004).

Martensite is a metastable phase. That means it does not appear on equilibrium phase diagrams but is present in CCT and TTT diagrams. It will decompose into ferrite (alpha) and cementite (Fe_3C) if it is heated up sufficiently high to allow phase transformation to occur (Shackelford, 2004). However, if kept at or near room temperature the martensite will remain as body centered tetragonal and retain its strength.

One of the issues with quenching is converting all of the austenite into martensite. It is difficult to convert all austenite into martensite and so there is some retained austenite in the quenched product. This is austenite that was cooled and did not transform into martensite but cooled faster than equilibrium so that it did not have time decompose into the stable phases of ferrite and cementite.

In the quenching process the important factor for development of the microstructure is heat transfer. To achieve more control over the phases present after heat treating it is desirable to have the capability of high heat transfer rates. Since residual compressive stresses are desirable in applications that will experience tensile loading the

more residual compressive stresses that can be added to the part during heat treatment the longer the fatigue life. Figure 2 shows how a higher flow rate produces higher compressive stresses. This phenomenon is explained by fluid mechanics and heat transfer. When a fluid moves past a heat source heat is absorbed by the fluid through convection. The higher the fluid flow rate, the more molecules come in contact with the heat source and the faster that heat can be exchanged between the fluid and heat source.

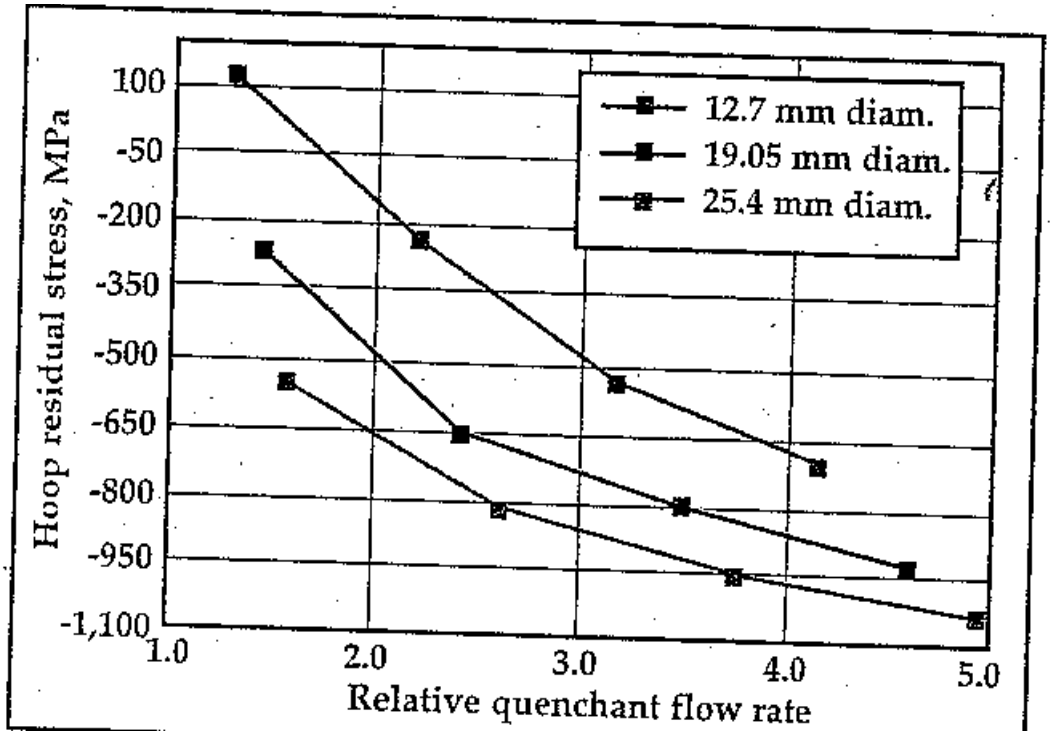

Figure 1: Predicted residual surface stress for AISI 4140 alloy steel rods as a function of quenchant flow rate (instantaneous flow is assumed) (Z. Li, 2008).

Cryotreating

Cryotreating is a process that cools the part to transform the retained austenite to martensite and redistribute the residual stress. It is done after quenching the part and before any tempering. The purpose is to have less retained austenite so that the part will be stiffer and stronger ("Cold Treating…").

It is important to cryotreat soon after quenching so that the part does not have enough time at room temperature for austenite stabilization to occur (Stratton). If equilibrium occurs the ferrite and cementite, Fe_3C, phases will appear and there will be

no retained austenite. In particular the Fe_3C phase more commonly known as carbides creates several problems. Carbides are very hard and during cyclic loading they do not flex like other steel phases but instead force the surrounding lattice to accommodate their unique size. Inevitably that means that cracks form as the lattice is forced apart. On heavily alloyed iron where the martensitic end temperature has been sufficiently lowered Cryotreating is necessary or carbides will form and dramatically reduce fatigue life.

Factors influencing hardness

The hardness of steel is influenced by a number of different factors. Those factors are: carbon content, other alloying elements, cooling rates, cooling temperatures and cryotreating parameters.

First carbon content is one of the most important factors controlling the hardness of steel. All steel has carbon by definition otherwise it would be iron. Carbon has a low molecular weight of only 12 while carbon has a molecule weight of 56 which means it has more protons, electrons, and neutrons that make it much larger than carbon. There are several ways that diffusion can occur in metals. Vacancy diffusion is one of the most common forms of diffusion where vacancies in the crystal lattice of a materials are taken by an adjacent atom which then creates a vacancy in the lattice point where that atom used to be. This is the most common form of diffusion for similar sized atoms. There is also exchange diffusion which consists of atoms at two adjacent lattice sites exchanging position with each other. However, this method requires a very large amount of energy in relation to the other diffusion mechanisms so it is not encountered as often as vacancy diffusion. The second predominant method of diffusion is interstitial diffusion. That is when relatively small atoms compared to the main atom in the crystal lattice move through a crystal lattice in the voids between atoms in lattice sites. This is common for small atoms like hydrogen and carbon. This type of diffusion also places large amounts of stress on the surrounding lattice because instead of a void there is an atom pushing out against the nearest atoms in the lattice.

Another factor influencing harness is the amount of martensite and retained austenite in the steel. This can be affected by a number of factors one of them being the composition of the alloy. In the 1960's a simple formula was developed by Steven and Haynes to describe the basic relationship between the composition of a steel alloy and the

martensitic start temperature. This theory also assumes that the martensitic end temperature is about 215^{o}C (419^{o}F) below the martensitic start temperature. The formula is valid only up to about .5% carbon after that the relation between carbon and the martensitic start temperature becomes a quadratic formula (Haynes, 1966). The formula is:

$$\mathbf{M_s\ (^{o}C) = 561 - 474C - 33Mn - 17Ni - 17Cr - 21Mo}$$

This formula uses the percentage of a given element multiplied by its coefficient. So if there is .1% carbon in the alloy .1 would be multiplied by 474. In addition vanadium also promotes hardness at higher temperatures (Preston). By looking at the coefficients it is easy to see that carbon has the largest effect on martensitic start temperature.

At higher carbon concentrations than .5 weight percent the relationship between carbon and martensitic start temperature vary as a function of composition of other elements such as chromium and molybdenum as well as the amount of austenite before the transformation. With empirical data it becomes evident that complicated prediction of phase transformations is best done using computer simulations (Haynes, 1966).

The addition of carbon lowers the martensitic start temperature as well as modifying the exact profile of the pearlite and bainite start curves (Shackelford, 2004). One method to reduce distortion is to cool the part to just above the martensitic start temperature and hold for a short amount of time to relieve some of the residual stress before quenching it to room temperature. With the higher carbon content steel, which is representative of a carburized surface, the part can be held for about two minutes while for the lower carbon content steel it can only be held about 10 seconds before it begins to form bainite. This shows that while the carburized surface finish will probably remain entirely austenite before most quenching processes if the interior cools too much bainite will form which is not as desirable as martensite because it is not as hard.

The DANTE material database specifies a martensitic start temperature of 135^{o}C and 99% finish of approximately for -85^{o}C for Pyrowear 53 with .8 weight percent carbon (Appendix 1). This comes from empirical data and justifies the cryotreatment of helicopter gears. If the gears are not cryogenically treated the retained austenite will remain above the specified 20 percent or lower. Now that all of the aspects of the carburizing and quenching process are described it becomes is important that to get the

most martensite in the part it must be fully austenized so that there is very little bainite or pearlite in the part before quenching. Then the fully austenitic part must be moved to the quenching facilities quickly so that the noncarburized areas of the gear will not begin forming pearlite and bainite. It is then quenched. After quenching it must be cryotreated before it starts to cool to equilibrium so that all of the carburized parts of the gear will form martensite and not some other phase like Fe_3C.

Effect of other alloying elements on carbon

From thermodynamics it can be mathematically explained that as the composition of an alloy changes the activity of elements in that alloy change. The change is also not linear and it is not the same for all elements. This can best be described by diffusion coupling experiments. As the content and thus the activity of element A is higher in alloy X it will force diffusion toward alloy Y with a lower activity of element A even though it may have a higher concentration of element B than alloy X.

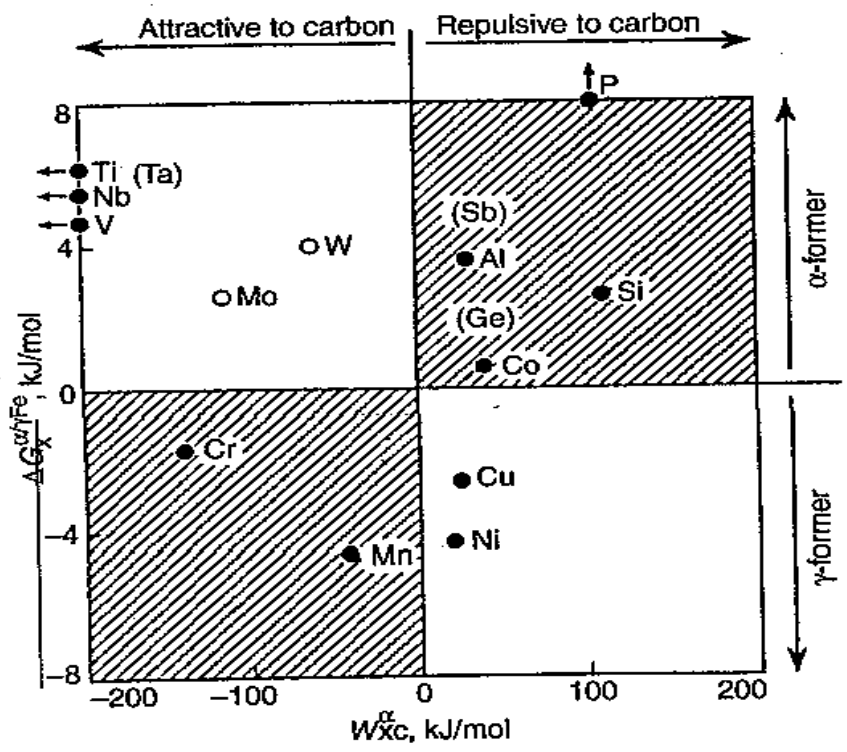

Figure 2: Gibbs energy ($\triangle$G) plotted against the interaction energy (Wx) for alloying elements added to steel (Parrish, 1999).

Property	AISI 9310	Pyrowear 53
RC 60 Depth, mm (in)	0.64 (0.025)	.074 (0.029)
RC 50 Depth, mm (in)	1.17 (0.046)	1.19 (0.047)
RC60/RC50 Ratio %	54	61
Maximumm Hardness	62.4	62.4
Core Hardness RC	38.0	38.0
Retained Austenite %	8.0	10.5

Table 2: Carburized case properties of AISI 9310 and Pyrowear 53 Carburized at 7.5 hours at 927^{o}C (Thomas, 1989).

It can be seen from Table 2 that while the surface hardness and core hardness are the same the depth of Rockwell C 60 is deeper for the Pryowear 53. This implies that there has been more carbon absorbed by the Pryowear 53 than the 9310. It can be seen from Figue 2 that the addition of Vanadium and Molybendenum which are attractive to carbon create a larger potential for carbon absorbtion than the 9310 steel.

A steel that has a greater affinity for carbon and thus a carbon profile that maintains a high hardness farther into the steel will produce more residual compressive stresses in the carburized area due to the higher carbon content. The higher residual compressive stress correlates to the ability to withstand higher tensile loading. The load on the carburized surface can then be increased or if the load is kept the same the fatigue life will be longer because the stress experienced at any given time is a smaller percentage of the yield strength.

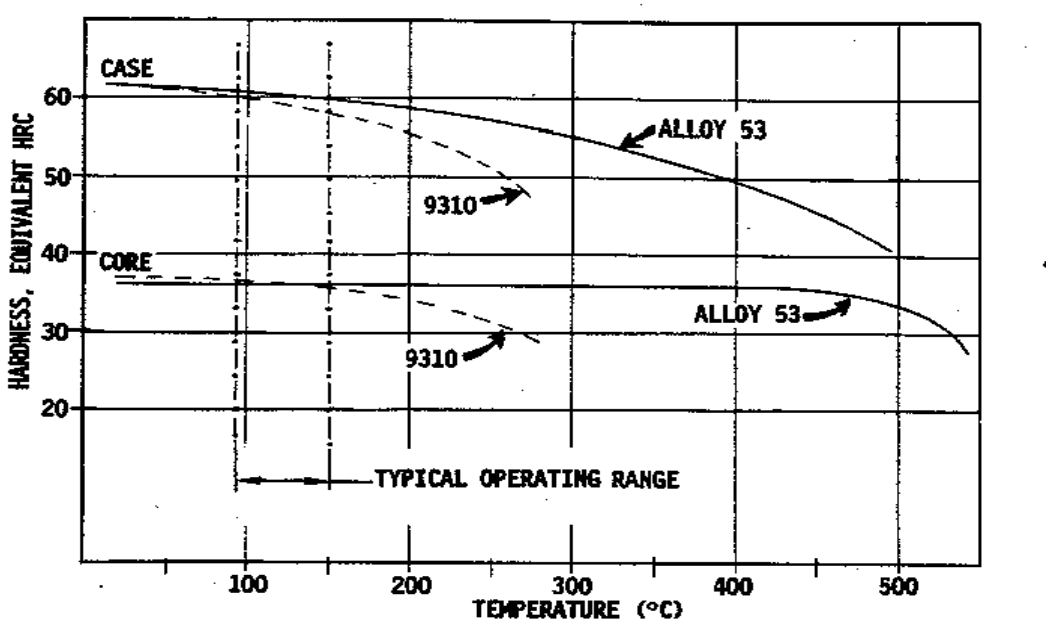

Figure 3: Hot hardness Data Summary, illustrating the nardness at temperatures. Developed from a summation of published data (Saulnier, 1989).

Figure 3 shows a comparison between 9310 and Pyrowear 53 for the hardness as a function of operating temperature. This is a critical comparison for helicopter gear transmissions. Helicopter transmissions are important because the turbine engines lie horizontally just like in an airplane and a transmission is needed to turn the horizontal rotation into a vertical rotation for the main rotor and for the tail rotor. If the transmission fails the helicopter will fall out of the sky. This could be a problem because many helicopters fly over terrain that is undesirable for landings such as large bodies of water or hostile enemy territory. For this reason helicopter transmissions are designed to operate for a period of time without any oil. Without any coolant the engine and transmission will quickly heat up. The longer than the gears can maintain their hardness the longer they will last before they fail under extreme conditions.

Effect of retained austenite on fatigue lifetimes

Austenite has a face centered cubic structure. It is more ductile than body centered tetragonal. The more retained austentite a part has the more ductile the part will be and ductility is directly related to fatigue lifetimes. However, it is important to remember that it is most important for the part to be strong enough for the desired application in the first

place so a part with 50% retained austenite will probably not be strong enough for most desired aerospace applications. Table 2 shows the retained austenite in both 9310 and Pyrowear 53 with the same heat treatment. The Pyrowear 53 has more retained austenite but is still quite low. Figure 4 below compares the longer fatigue lifetimes of Pyrowear 53 than 9310. Pyrowear 53 has a longer fatigue life due in part to the slightly larger amount of retained austenite.

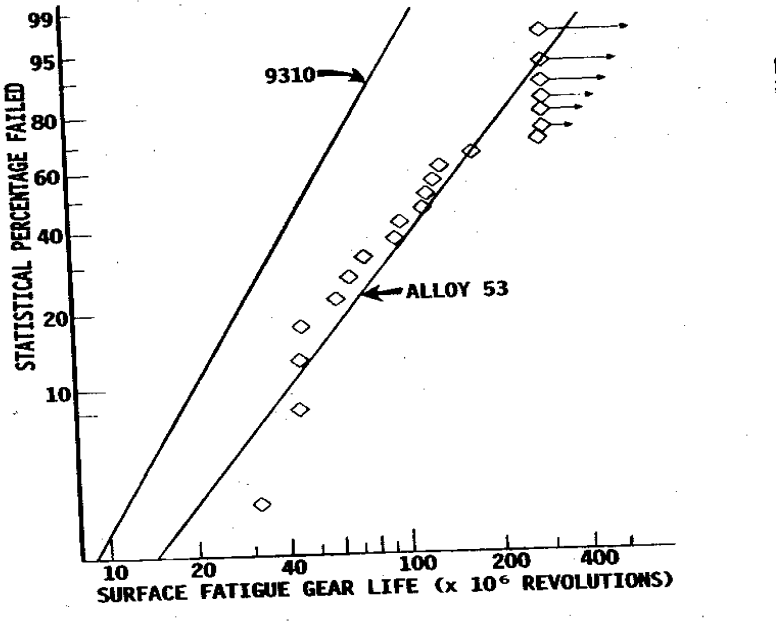

Figure 4: Surface Fatigue Lives of Carburized and Hardened AISI 9310 and Alloy 53 (Pyrowear 53) Gears (Saulnier, 1989).

Mechanisms of Distortion

One simple example of the effect of residual stresses from heat treating is again the samurai katana sword. It is carburized and austenized in a straight line with the ceramic paste on one side of the sword. When the sword is taken out and quenched the ceramic paste insulates the metal on the dull side of the sword and the sharp side which has no coating will cool much faster (World's Sharpest, 2008). This uneven quenching curves the sword into the characteristic curved shape that is associated with samurai katana swords.

As a part is cooled the outside cools faster than the inside causing thermal stresses

due to the thermal gradient between the hot inside and cool outside. The part also undergoes the transformation from austenite to martensite which involves a change in phase of the steel from face centered cubic austenite to body centered tetragonal martensite which causes an increase in volume (Callister, William D. Jr.) (Rakhit).

As the part is quenched and develops residual stresses, these stresses are often enough to distort the part. The major factors that affect the distortion directly due to quenching are quench fluid temperature, quench fluid velocity, which section of the part that is first touched by the quench fluid, the phase composition immediately before quenching, and any contact points that the part has with the structure holding it.

Often times, residual stress distortions are taken into account in the manufacturing process. The manufacturing process designers will give some tolerance for the part. In the aerospace industry there are many flight critical parts that dimensions and tolerances are extremely important for safe operation of human carrying aircraft. For this reason there are tolerances that are specified for the size of the part after heat treating. If the part is within those tolerances then a small amount of the part will be machined off so that each part meets blue print specifications. If the part is not within those tolerances it will be scraped at a loss to the company. The unfortunate aspect of the post heat treating machining process is that as the outer surface is machined away the stress field of the part will change and more distortion can occur. Unfortunately this is somewhat difficult to predict. That is why computer finite element method simulations are gaining popularity as a way to simulate different heat treating and machining scenarios so that parts can be processed with low or even no measurable distortion. This could potentially save large aerospace companies millions of dollars.

As an example one helicopter company produces a large ring gear for helicopter transmissions that is about two feet in diameter. About one third of the cost of any heat treated gear produced is from the heat treatment process. Aerospace gears are expensive because they are manufactured from forgings of exotic alloys that have long lead times. Aerospace companies scrap millions of dollars of partially or fully processed gears due to the effects of distortion. In 2007 Sikorsky Aircraft scraped over one millon dollars worth of helicopter gears that was partially or fully processed and did not end up the right size because distortoin affected the post processing (Benitez, Frost, 2008). As the world

strives to make larger and lighter aircrafts with increased payload capacity, quality control becomes an issue as companies stretch the limits of precision production.

Computer Modeling

The thermal processing of metals continues to be a problem in quality control for many companies. From the automotive industry to the aerospace industry heat treating of complex shapes fails to produce the same product every time. For example, Ford Motor Company was experiencing difficulty heat treating a ring gear and were tolerating a 3-5% rejection rate for that gear (Mgbokwere, 2000). Through computer simulation using Abaqus, one of the major finite element software packages available, they were able to effectively simulate the heat treating process. When a process is simulated so that it matches what happens in actual production each step can be evaluated to examine what is actually happening. Corrective steps can then be taken to ensure consistency and minimize the rejection rate of complex parts. This is beneficial because it is not feasible to take measurements at the every stage of the heat treatment process such as the variation of distortion as a function of time while a gear is in a press quench or in any quenching method for that matter.

The heat treating of gears in particular poses many problems for many companies. As new methods of heat treating become feasible a demand grows for comparison between the various methods so that production companies and furnace companies can find the best solution for every problem. Using computer simulation to model heat treating processes is one of the most cost effective techniques to compare new and old heat treating processes. Compared to analytical methods finite element methods are simple and fast for complex processes using modern computers (Moser).

An example of one way that computer simulation is being used to evaluate new processing methods is by comparing those methods to current processing methods. One new quenching method is intensive quenching. Intensive quenching uses highly agitated water followed by cooling in air so it is more environmentally friendly than oil and polymer quenching, and produces higher cooling rates than traditional oil quenching (Aronov, 2008). The U.S. Army was searching for methods to make helicopter gears with longer fatigue lives and intensive quenching was suggested as a possible solution. Using Abaqus software and DANTE, a supplemental material property database, Deformation

Control Technology Inc. simulated the processing of both oil quenching and intensive quenching.

Using the software stresses were evaluated and compared between the two methods. Figure 5 shows the residual stresses after quenching. The intensive quench process produced higher compressive stresses at the root of the teeth. That is a very critical area for fatige lives. As the teeth are subjected to forces perpendicular to the flank of each tooth there is a tensile stress concentration at the root of the tooth. That area is vunerable to cracking and thuse failure of the part. If residual compressive stresses can be maximized at the root of the tooth than fatigue lifetimes will be increased or the load on the teeth can be increased.

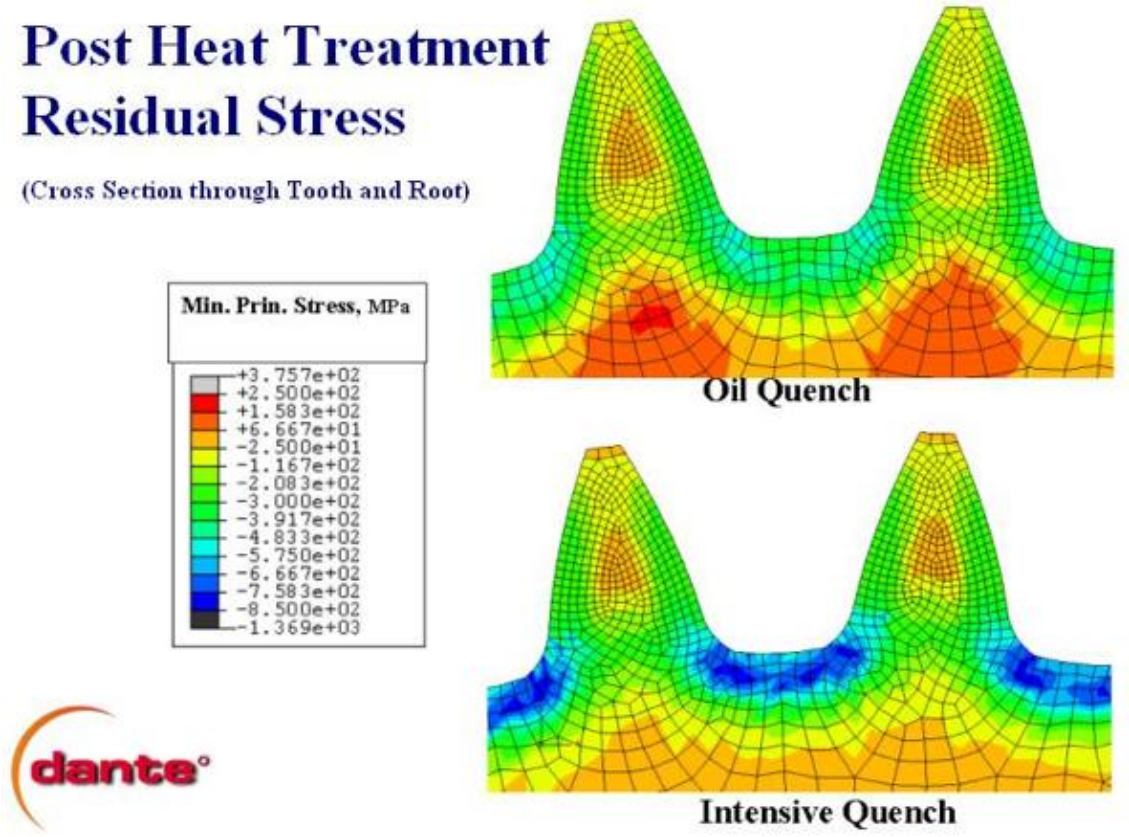

Figure 5: Post heat treament residual stress for two different quench methods (A.M. Freborg, 2006).

Figures 6 shows the residual stress profiles at the root of the tooth. The lower line in all three graphs corresponds to the intensive quench and the upper line for the oil quench. This graph shows that the magnitude of the intensive quench residual

compressive stresses are greater than the oil quench residual stresses. This graphs shows that the simulation predicts a significant increase in desirable residual compressive stresses at the root of the tooth. With this information it would be appropriate to move onto a full scale physical experiment where the simulation can be validated and the intensive quench process can be implemented.

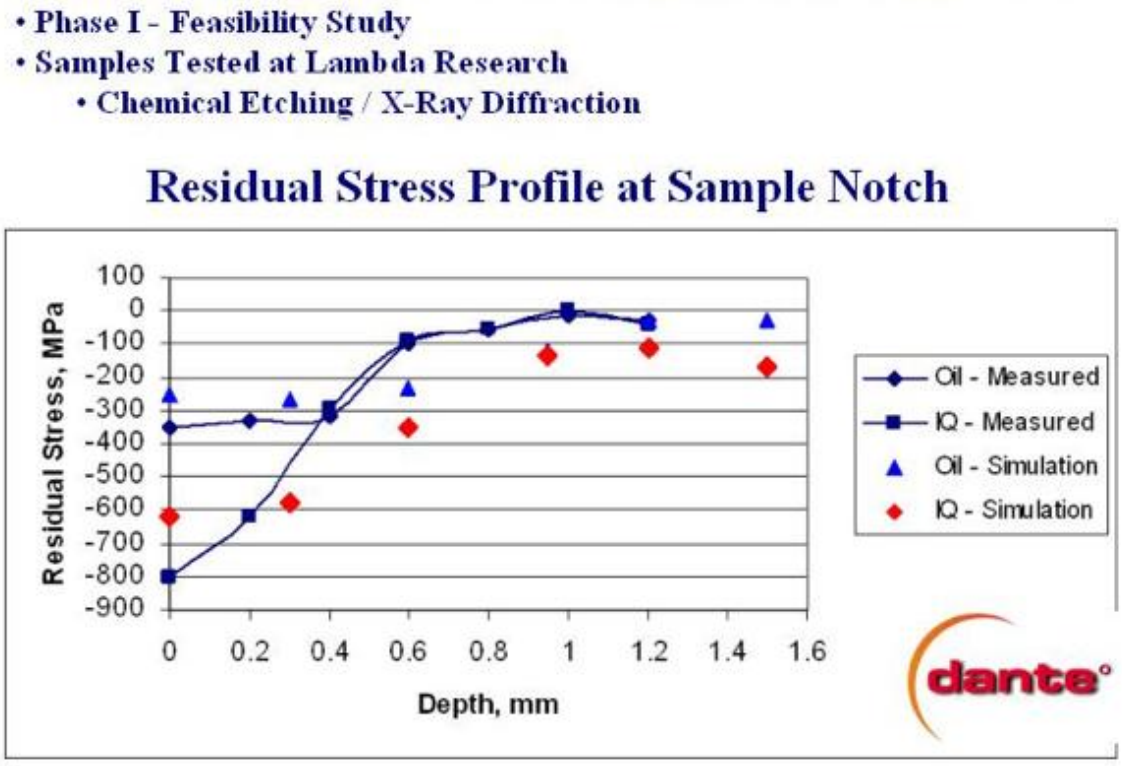

Figure 6: Predicted vs. Measured Residual Stress Profiles for two quenching simulations (A.M. Freborg, 2006).

Figure 7 shows the reaction of the the oil quenching method to an applied force on the flank of the tooth. It is a goal of gear manufacturers to minimize the tensile stresses during operation of gears. Any tensile stress that occurs in the root of a tooth in a gear during operation could reduce the life of the gear.

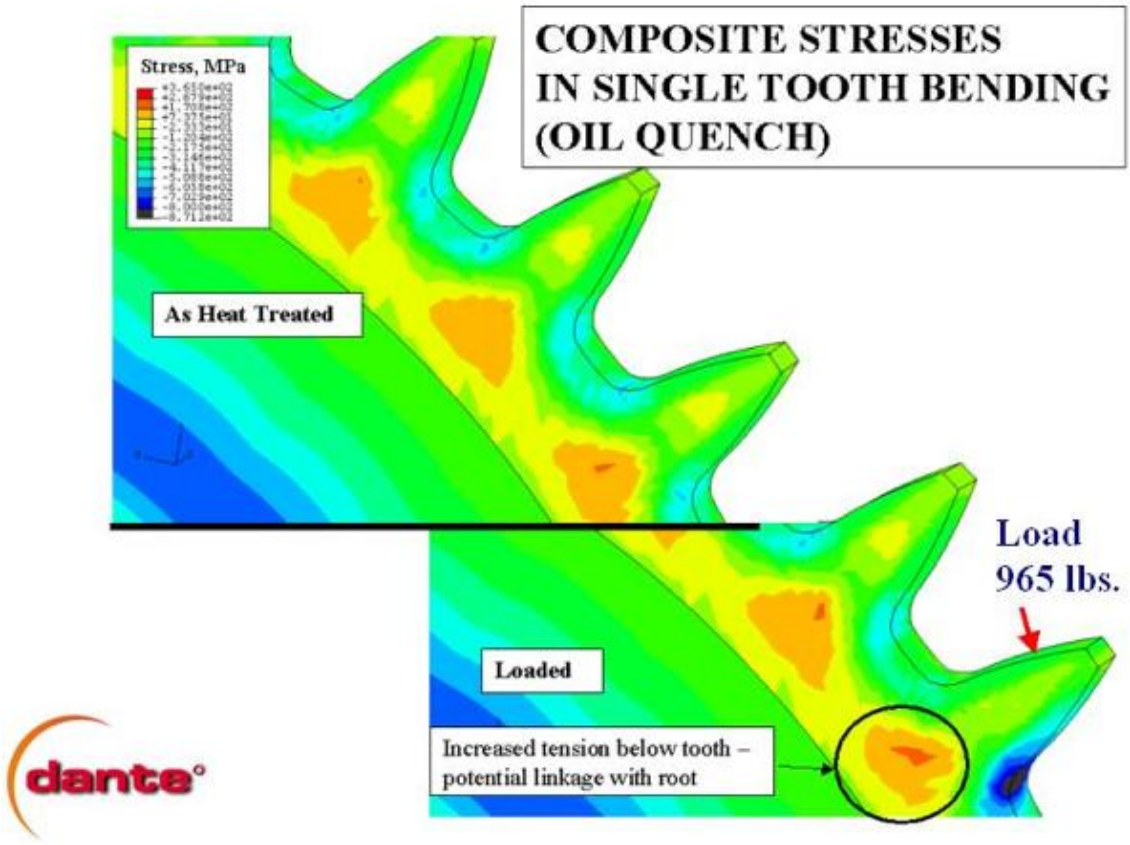

Figure 7: Composite Stresses in Single tooth Bending (oil quench) (A.M. Freborg, 2006).

One important factor to remember is that computer simulations are just simulations and not physical experiments. There are often factors in actual production that may not be accounted for in computer simulations such as sand blasting cleaning after quenching. While the effect of these unmodeled steps may have very little effect on the end result; any effect at all may prove important. The importance of details has been demonstrated by the use of square aluminum airplane windows and humid conditions, which limit fatigue life (Atkinson).

Another advantage of computer simulation to heat treating is the ability to quickly compare several different heat treating methods for a fraction of the cost and time of physical experiments. The major determining factor in the accuracy of computer simulations of heat treating is determining correct boundary conditions. There are many necessary boundary conditions that are needed to ensure an accurate simulation. Two of the biggest problems with boundary conditions are determining appropriate heat transfer

rates as well as the physical fixture of the part.

The heat transfer between the part and the fluid or solid in contact with the part determines how fast or slow the part changes temperature. For quenching operations of steel the rate of cooling is important to determine the amount of martensite that is formed and at what depth it forms in the material. There is also the problem of the type of heat transfer, especially in a press quench. Heat transfer occurs by free convection while the part travels between the furnace and press quench. Heat transfer by conduction and radiation occurs at all stages because the part is always touching some sort of fixture in the heat treating process. Finally, forced convection from the quenching medium contributes to the cooling of the part. All of these factors contribute, specifically to the transition from austenite to martensite, and the stress field generation and distribution that occurs during heat treating. Fortunately, heat transfer rates for many mediums have been published and are available.

The physical constraints on the part in a simulation determine both how the stress pattern develops as well as how the part deforms. Applying the correct fixture boundary conditions determine if a simulation will provide accurate results. One of the challenges in simulations is that the fixturing in the computer model may not be identical to the physical situation. This may cause a simulation which has deformation equal to the measured values yet has boundary conditions different than those which created the physical part.

Another factor that influences the accuracy of models is the simplification of the geometry and/or mesh. Many parts contain rounded edges that are not conducive to cubical shaped elements. This could be simplified by simplifying the geometry to have a square corner. This could cause a stress concentration that does not occur in the actual part, if it is an inside corner or a way to slightly reduce stress if it is an outside corner.

Methodology

The software used for these simulations included Solidworks for the modeling of complex geometries associated with the ring gear and press quench, Abaqus 6.7 for the finite element model creation and simulation, and DANTE for the material phase transformation database (Abaqus, SolidWorks, DANTE). To investigate the effects of the current heat treating process first a number of 2D models were created. These 2D models were also used as training to gain familiarity with the software packages. These models represent the cross section of the ring gear. They provided a simple way to evaluate basic mass transfer and heat transfer within the ring gear. The simulation below represents a 2D mass transfer simulation of the carburizing process at the root of a tooth in the gear. The concentration of carbon is graphed according to the scale on the left. The results of this simulation match the specs for the carburizing operation with a surface carbon content of about .8 wt% which is within the specified surface carbon content.

The heat treating process that this paper describes is shown below in Figure 9. To further simplify the simulation both temper steps were ignored. It is assumed that they contribute very little to the distortion that occurs during heat treating. The simulation was further broken into smaller simulations based on complexity and type of analysis, that is mass transfer, heat transfer, and stress analysis. A mass transfer simulation was performed for the carburizing operation. A thermal simulation was performed for both the carburizing operation and the through hardening operation. A stress simulation was then performed for both the carburizing operation and the hardening operation.

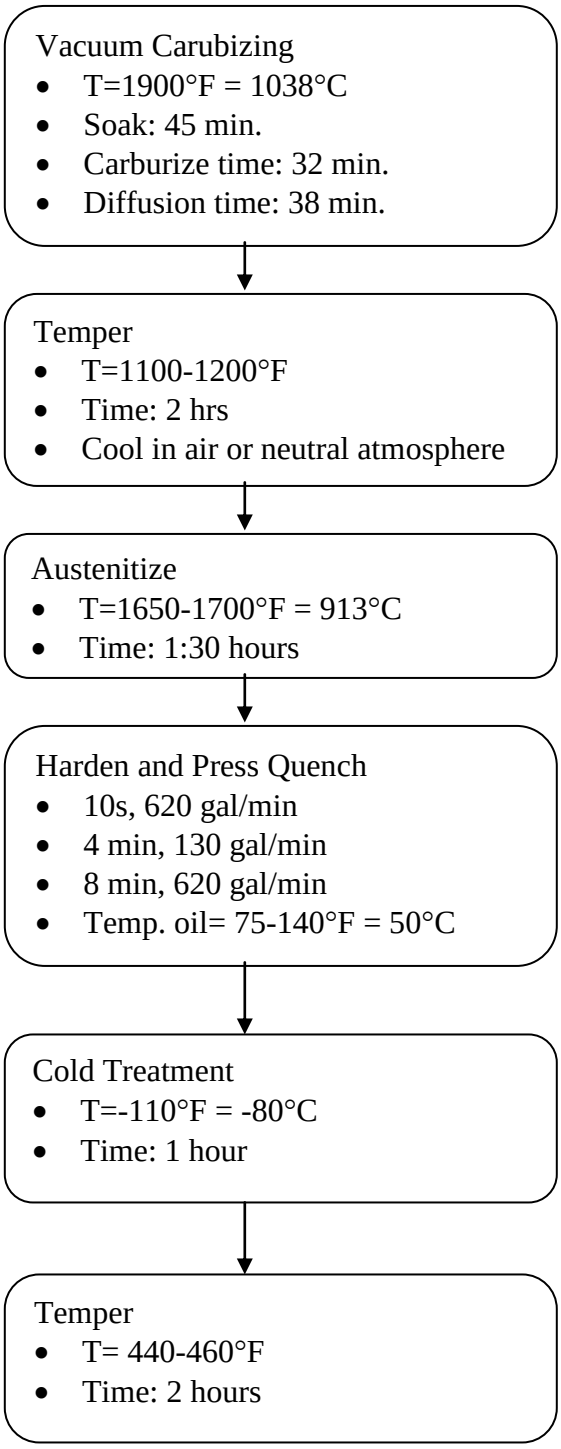

Figure 8: Flow chart of heat treating process that was the goal of the project to simulate

2D Simulations

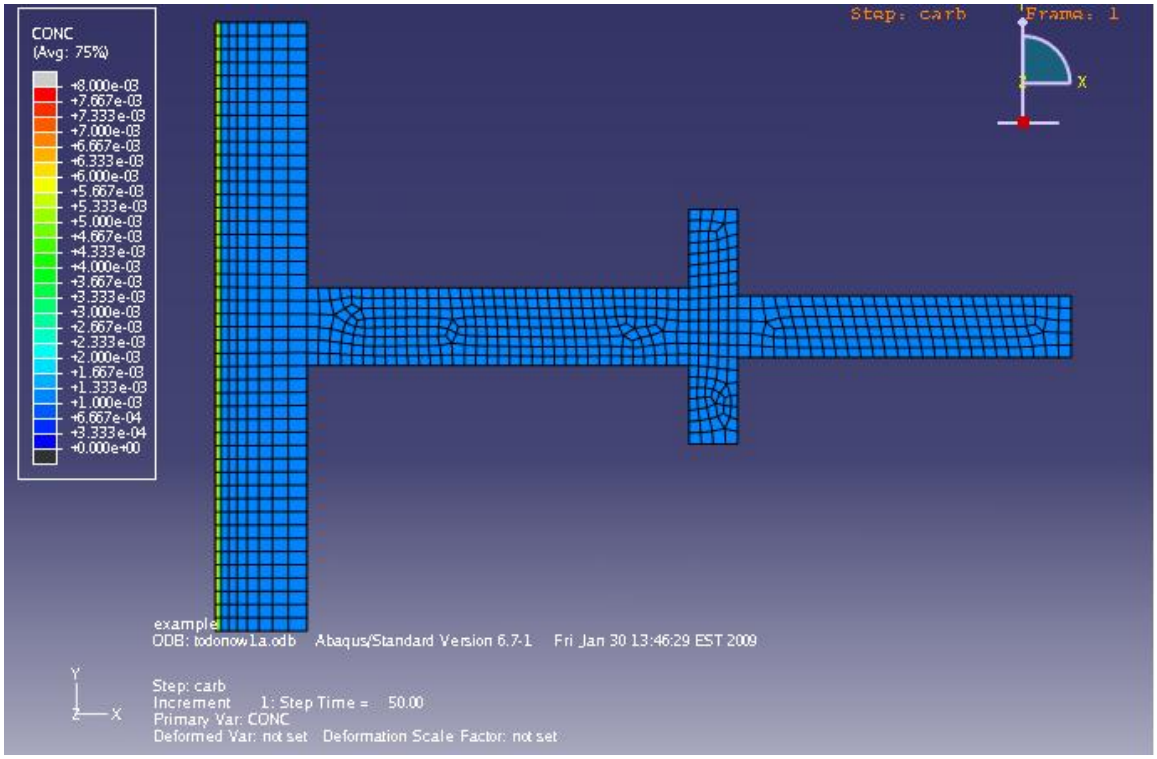

Figure 9: 2D carburizing simulation of ring gear

In a similar fashion several 2D thermal simulations of the process were performed. The following picture is of a simulation that had convective heat transfer from oil on the bottom and no heat transfer on the top. The retained austenite percentages are shown which clearly show that a slower cooling rate leaves more retained austenite while a fast cooling rate reduces the retained austenite to only fractions of a percent. The simulation was for Pyrowear 53 which at .1 wt% carbon (the amount of carbon in the alloy) has a martensitic start temperature of 437 degrees Celsius (819^{o}F) with 99 percent of the austenite transformed to martensite at 222 degrees Celsius (432^{o}F). This high start temperature means that relatively little cooling from pure austenite at 913 (1700^{o}F) degrees Celsius is necessary to eliminate all of the austenite in the noncarburized material.

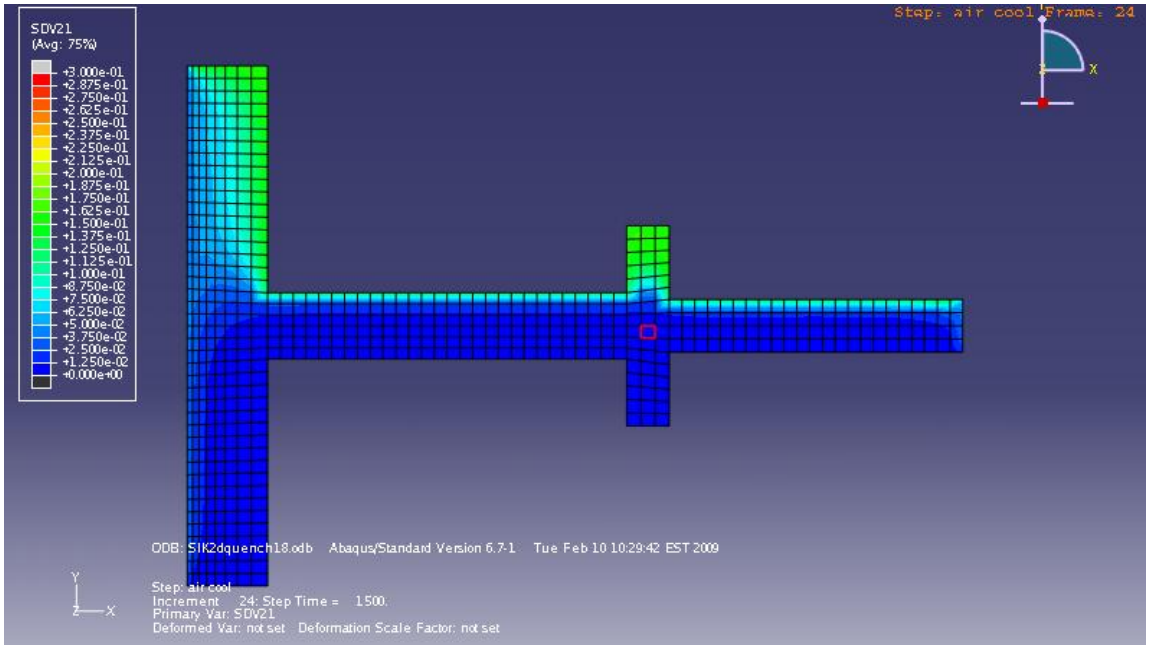

Figure 10: 2D Heat Transfer simulation of Ring Gear

All of the simulations featured in this paper several different heat transfer coefficients were used based on the desired medium of heating and cooling. Those values are represented in the graph below.

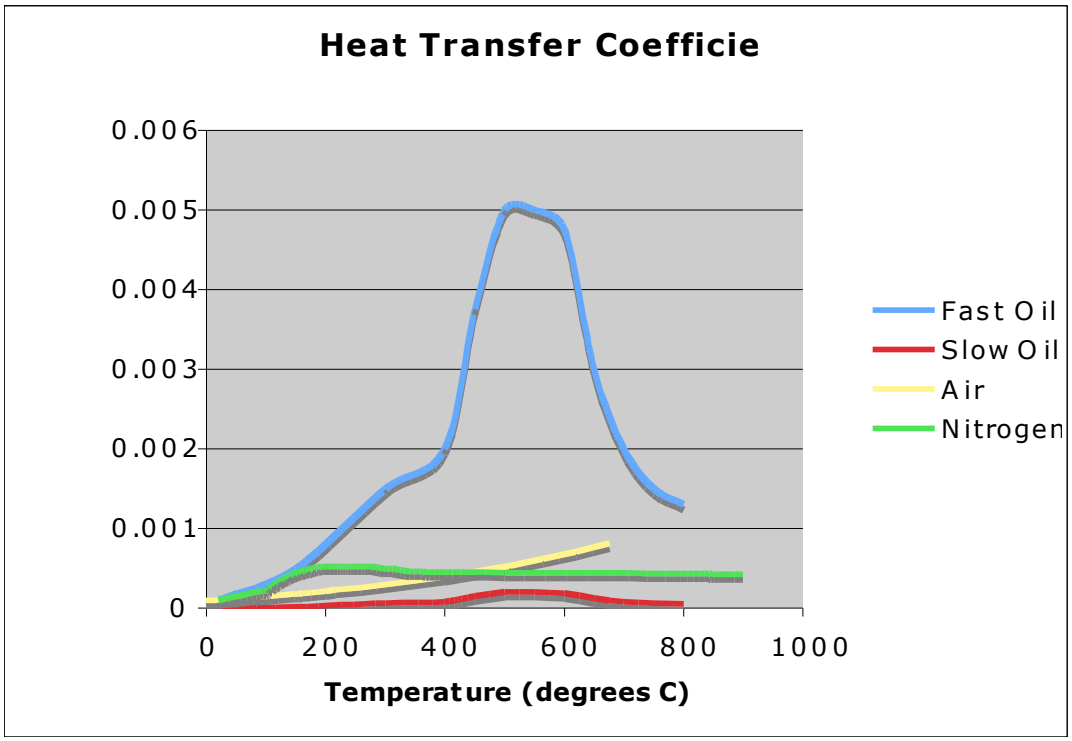

Figure 11: Graph of Heat Transfer coefficients used throughout these simulations to simulate the heat transfer at all steps of the heat treating process

3D Simulations

After the 2D simulation multiple 3D simulations were performed to evaluate different aspects of the heat treating process. The smallest possible geometry to accurately simulate the carburizing on a detailed level is one quarter of one tooth. This geometry allows the rest of the gear to be a series of reflections. The mesh that was created can be seen in Figure 12 as well as a close up of the chamfered edge between the flank and side of the tooth in Figure 13. The model consists of 48348 linear hexahedral elements (generally cube or brick shaped) of the type DC3D8 and 54373 nodes.

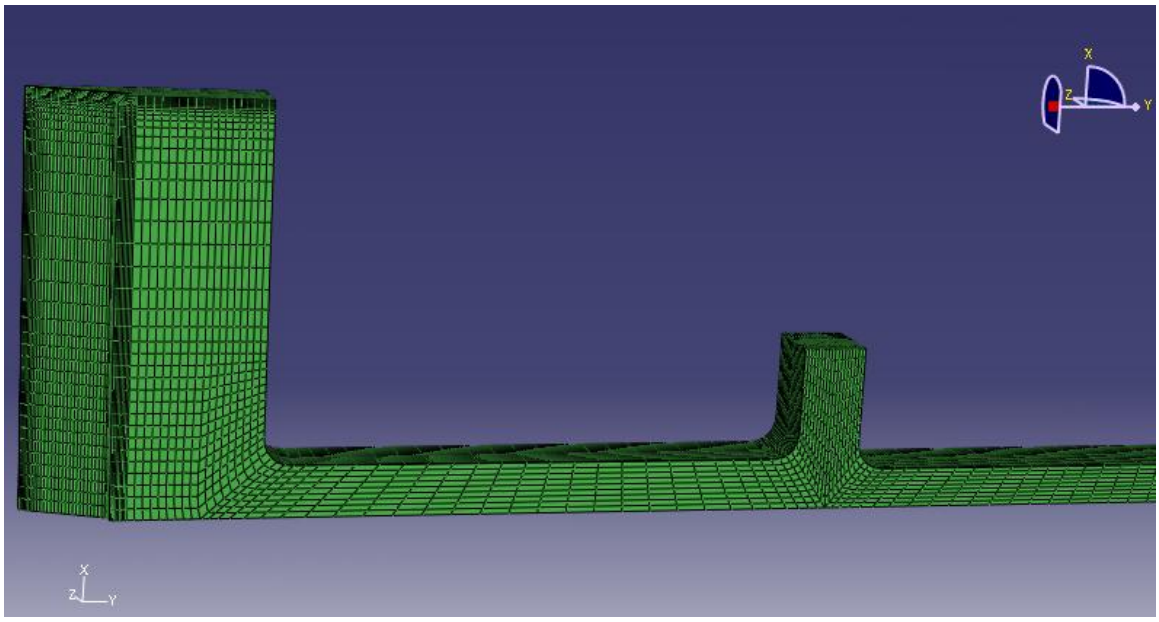

Figure 12: Overall view of Mesh created to simulation One Quarter of One Tooth in the Ring Gear geometry

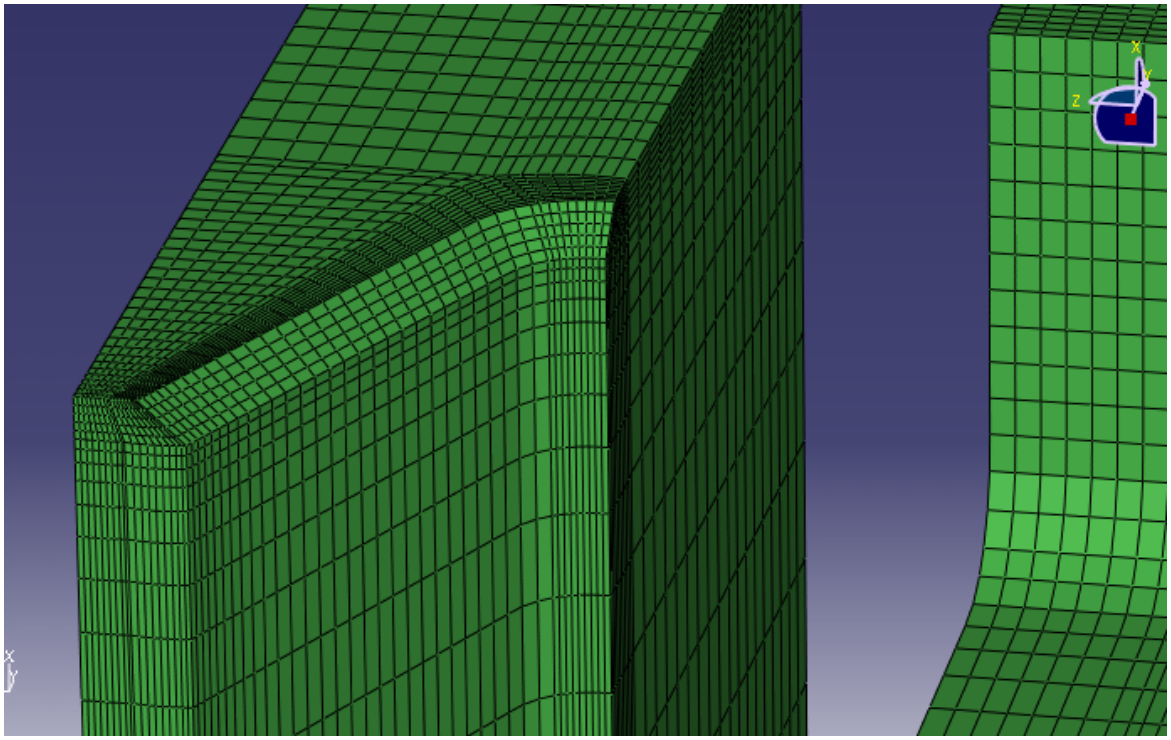

Figure 13: Close up View of Flank, Chamfer, Side, Root, and Top-land

To investigate the out of round distortion that was occurring a model of the gear was created excluding the teeth as shown in Figure 14. This was done to greatly reduce the complexity of the model and computation time required. The ring gear was subjected to several thermal and stress simulation to discover how factors, specifically variations in heat transfer and physical constraining, affected the distortion. The model created contains 52,373 nodes and 38,784 linear hexahedral elements of the type C3D8.

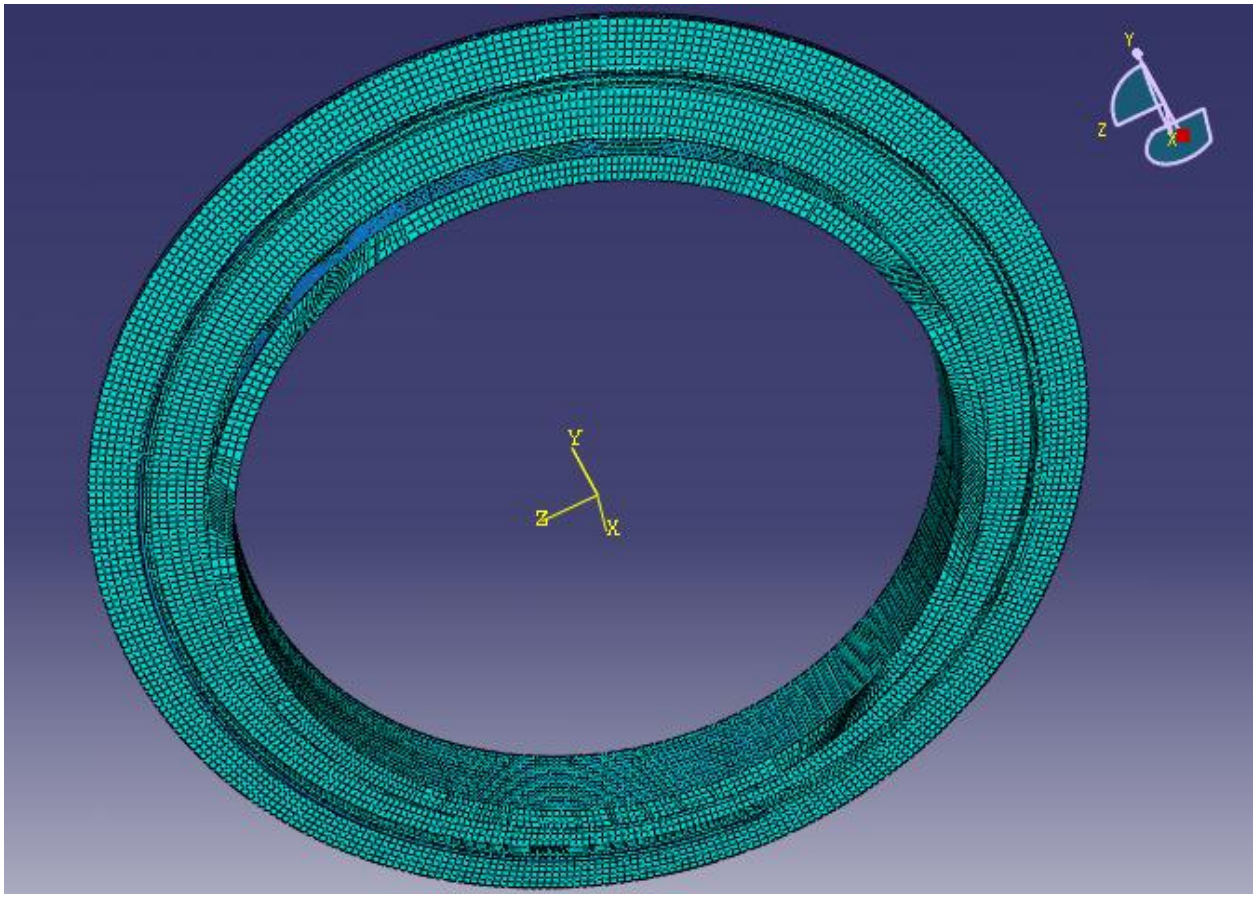

Figure 14: View of Ring Gear used to Simulate Out of Round Distortion

These models were used with the heat treating process described in Figure 8 to simulate the heat treating process of the gear. After a heat treating simulation was completed the stress simulation were run using the thermal boundary conditions of the matching heat treating simulation as well as the boundary conditions of fixing several nodes. In each simulation three nodes were fixed. One node was fixed in from all three lateral movements and from rotation about each of those axis. One nodes was fixed in two lateral directions to prevent the entire body from rotating in two directions. Then a third node was fixed in one lateral direction to prevent rotation about the remaining direction. This allowed the gear to expand and contract and move but not rotate.

The simulation process consisted of two or three steps depending on the geometry. First the carburizing was implemented if the geometry included the flank and root of the teeth. That step was neglected in the simulation of a simple toothless ring gear. Second a heat transfer simulation was completed. This simulated the heating and cooling that was specified and observed. This simulation calculated the microstructure and phase

transformations during heat treating. Third a stress simulation was completed using the same finite element mesh as both the carburizing and heat transfer simulations. This simulation used the phase transformations calculated in the heat treansfer simulation to calculate the volume change stresses that develop during heat treating. Those transformation and thermal stresses were used to calculate the distortion that occurred during heat treating.

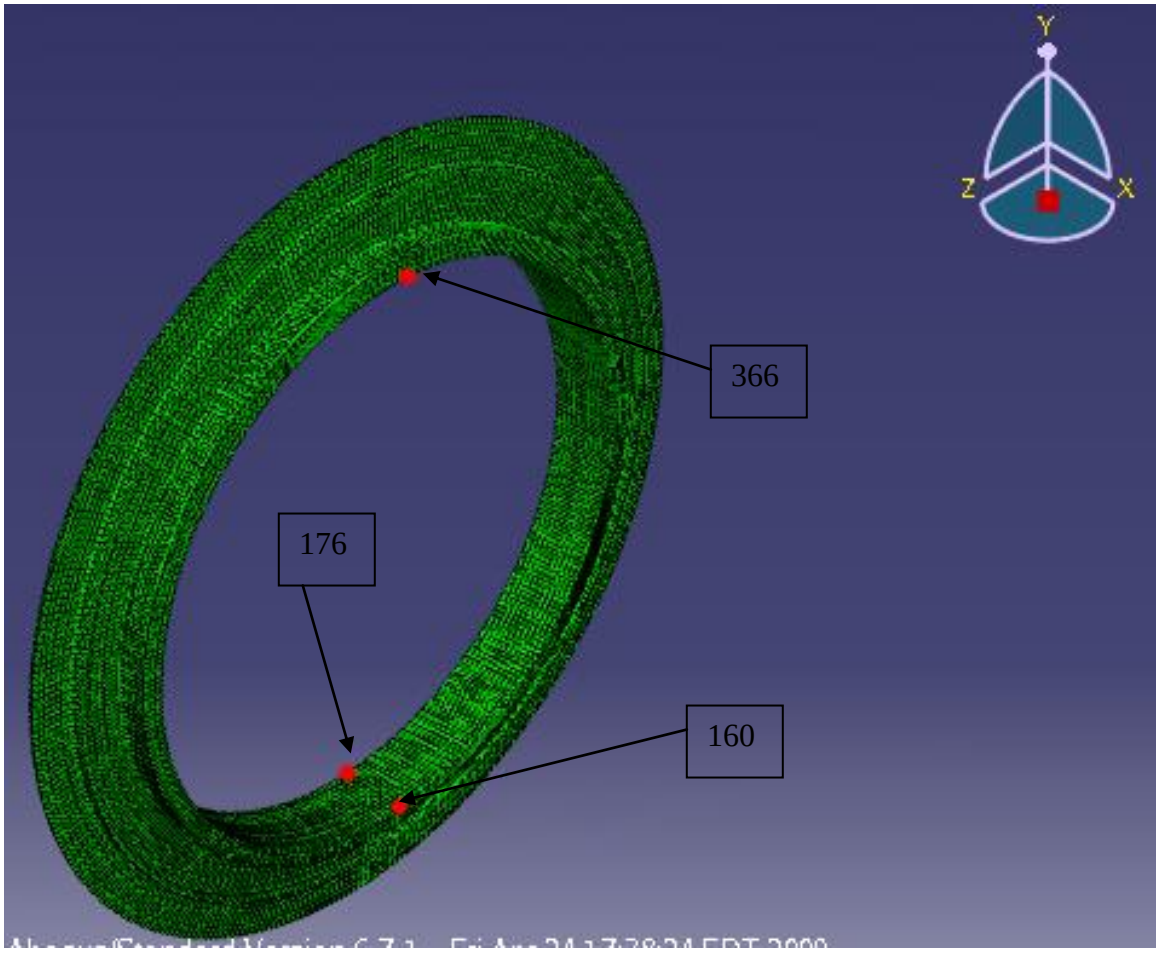

Figure 15: Nodes Fixed during Stress Simulation

Figure 17 shows the nodes that were fixed during the stress simulation. Node 160 is constrained in all six directions. Node 366 is constrained only laterally in the z direction. Node 176 is constrained laterally in the y and z directions. The details of the stress input files can be seen in Appendix 4.

Results and Discussion

Carburizing Simulation

The first step in the heat treating process that was simulated was carburizing. To simulate a low pressure/vacuum carburizing operation a surface mass flux was used. In a vacuum a small amount of carbon in the atmosphere was an unlimited potential and the steel with a much lower carbon potential absorbs the carbon at a rate that is assumed to be constant.

Parameters: 32 minutes at Carbon flux = 2.5×10^{-11} kg/mm^2/s (2.5×10^{-6} g/cm^2/s) at chamfer, flank, and root, 38 minutes of zero carbon flux at the chamfer, flank and root 1038^{o}C (1900^{o}F) Explanation of Figure 16: the concentration is in kg/mm^3. So dark blue at 9.71×10^{-9} corresponds to 0.1 wt.% carbon, the green on the surface of the root of the tooth corresponds to about .67 wt.% carbon, and the red on the surface between the chamfer and the flank corresponds to about 1.06 wt.% carbon. This is within the required carbon case content at a depth of .005-.010 inches (.12-.24mm) from the surface of .6 to 1.0 wt.% carbon.

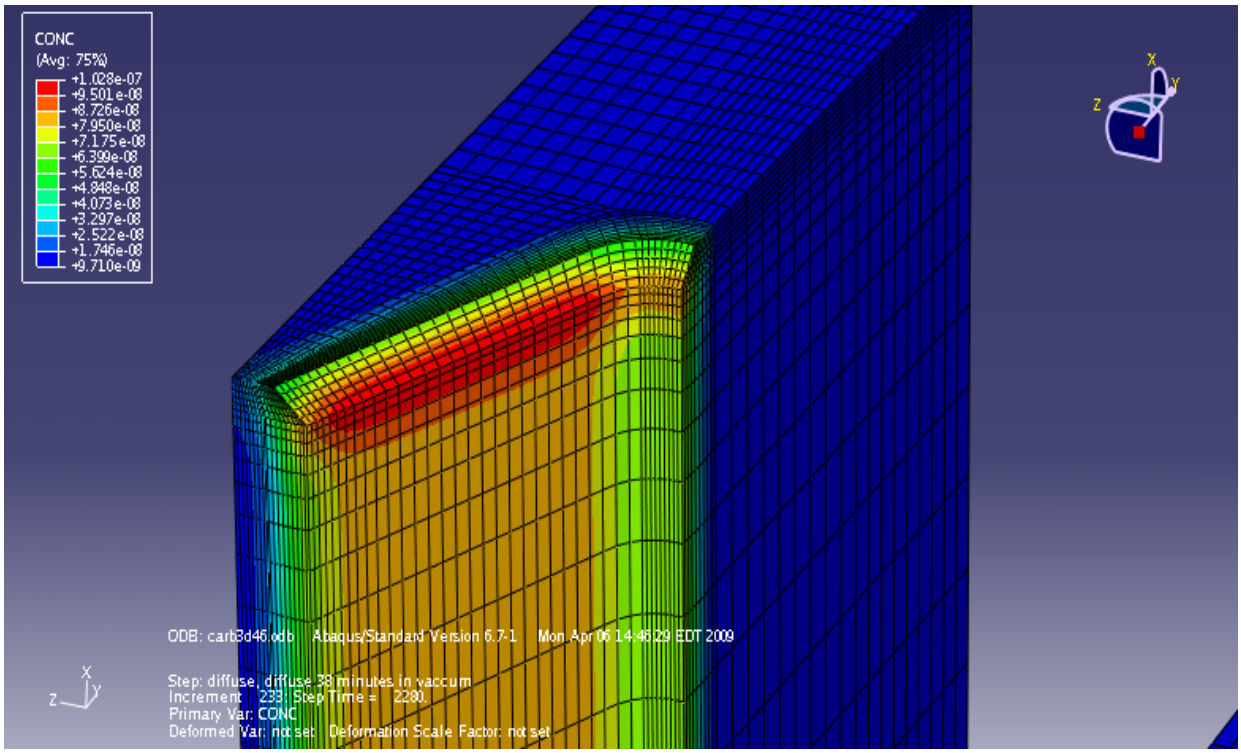

Figure 16: Carbon Concentration Results of 3D Vacuum Carburizing Simulation

Heat Transfer Simulations

A heat transfer simulation of the carburizing process was preformed with completely symmetrical heat transfer. The goal of this simulation was to compare the simulation results with the measured values. The maximum temperature used were those for the carburizing furnace (1038C, 1900F). The time was the same as the carburizing operation (70 minutes). The ring gear was heated from 20^{o}C to 1038^{o}C (68^{o}F to 1900^{o}F) and held there for the remainder of 70 minutes before it was cooled in air back to 20^{o}C (68^{o}F).

A heat transfer of the quenching simulation was carried out on the quarter of one tooth model with the carburizing completed to see how the carbon had an effect on the retained austenite in the case. As you can see from Figure 17 the carbon in the case of the gear prevented austenite from forming at that point 10 seconds into the quenching process. This demonstrates that the steel with higher carbon content has a lower martensite start temperature than the low carbon steel. While this is a well documented phenomena, it demonstrates the ability of the model to mimic the physical situation.

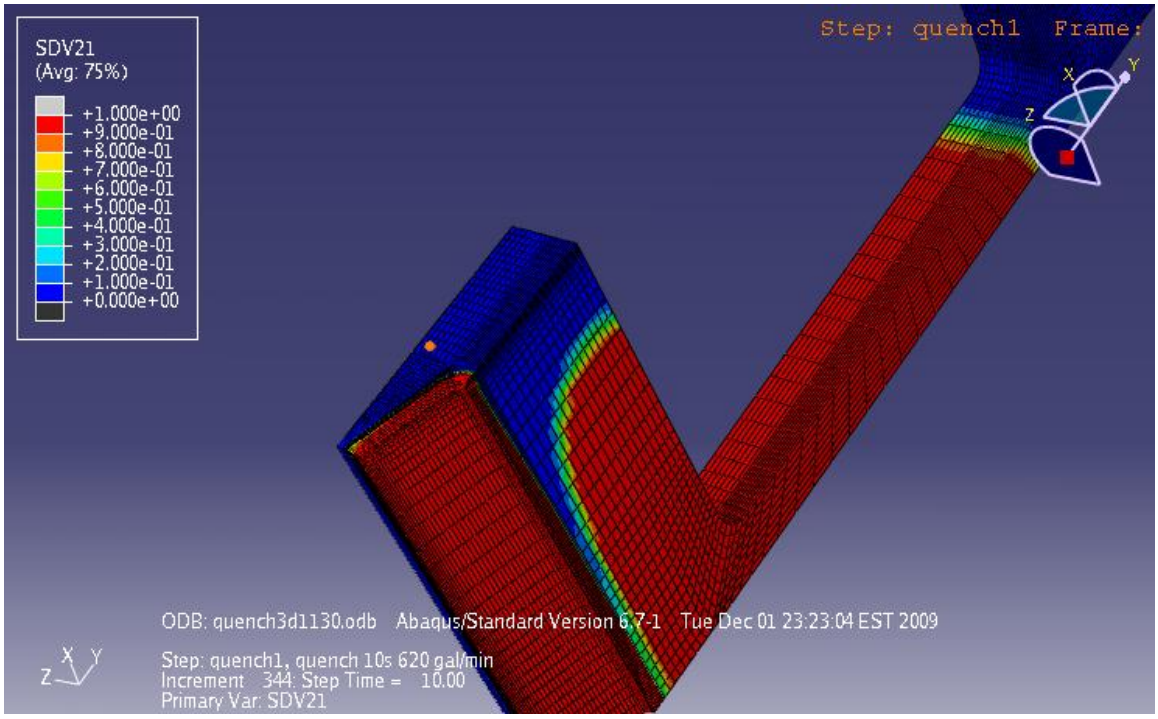

Figure 17: Austenite after First Step in Oil Quenching (10s)

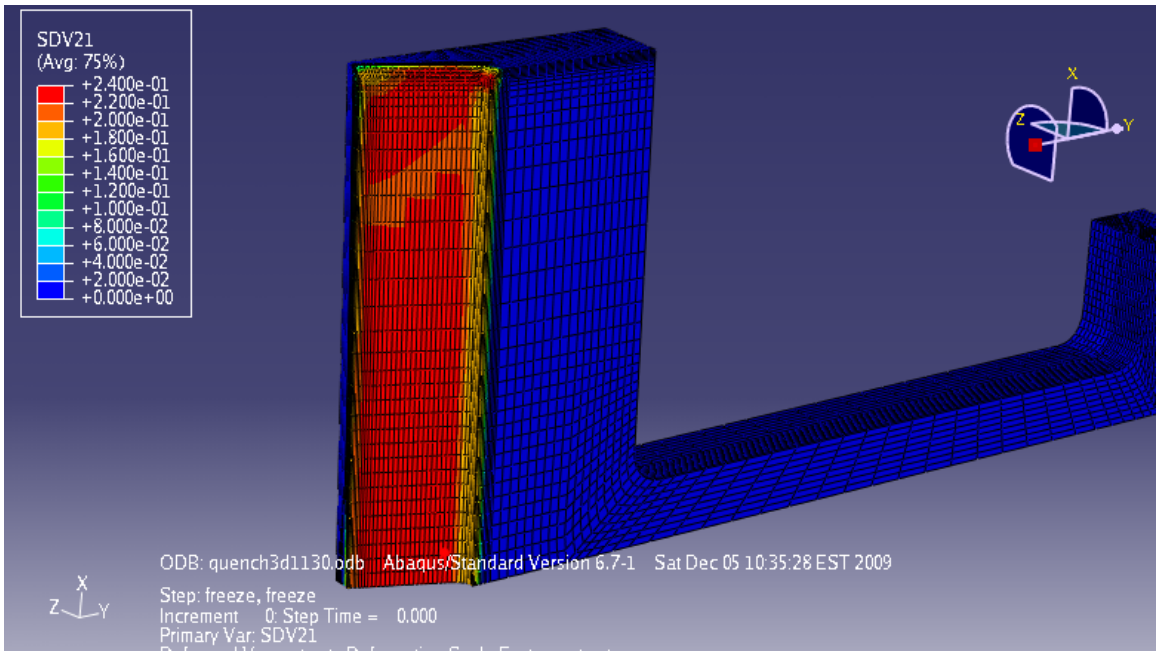

Figure 18: Retained Austenite Between Quenching and Cryogenic Treating

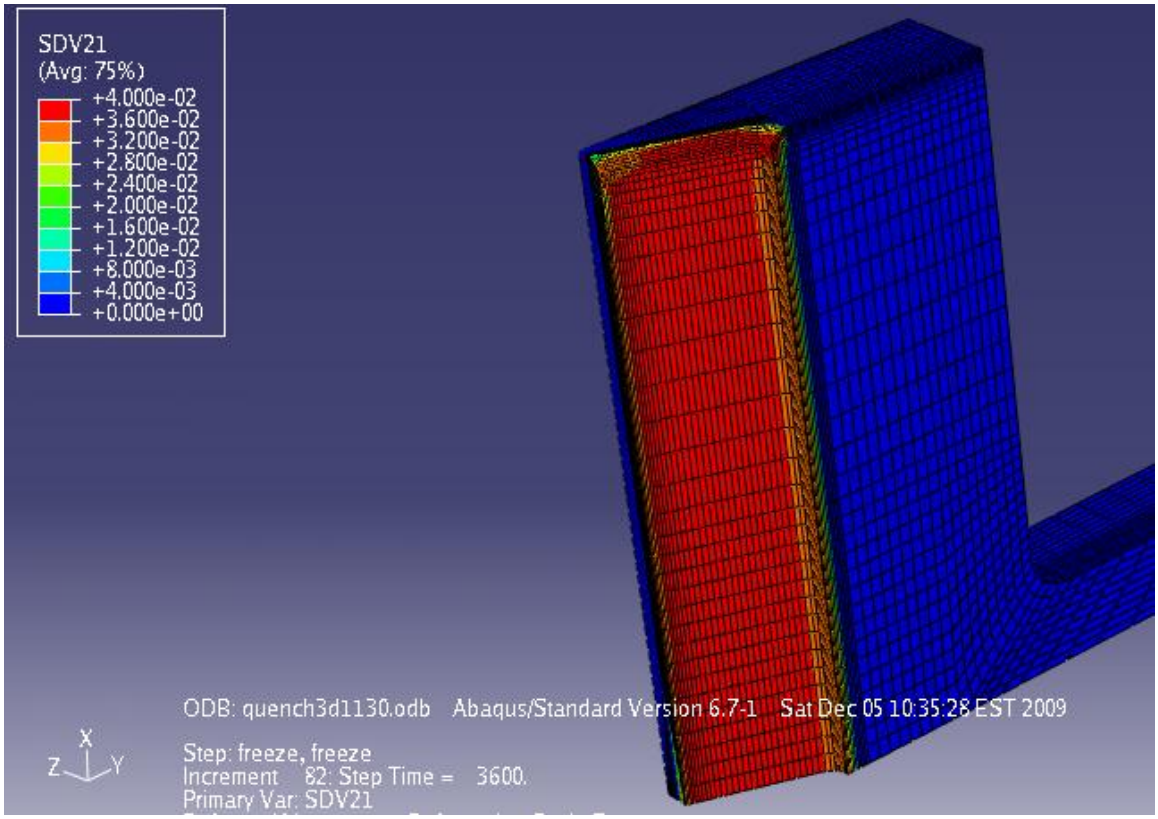

Figure 19: Retained Austenite after all Quench, Harden and Cryogenic Treatment

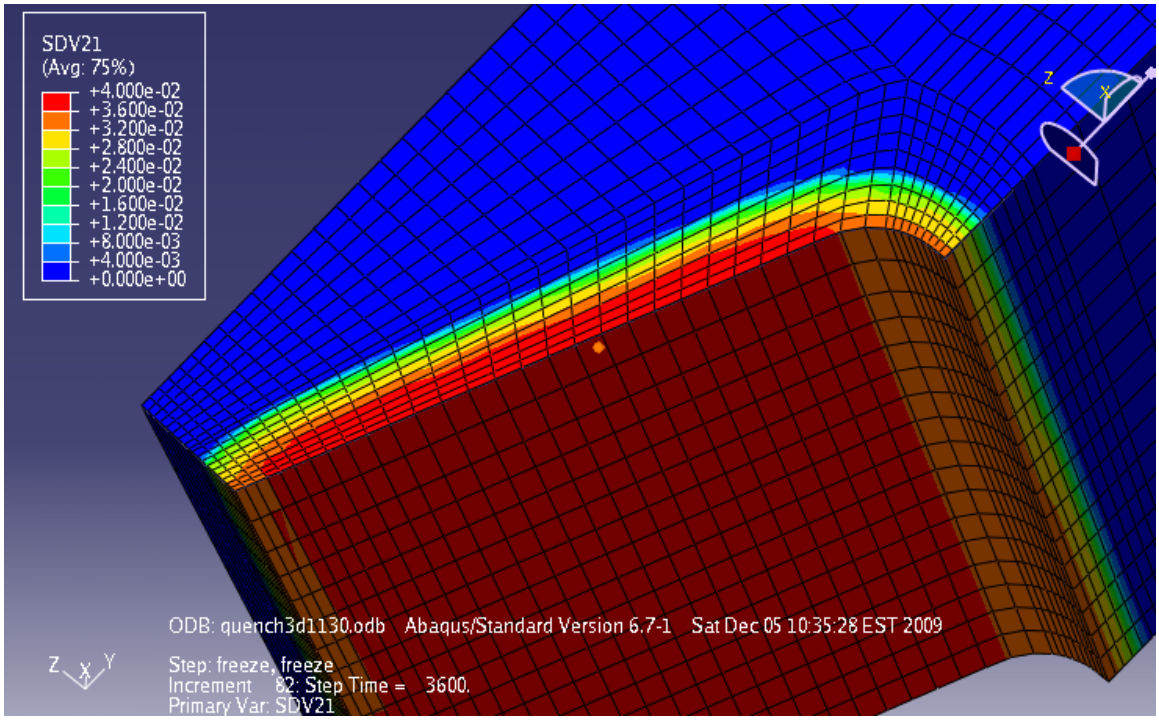

Figure 20: Close up section view of Retained Austenite After Quench and Harden

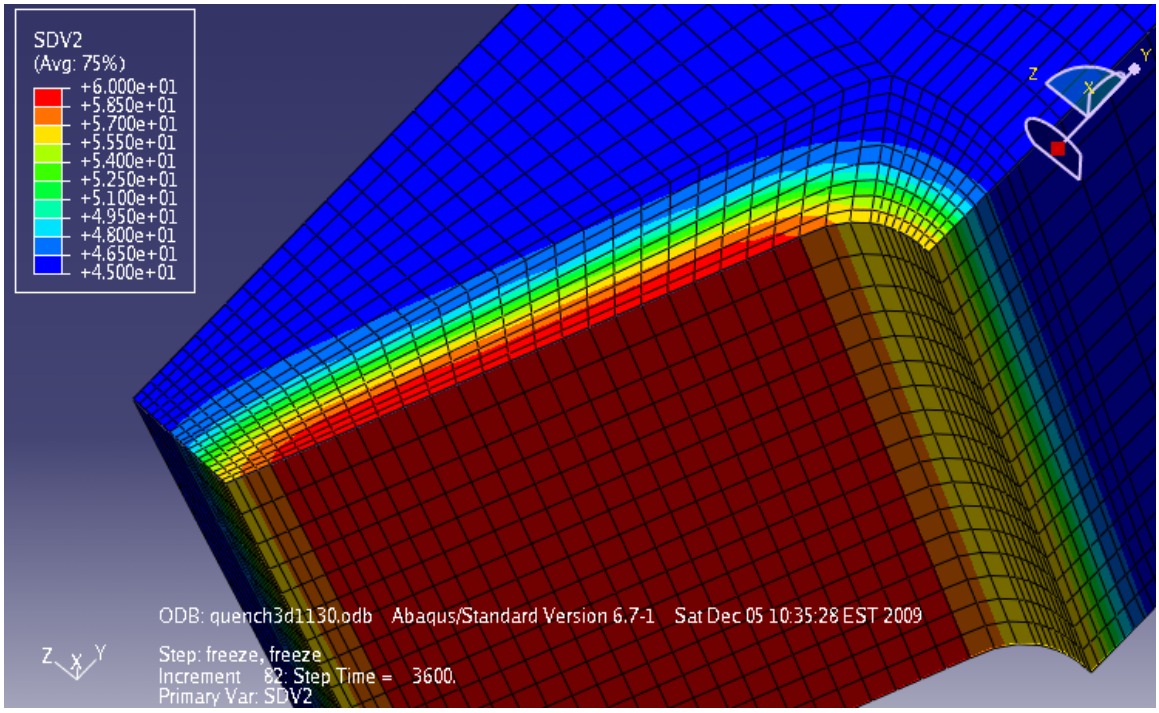

Figure 21: Close up section Hardness (Rockwell C) after Quench and Harden

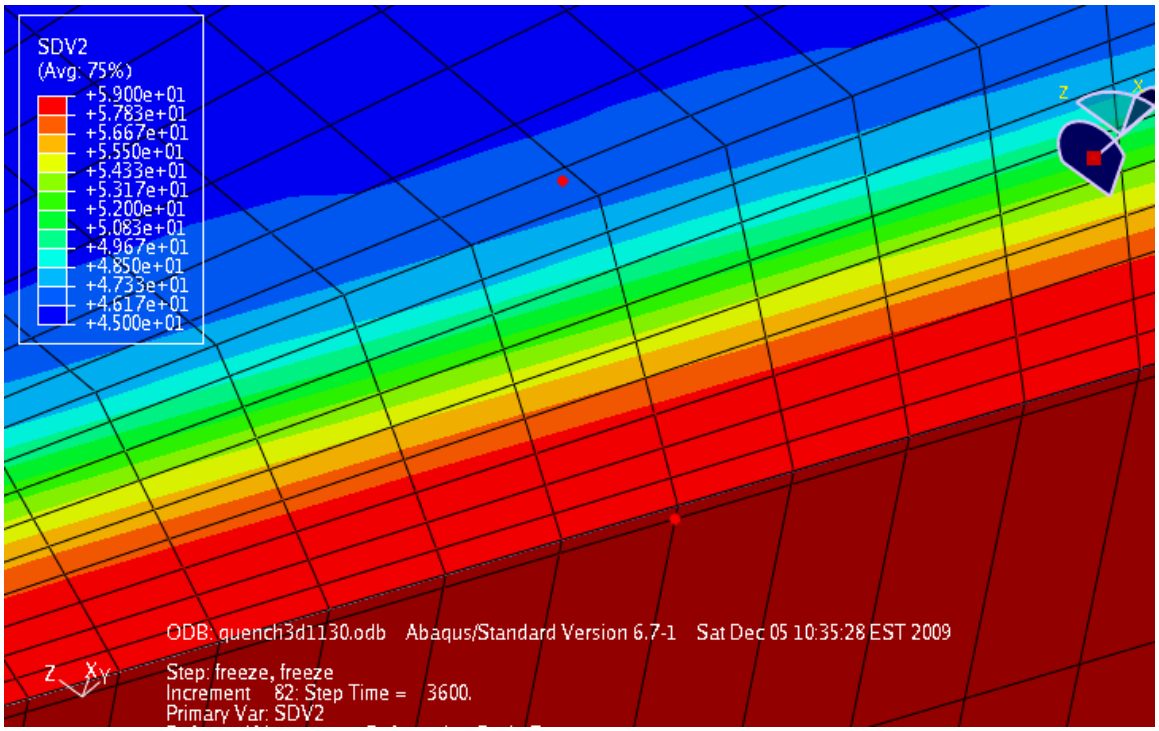

Figure 22: Close up Section Hardness (Rockwell C) after Quench and Harden

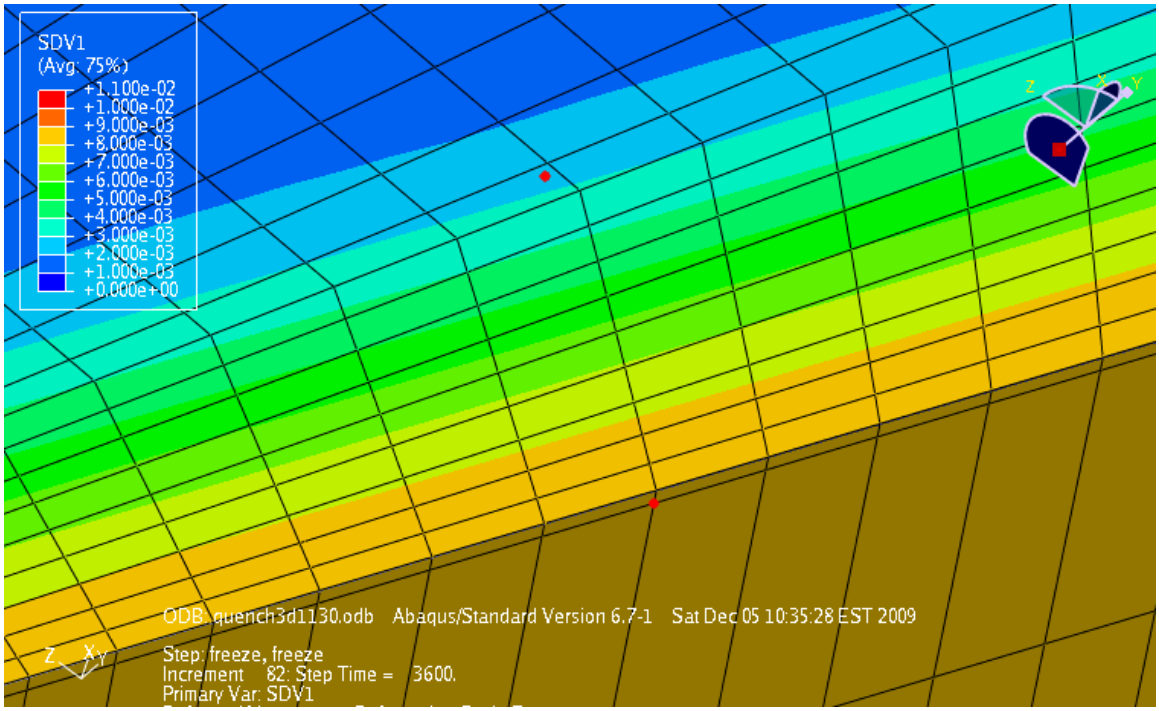

Figure 23: Close up Weight Percent Carbon content after Quench and Harden

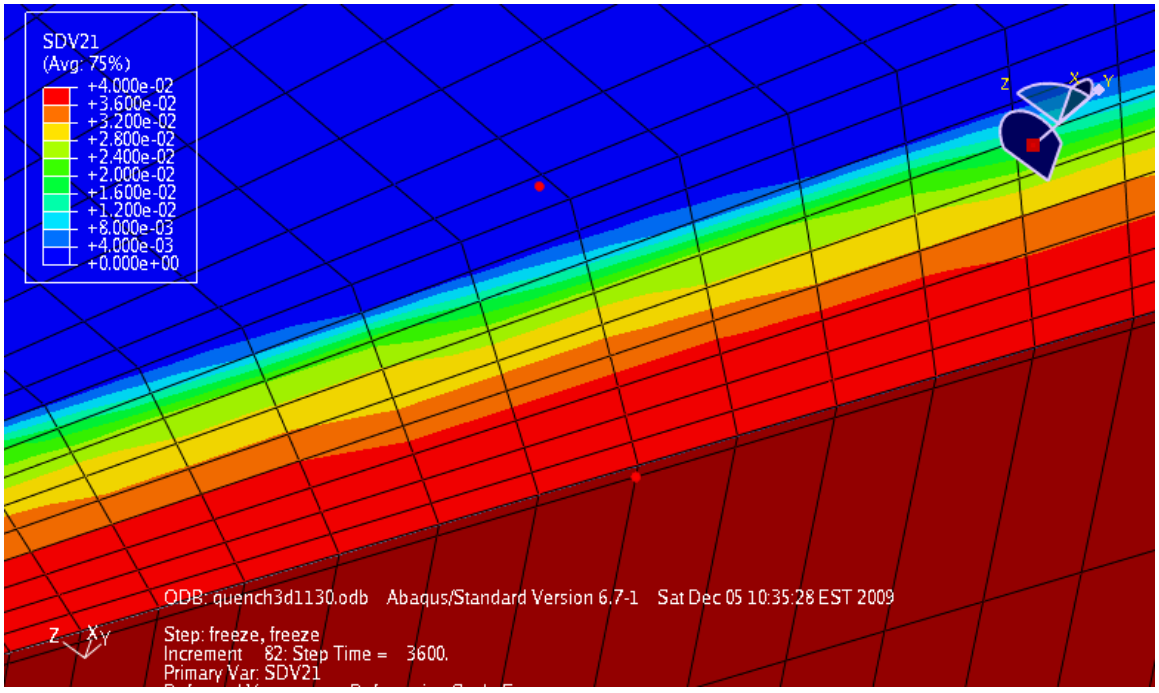

Figure 24: Retained Austenite Percentage after Quench and Harden

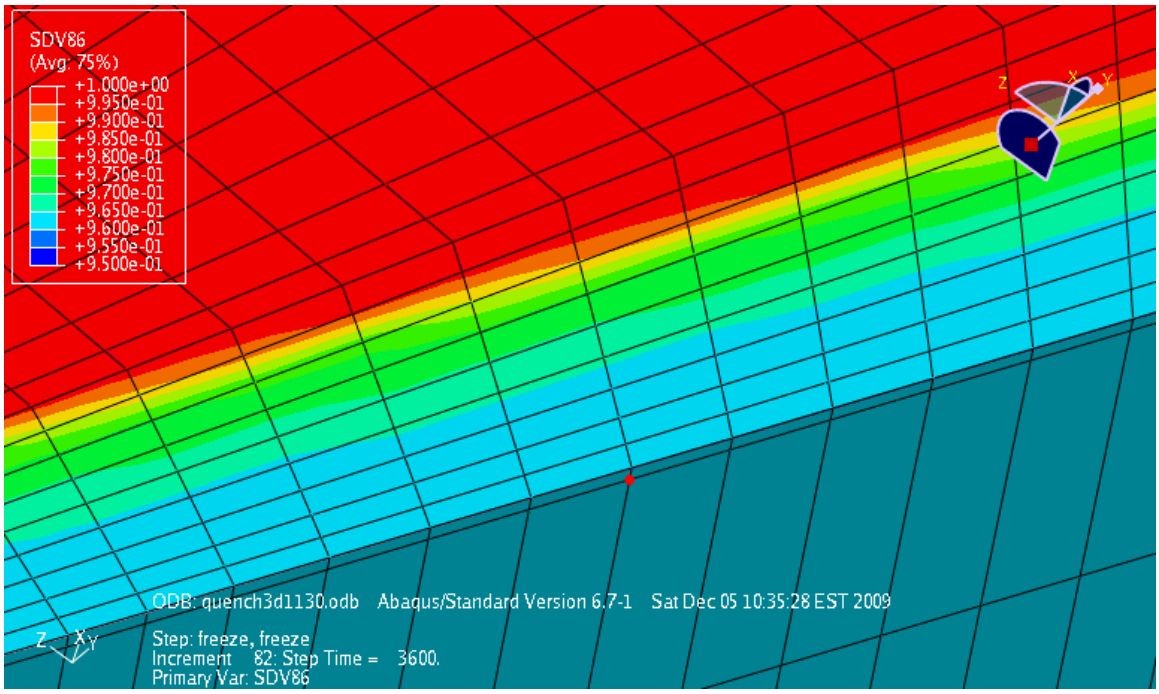

Figure 25: Percent Martensite after Quench and Harden

Figures 15 and 17-25 show the microstructure and hardness of the gear near the carburized layer. Figure 18 shows the austenite between the quenching and cryogenic treatment. At the surface of the carburized case the retained austenite is 22-23 percent of the microstructure. This demonstrates that the gear needs to be cooled further to reduce the retained austenite to less than 20 percent as specified by the manufacturer. Figure 19 and Figure 20 show the retained austenite after quenching and cold treatment. The maximum retained austenite is about 3.9 percent of the microstructure. That is below the specified maximum value. Figures 21 and 22 show the hardness in the carburized case. The hardness in Rockwell C varies from a value of about 59 at the surface to 46 in the core. The 46 is higher than the expected from the literaturebecause the DANTE material database specifies the same hardness for all Pyrowear 53 with 0.2 weight percent carbon and below. Figure 23 shows the levels of carbon at a typical section of the flank. Figure 24 shows the retained austenite after cold treatment. Figure 25 shows the martensite after cold treatment.

The values shown in these figures are the values expected with the exception of the through hardness of 46 Rockwell C which was explained by the specifications of the material database used by the software. This phase property data is shown in Appendix 1.

For these simulations all of the martensite with a carbon content of less than .2 weight percent have a hardness of 46 Rockwell C. There is no division between .1 weight percent and .2 weight percent.

One of the issues reducing the extensive use of high pressure gas quenching is the question of heat transfer rates and retained austenite levels. Using the same fixturing boundary conditions a simulation was performed using oil quenching and another was performed using high pressure gas quenching. The oil quenching simulation results shown below in Figure 26 with the variable graphed is retained austenite. The gas quenching simulation values for retained austenite are shown in Figure 27. In the uncarburized material the retained austenite is below one percent which is expected. Pyrowear 53 contains .1 wt% carbon in the bulk material and starts forming martensite at 437 degrees Celsius (819^{o}F) and 99 percent transformation is complete around 222 degrees Celsius (432^{o}F).

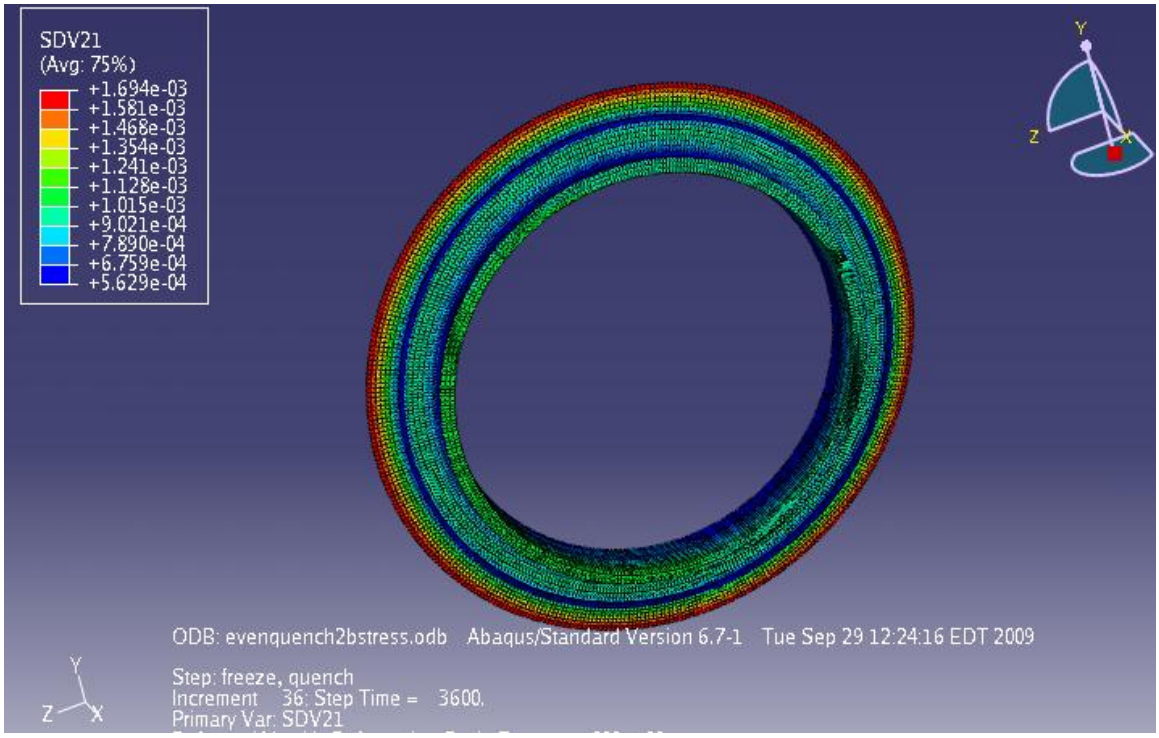

Figure 26: Retained Austentite in Oil Quenched Simulation

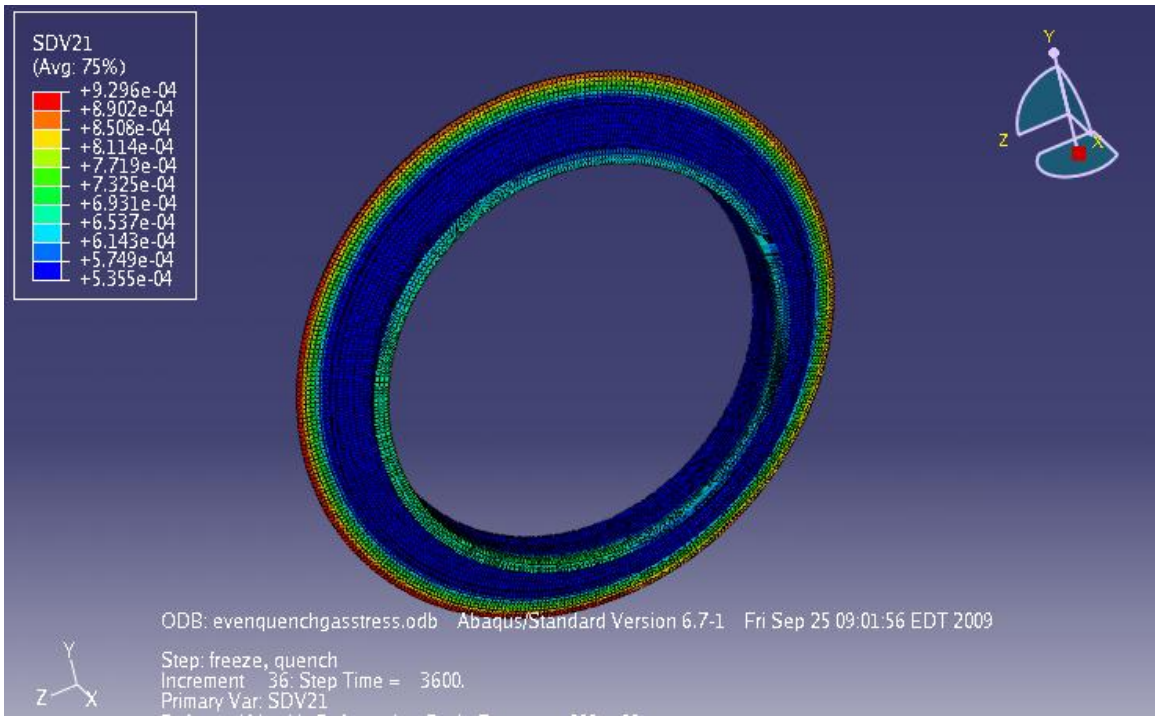

Figure 27: Retained Austenite in high pressure gas quenched simulation

The hardness from the oil quenched and high pressure gas quenched is about the same, ranging between 45.9 and 46 Rockwell C. These values are higher than the measured values from coupons processed with the gears which showed a hardness of 34 to 44 Rockwell C (Figure 28) and the literature which give a through hardened value for Pyrowear 53 of martensite of 38 (Thomas). Figure 29 shows the Rockwell C hardness of an oil quenched section of the gear. Figure 30 shows the Rockwell C hardness of a gas quenched gear section.

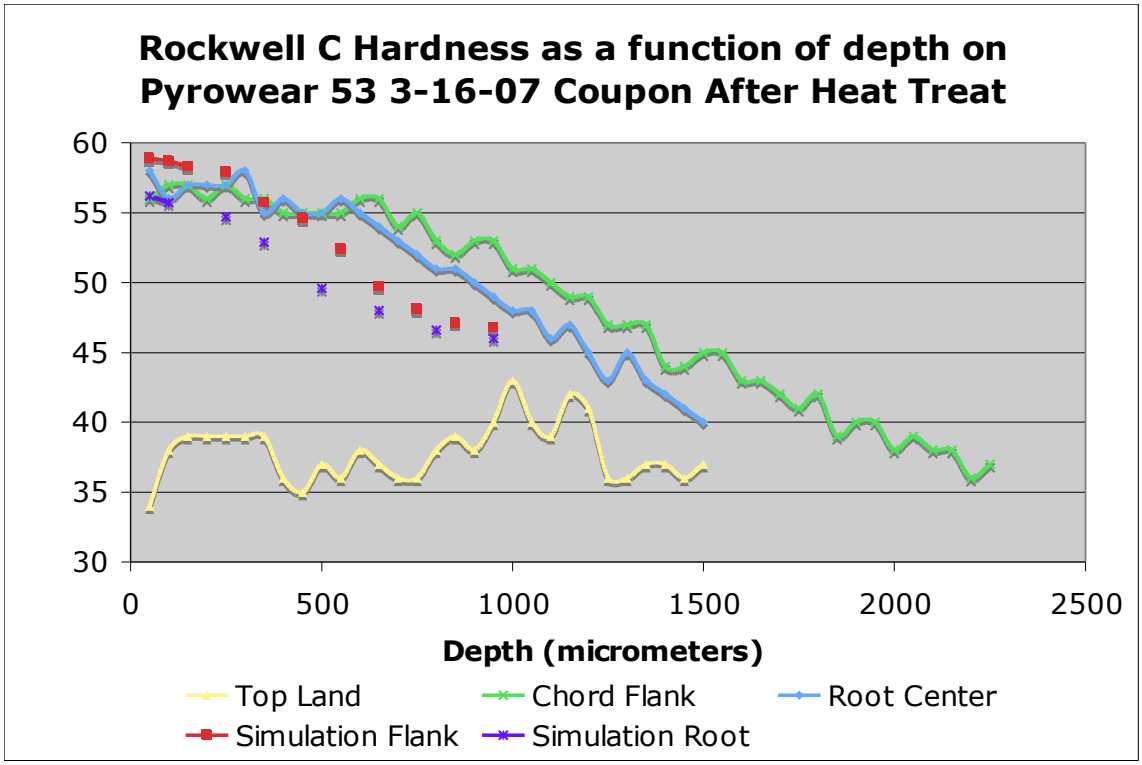

Figure 28: Hardness as a Function of Depth on test Coupon and Simulation

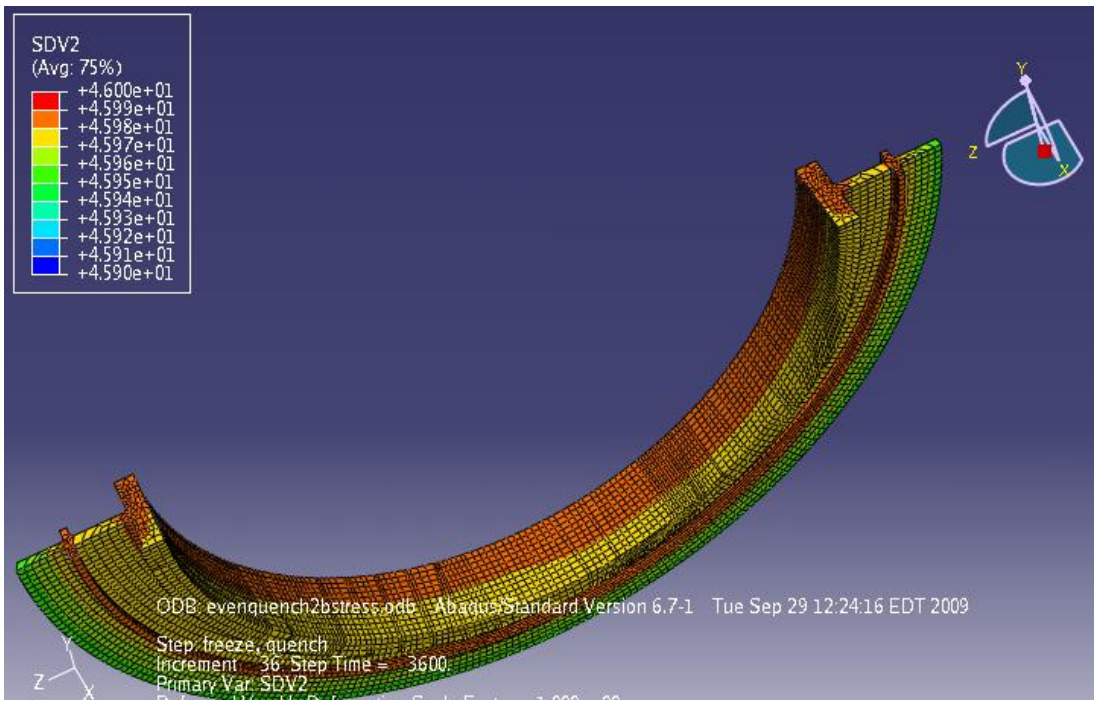

Figure 29: Rockwell C hardness of oil quenched simulation

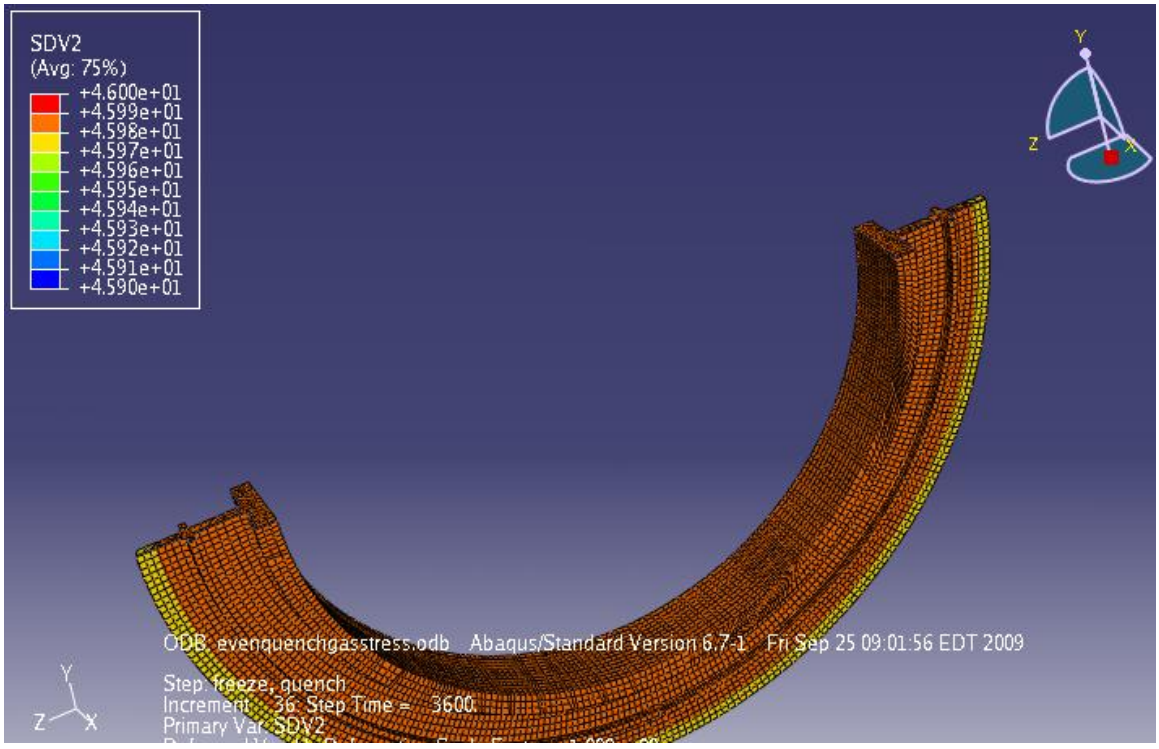

Figure 30: Rockwell C hardness of gas quenched

Stress Simulations

A stress simulation was performed using the results of the symmetrical heat transfer simulation. This provided a base for knowledge of boundary conditions which would show that the gear simply expanded and contracted and was a perfect circle as it started. The maximum and minimum principal stresses are shown below. Due to the symmetrical heat transfer the stress fields are nearly perfectly symmetrical. Figure 31 shows the maximum principal stresses for a gear that is simply heated up and cooled down simulating the carburizing operation. Figure 32 shows the minimum principal stresses for the same simulation. The positive values refer to tension and the negative values refer to compression. All stress values are in megapascals (MPa).

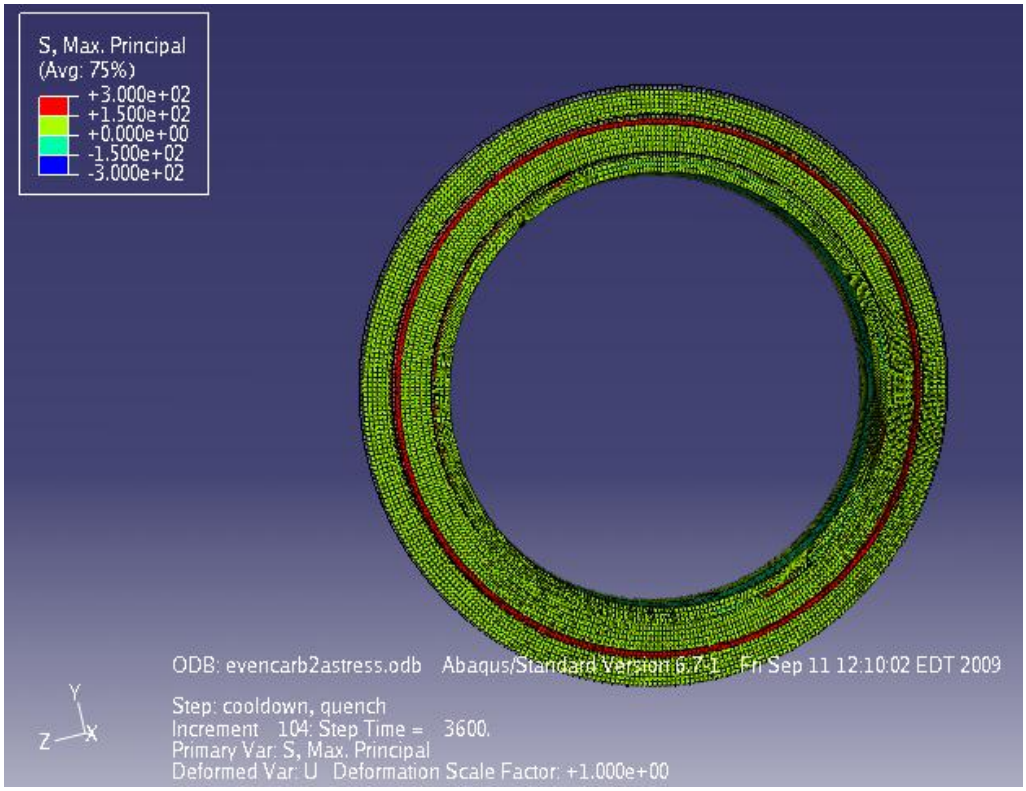

Figure 31: Maximum Principal Stresses for Evenly Quenched Simulation

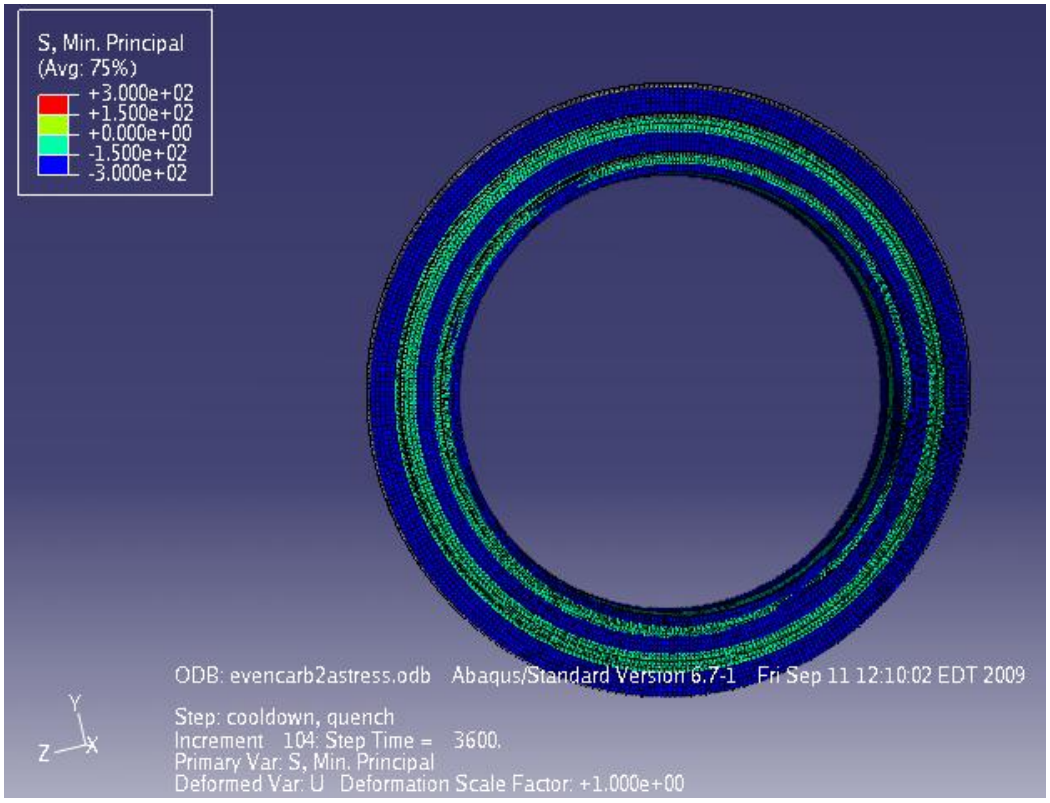

Figure 32: Minimum Principal Stresses for Evenly Quenched Simulation

The results of this simulation are shown in Table 3 below. This demonstrates the importance of minor variations within the mesh as well as constraining the part. The distortion is nearly zero as expected.

Carburizing Simulation Evencarb2astress.odb 9-11-2009	**Internal Diameter goal = 20.320 in.**	
Nodes 4 to 310	**millimeters**	**inches**
Initial t=0	516.128	20.320
Air cool t=5000	510.811	20.111
Nodes 1290 to 2620		
Initial t=0	516.128	20.320
Air cool t=5000	510.694	20.106
Out of Round	**.117**	**.005**

Table 3: Distortion measurements for Evenly Quenched Simulation

Physical distortion measurements were taken at several stages during the heat treating process at the manufacturer. Measurements were taken after machining, after carburizing, and after harden and temper. The measurements taken after machining before any heat treating are show below in Table 4 for a series of gears run through the same batch.

Root	(inches)			
	S/N 178	**S/N 179**	**S/N 180**	**S/N 181**
Out of Round	**.003**	**.001**	**.002**	**.002**

Table 4: Measured Distortion Values before Heat Treating

The gears were also measured after the carburizing process and measurements are summarized in the Table 5 and Figure 33 below as well as Appendix 5. The results of these measurements showed that the gear had significant distortion that occurred during carburizing.

Root Diameter	Master Diameter =20.930"	(inches)		
	S/N 178	**S/N 179**	**S/N 180**	**S/N 181**
Out of Round	**0.1**	**0.105**	**0.92**	**0.018**

Table 5: Measured Distortion Values after Carburizing

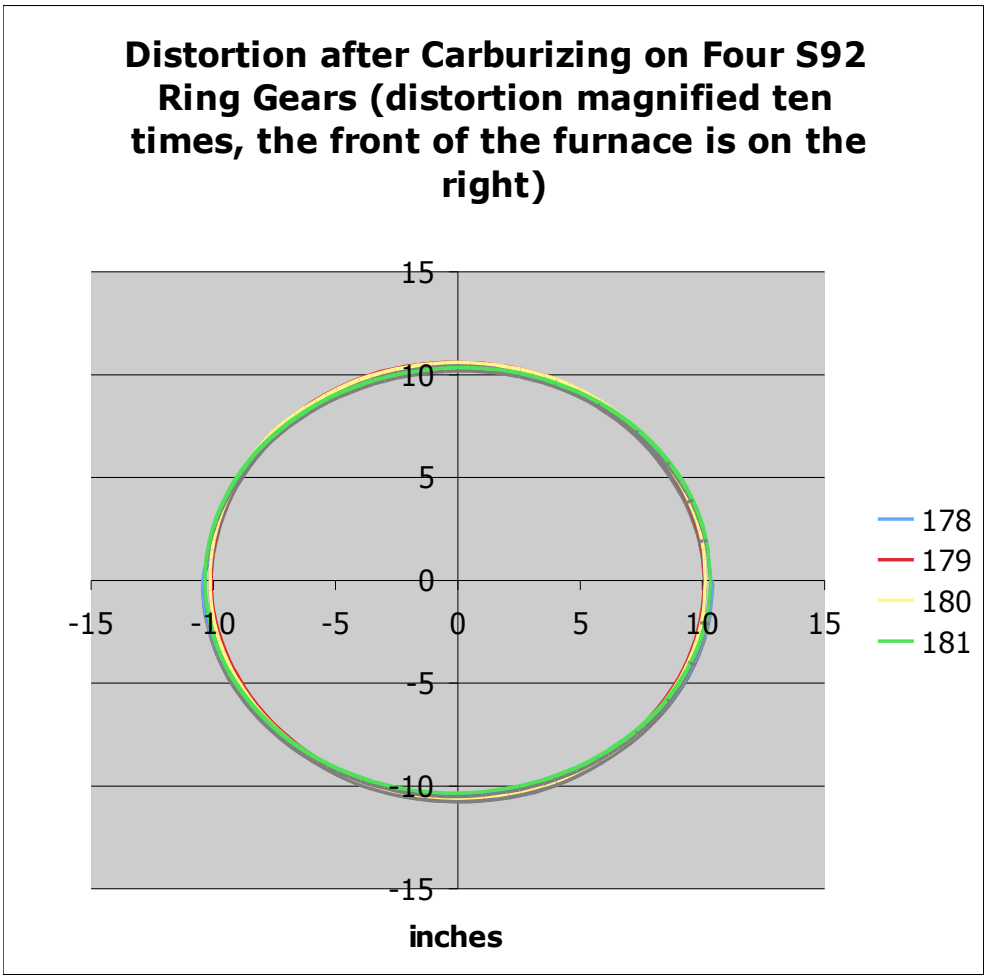

Figure 33: Measured Distortion after Carburizing (distortion magnified 10x)

The results of these measurements show uniform distortion occurring on three out of four samples in the carburizing furnace. The gears contracted in the direction perpendicular to the door and expanded in the direction parallel to the door. This could be due to the racking system. It is possible that the carbon gases are not evenly distributed over the parts. This could cause more compressive stress on the part of the gear that absorbed more carbon (Rakhit). The racks that the ring gears rest on could also be warped causing deformation (Frost). The results of these measurements compared to the symmetrical heating and cooling simulation demonstrate that some force is acting on the gears which is not accounted for in the simulation. Some of the possible causes include residual machining stresses, an uneven carburizing rack, and uneven cooling.

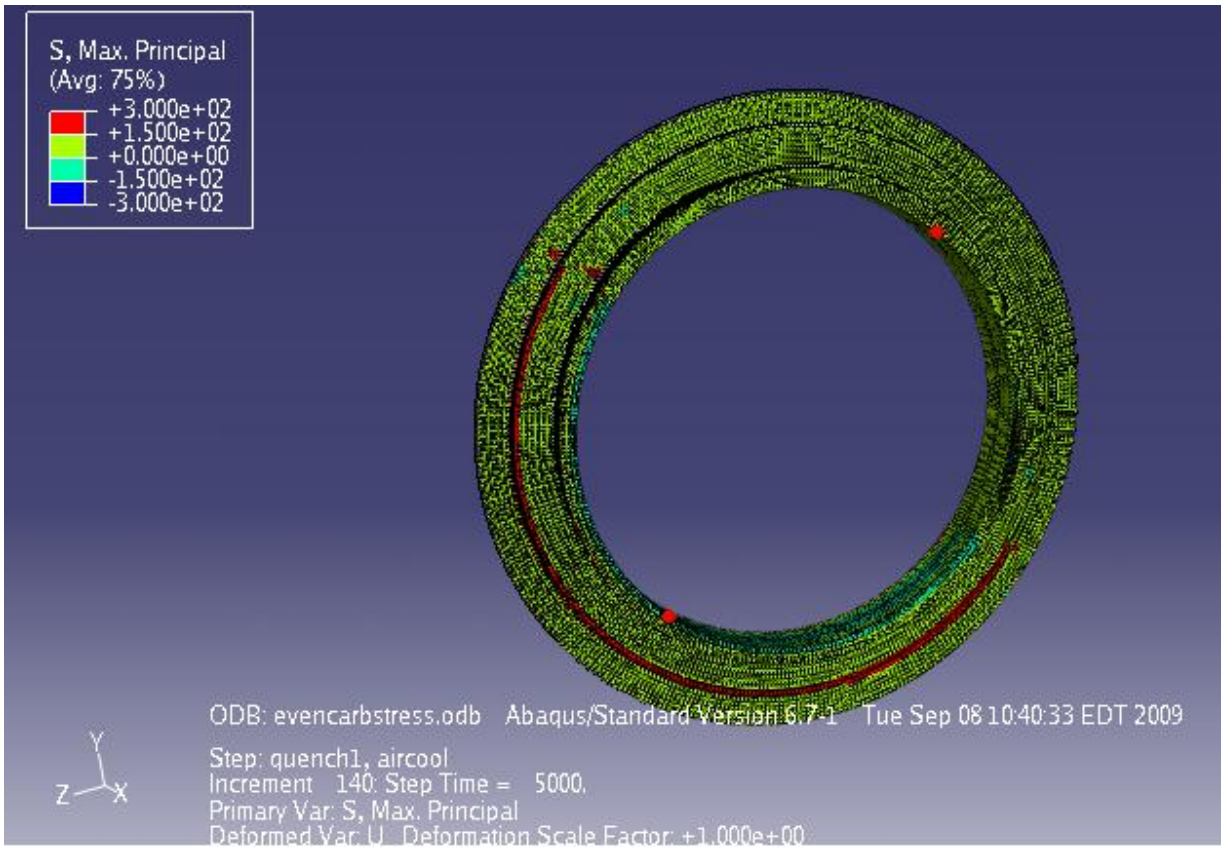

Figure 34: Maximum Principal Stresses on Unevenly Oil Quenched Simulation

To simulate some of the possible causes of distortion in the carburizing process a simulation was completed that cooled half of the ring gear for 30 seconds and then cooled the entire gear evenly. This was to simulation an uneven cooling such as the door of the carburizing furnace opening and allowing in cool air. It is obvious from the images that the stress field was uneven. The half of the gear that cooled faster had larger compressive principal stresses and larger tensile principal stresses. The maximum principal stresses are shown in Figure 34 with nodes 1290 and 2620 shown in red. The minimum principal stresses are shown in Figure 35 with nodes 4 and 310 shown in red. Nodes 4, 310, 1290, and 2620 were are right angles to each other and were used to measure the distortion.

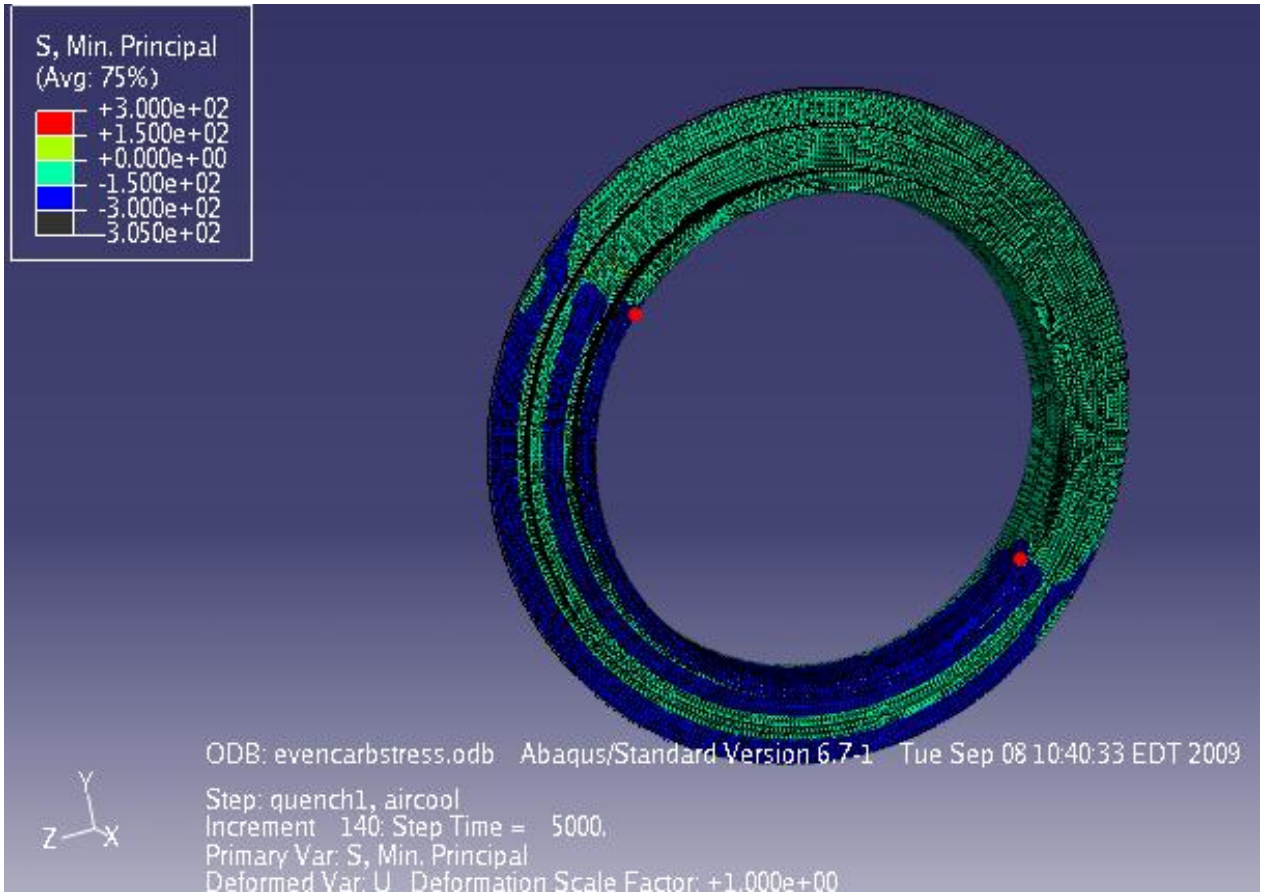

Figure 35: Minimum Principal Stresses on Unevenly Oil Quenched Simulation

The measured deformation results of the simulation are shown below in Table 6. These results show that while uneven cooling is responsible for about three times more distortion than even cooling it still does not compare to the measured values.

Carburizing Simulation Evencarbstress.odb 9-8-2009	**Internal Diamter goal = 20.320 in.**	
Nodes 4 to 310	**millimeters**	**inches**
Initial t=0	516.128	20.320
Air cool t=5000	513.062	20.199
Nodes 1290 to 2620		
Initial t=0	516.128	20.320
Air cool t=5000	512.728	20.186
Out of Round	**.334**	**.013**

Table 6: Distortion Measurements on Unevenly Oil Quenched Simulation

To evaluate the effect of different quench methods on the ring gear simulations were performed that demonstrate the relative heat transfer differences between high pressure gas quenching and oil quenching. The same four gears that had previously been measured were again measured for distortion after they were quenched and hardened and the results are in Table 7.

(dimensions in inches)	**Root Diameter**	**Master = 20.930"**		
	S/N 181	**S/N 178**	**S/N 179**	**S/N 180**
Out of Round	**.012**	**.009**	**.005**	**.005**
TAPER	0.019	0.024	0.021	0.012

Table 7: Measurements after Quench and Freeze

First a simulation of free quenching in oil was carried out. The results of that simulation are shown in Figure 36. The Von Mises stresses are shown on the distorted gear which is magnified 66.58 times and compared to the original size of the gear. The gear has a slight potato chip effect where the gear appears to curl up about the z axis.

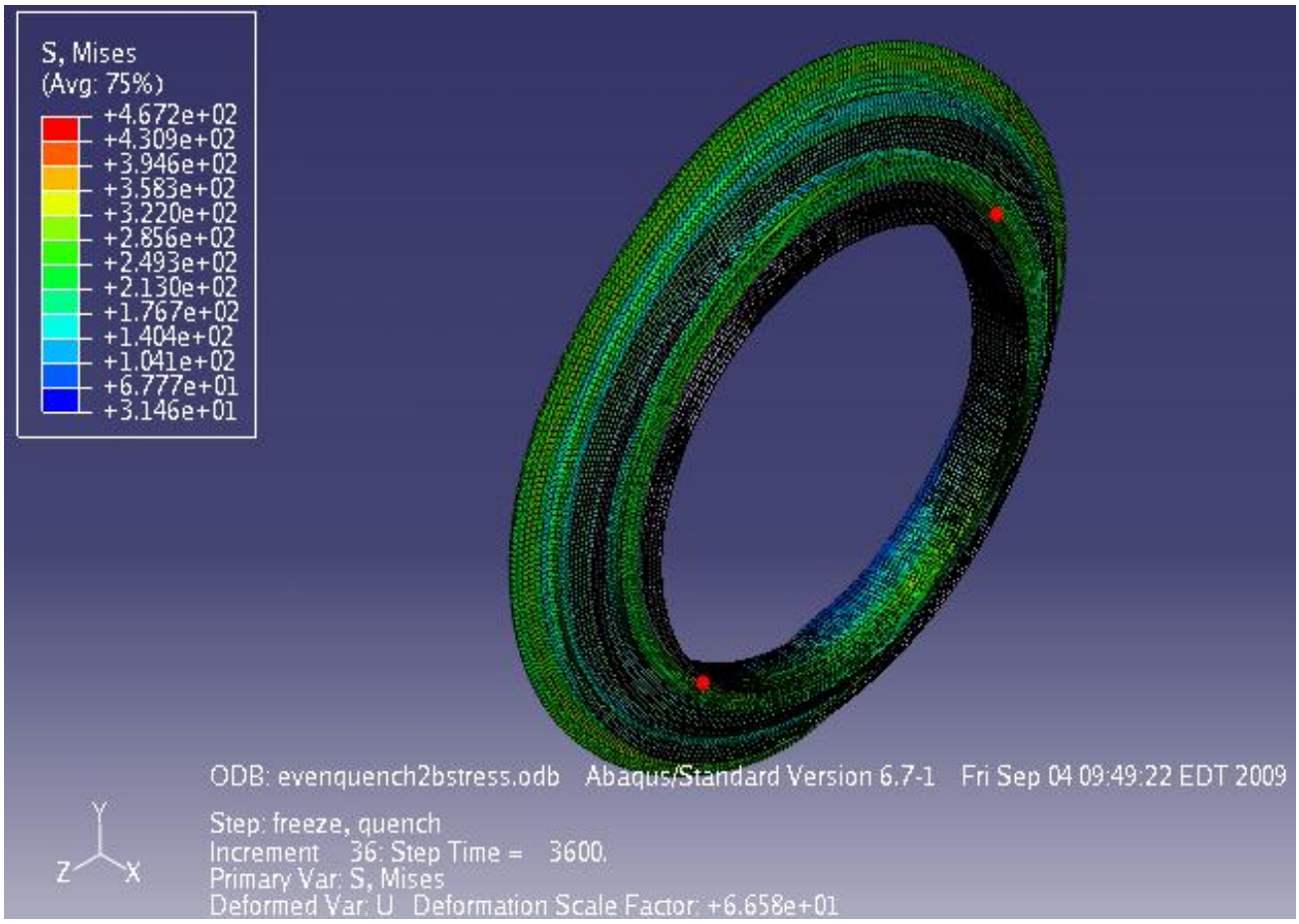

Figure 36: Von Mises Stress on Free Quenched in Oil Simulation

The results of the out of round distortion for this gear simulation show very little distortion as shown in Table 8. This is to be expected considering the symmetrical quenching. The numerical results of this simulation can be seen in the table below. This model was also over constrained with four separate nodes fixed to simulate an even rack where the gear was resting on four points at once.

Quench and Freeze Simulation Evenquench2bstress.odb 9-4-2009	**Internal Diameter goal = 20.320 in.**	
Nodes 4 to 310	**millimeters**	**inches**
Initial t=0	516.128	20.320
Air cool t=5000	516.724	20.343
Nodes 1290 to 2620		
Initial t=0	516.128	20.320
Air cool t=5000	516.740	20.344
Out of Round	**.016**	**.001**

Table 8: Distortion of Free Quenched in Oil Simulation

Using the exact same boundary conditions as the simulation above, maintaining the same fixed nodes in the same directions, a high pressure gas quenching simulation was performed. The maximum and minimum principal stresses are shown below in Figure 37 and Figure 38 respectively. Nodes 4 and 310 are shown in red.

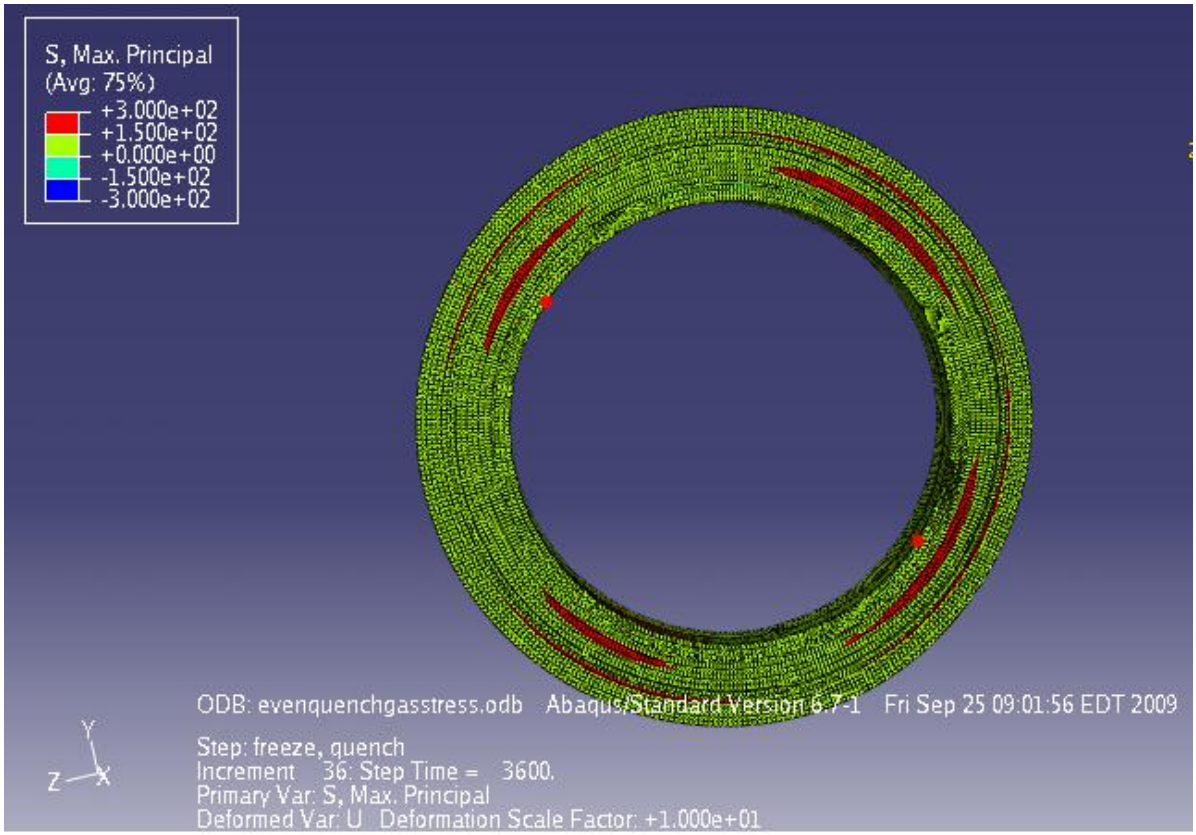

Figure 37: Maximum Principal Stresses on High Pressure Gas Quenched Simulation

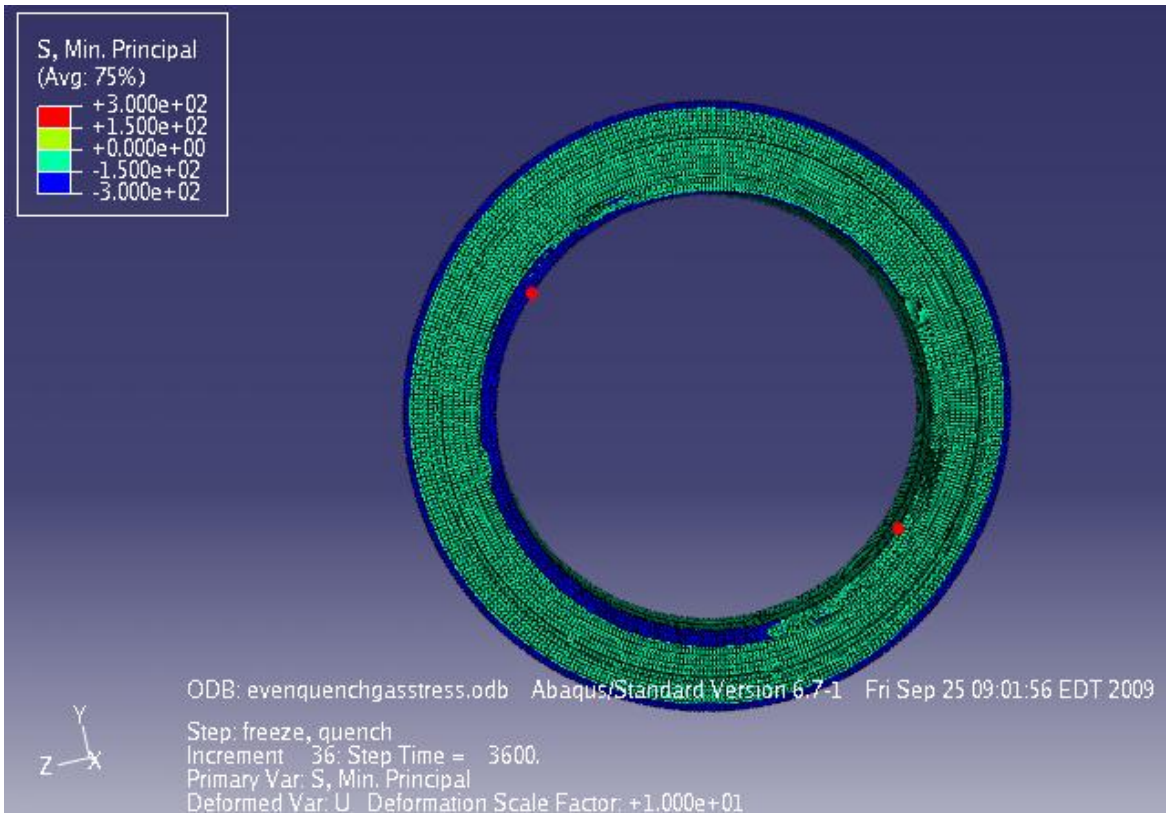

Figure 38: Minimum Principal Stresses on High Pressure Gas Quenched Simulation

Table 9 shows the measured distortion in the high pressure gas quenching simulation. It is interesting to note that using the same fixed boundary conditions as the both carburizing simulations the gas quenching provides much more distortion.

Nitrogen Gas Quenching Evenquenchgasstress.odb 9-25-2009	**Internal Diamter goal = 20.320 in.**	
Nodes 4 to 310	**millimeters**	**inches**
Initial t=0	516.128	20.320
Air cool t=5000	514.636	20.261
Nodes 1290 to 2620		
Initial t=0	516.128	20.320
Air cool t=5000	514.222	20.245
Out of Round	**.414**	**.016**

Table 9: Distortion for High Pressure Gas Quenching Simulation

To further investigate the detailed heat treating process a model was created that contained half of the entire gear and is shown in Figure 39. The goal of this model was to simulate the carburizing, quenching, and hardening process for the ring gear paying attention to previously ignored details. The details previously ignored to be included in this model include the teeth of the gear and the parts of the press quench in contact with the gear. The model contains 406,576 elements, 6336 linear hexahedral of the type C3D8R and 400,240 linear tetrahedral elements of the type C3D4. The model contains 112,195 nodes.

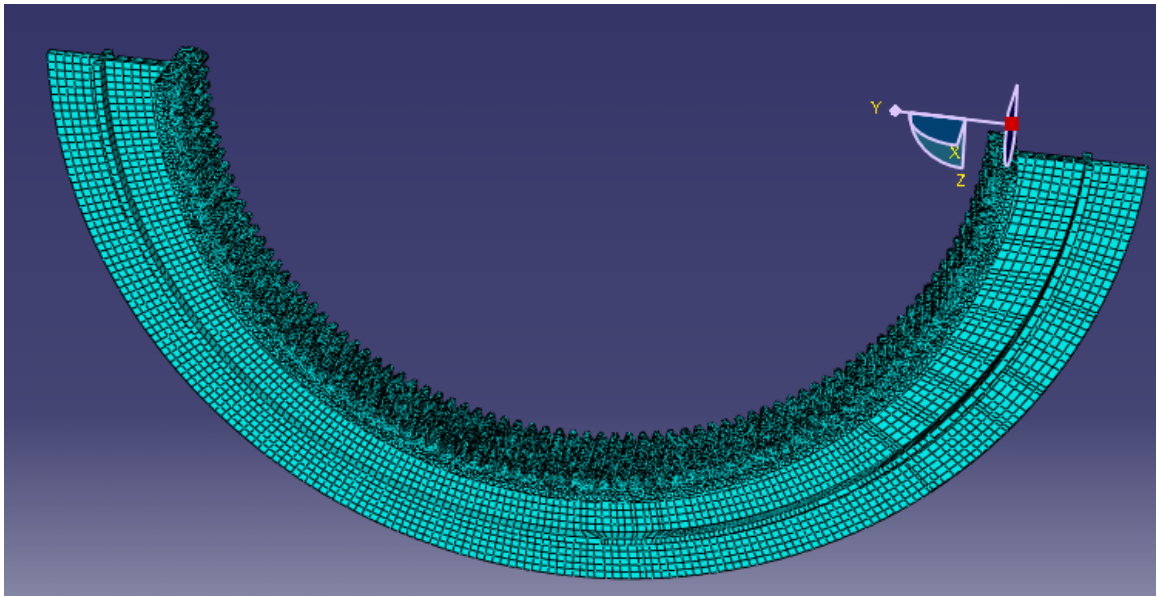

Figure 39: View of Gear for Combined Carburizing and Stress Analysis Simulation

The part was carburized using the same boundary conditions as the quart tooth section and the results representative of that simulation are shown in Figure 40.

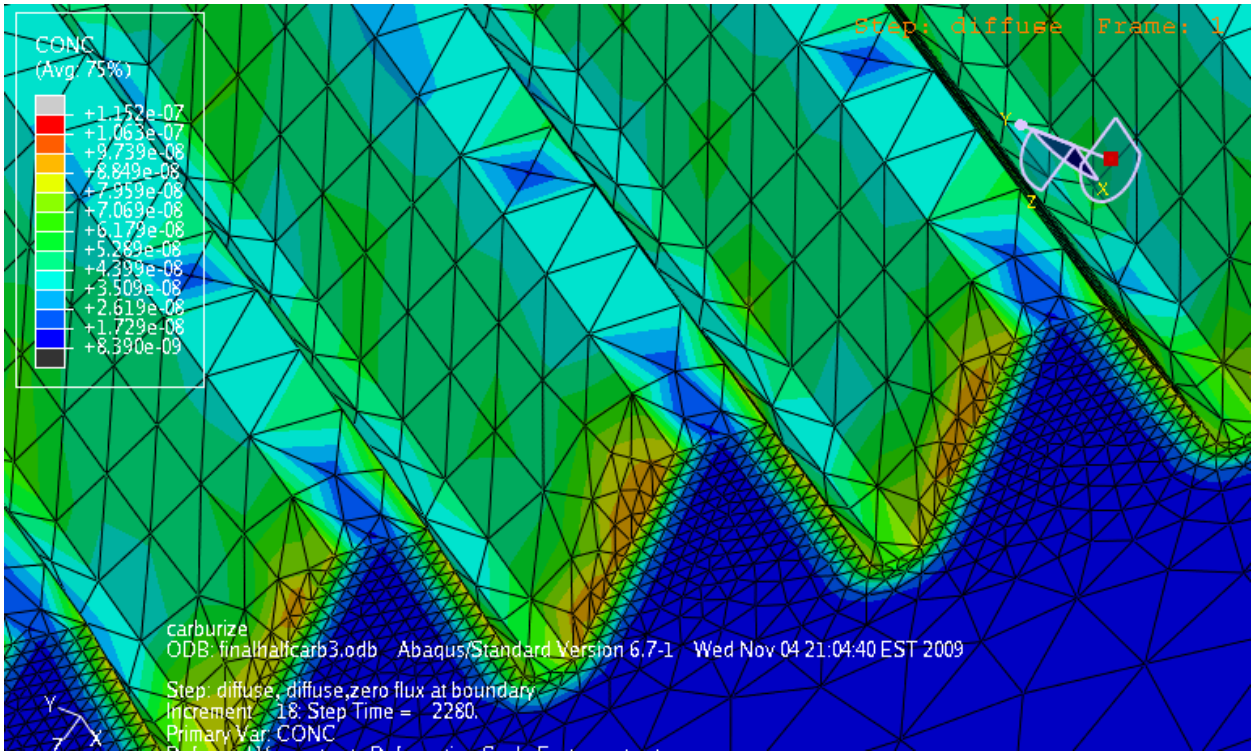

Figure 40: Close up View of Gear After Vacuum Carburizing Simulation

The carburizing on of each individual tooth was rather inaccurate giving values along the flank of .6 weight percent carbon and along the top land (which is not

carburized) of .4 weight percent carbon. Those values should be about .8 weight percent carbon and .1 weight percent carbon respectively. This model is a good representation of the limitations of finite element analysis. A mesh that is too coarse will not provide accurate enough results. However, the number of elements needed to compete a large scale analysis of a problem is often prohibitive in terms of time required and computing power available.

Conclusions and Summary

Distortion in heat treated gears is caused by a number of variables. In computer simulations any variable not accounted for will cause inaccurate results. One of the benefits of computer simulation of heat treating is to identify potential variables such as unsymmetrical cooling or constraining boundary conditions before a new simulation is started. Once the correct combination of variables is found which emulate the physical situation steps can be taken to optimize the heat treating process.

The results of these simulations show that there are a number of different contributing factors to the distortion during this heat treating process. Uneven cooling such as that which would occur during transfer between a furnace and quench press is shown in these simulations to provide more distortion than an even cool down. This could be mitigated by using a larger heating plate to keep the ring gear warm. This could also be mitigated by the integration of a two chamber furnace with a heating unit and quenching unit so that no air transfer is necessary.

The press quench induces stresses into the ring gear by contact forces. This is difficult to quantify due to the friction between the shims and the gear. The shims are free floating and thus each shim most likely exerts a slightly different force on the gear.

This paper has demonstrated the following conclusions:

1. Simulations of heat treating processes can lead to an understanding of the causes of distortion and improved process parameters.
2. Simulations of heat treating processes offer an opportunity to compare methods of heat treating such as by changing only one or two parameters and comparing the difference in properties.
3. The simulations described in this paper demonstrate several causes of distortion, among them nonuniform cooling due to a simulated air transfer was shown to cause about three times greater distortion than uniform cooling.
4. The simulations in this paper compared to the measurements taken demonstrate the importance of fixturing design in heat treating systems as compared to

boundary conditions in computer simulations. The difference between fixing three nodes and four nodes was shown to greatly impact simulated distortion.

5. There is a large amount of distortion that occurs during the carburizing process. Possible causes include relaxation of residual stresses from machining, uneven cooling, uneven carburizing gas flow, or uneven racks.

Future Work

There are several physical experiments that could be included in future work to further investigate the sources of distortion in this particular ring gear. There are also several steps that could be taken to prevent distortion which could be implemented immediately.

To compare simulation data to physical data measuring the residual stresses at every step of the heat treating process would help quantify the changes that occur in the part. It would also be helpful to quantify the details of the racking system and gas flow in the carburizing furnace which may contribute to distortion. It would also be helpful to quantify the friction that occurs between the press quench and the ring gear so that can be compared to a simulation.

1. One of the possible causes of distortion in the carburizing furnace is the use of uneven racks. Using less thermally responsive racks such as carbon fiber racks or other ceramic rack that will not distort due to creep as quickly as Inconel racks will probably help reduce distortion.
2. Monitoring the orientation of the ring gear from the time it goes into the austenitizing furnace until it goes into the quench press. This may demonstrate any lack of symmetry of the quench press. This will also show if there is any effect on the distortion of the gear from furnace to quench press due to the uneven cooling that occurs during transfer.
3. Measure residual stress at each step of the process to compare with the stresses calculated in the model.
4. Determine how to model residual stress from forming and machining in the simulation model before heat treating to study the stress relaxation.
5. Determine how to include the effects of uneven rack support during carburizing in the simulation model.

6. Quantify the carburizing gas flow within the carburizing furnace and simulate with computational fluid dynamics to determine the effect it has on the symmetry of carbon uptake in the ring gear.
7. Incorporate press quench geometry into simulation to model forces in a stress simulation which more closely match those in the press quench than in the free quench simulation.

Bibliography

Abaqus/CAE Version 6.7-1. Dassault Systemes. 2007. http://www.simulia.com/products/products_legal.html

Aronov, D. M. (2008). *What is the IntensiQuench® Process?* Retrieved December 18, 2008, from IQ Technologies Inc.: http://www.intensivequench.com/intensiquench.html

"Cold Treating and Cryogenic Treatment of Steel" from ASM Handbook Volume 4 Heat Treating, p203-206.

Atkinson, R.J., Winkworth, W.J., and Norris, G.M. Behaviour of Skin Fatigue Cracks at the Corners of Windows in a *Comet* I Fuselage. Ministry of Aviation. Aeronautical Research Council: Reports and Memorandum. 1960.

Benitez, S. (2008, November). Sr. Engineer. (I. Janzen, Interviewer)

Chatterjee-Fisher, R. (1978). Internal Oxidation during Carburising and Heat Treatment. *Metall. Trans. A, Vol 9* , 1553-1560.

Callister, Willima D. Jr. Materials Science and Engineering seventh edition. John Wiley and Sons, Inc. 2007.

DANTE: Version 3.3. Deformation Control Technology Inc. 2007.

Davis, J. (2002). *Surface Hardening of Steels: Understanding the Basics.* ASM International.

Dudley, D.W. Handbook of Practical Gear Design. McGraw-Hill Book Company. 1984.

Easterling, D. P. (2004). *Phase Transformations in Metals and Alloys second edition.* Boca Raton, FL: CRC Press.

Freborg A.M., B. Ferguson (2006, July). Engineering Heat Treatment for Stronger Aerospace Gears. *Gear Solutions* , pp. 24-36.

Ferguson, B. Lynn, Freborg, Andrew M., Greg Petrus, and Melvin L. Callabresi Predicting the Heat Treat Response of a Carburized Helical Gear. Gear Technology. November/December 2002. Pg. 20-25.

Ferguson, B.L. *, Z. Li, and A.M. Freborg. Modeling Heat Treatment of Steel Parts. Computational Materials Science 34. 2005. Pg. 274–281.

Frost, Jonathan. (2009, September). Engineer. (I. Janzen, Interviewer)

Haynes, A. (1966). Interrelation of Isothermal and Continuous-Cooling Heat treatments of Low-Alloy Steels and Their Practical Significance. *Heat Treatment of Metals* (Special Report 95), 13-23.

Kozlovskii, I. K. (1967). Internal Oxidation during Case-Hardening of Steels in Endothermic Atmospheres. *Met. Sci. Heat Treat. (USSR) (No. 3)* , 157.

Mgbokwere, C. M. (2000). Numerical Simulation of a Heat-Treated Ring Gear Blank. *Trans. of the ASME Vol. 122* , 305-314.

Moser, Freidrich, Lawrence Jacobs, and Jainmin Qu. Modeling Elastic Wave Propogation in Waveguides with the Finite Element Method. NDT&E International. 8 June 1998.

Parrish, G. (1999). *Carburizing: Microstructure and Properties.* ASM International.

Preston, S. Influence of vanadium on the hardenability of a carburizing steel. In *Carburizing: Processing and Performance* (p. 191). Swedish Institute for Metals Research.

Rakit, A.K. Heat Treatment of Gears: A Practical Guide for Engineers. ASM International. 2000.

Saulnier, J. D. (1989). *Development of High Temperature Gearing for Helicopter Transmissions.* Kaman Aerospace Corp.

Shackelford, J. F. (2004). *Introduction to Materials Science for Engineers.* Prentice Hall.

SolidWorks: Education Edition. Academic Year 2009-2010 / 2009 SP4.0. Copyright 1995-2009.

Stratton, Paul and Graf, Michael. “The Effect of deep cold induced nano-carbides on the wear of case hardened components.” The Linde Group. Elservier Ltd. 2009.

Thomas, W. a. (1989). *V-22 Osprey - The Commitment to an Advanced Carburized Grade Gear Steel.* Bell Helicopter Textron Inc.

World's Sharpest (2008). [Motion Picture].

Z. Li, A. F. (2008). Applications of Modeling to Heat Treat Processes. *Heat Treating Progress* , 28-33.

ZAR 5. Software for Planetary Gearing Design. Hexagon Software. Berlin. 2009.

Appendix 1: Phase Transformation Data

Phase Transformation data:

```
** SPYRO Kinetics Data by Charlie 3/27/2007, new TRIP data
MAR2007        ! model implementation date : use UPPERCASE
SPYRO          ! matnam must be UPPERCASE
  1            ! itprdb=1, require tempering data; otherwise no.
  1            ! iheat=1, require heating data; otherwise no.
** stress effect on martensitic transformation
 6.500000E-02   !stress effect on martensite transformation
** Total number of kinetic data sets with different chemistry
 4
# Chemical composition of data set NO. 1  (0.1%C)
#  G.S.     Carb.    Mn.      Si.      Ni.      Cr.      Mo.      ...
   0.70E+1  0.10E+0  0.83E+0  0.22E+0  0.15E+0  0.80E+0  0.40E-1
** Austenite-->Martensite
4.370000E+02                    !Ms
0.120315203234569                !mobility
9.170411655680299E-002            !alpha
 0.45965163774981                !beta
2.000000E-01                    !epsilon_m
** Austenite-->Ferrite
 466.110                !1 Lower T Bound  T1
 765.000                !2 Upper T Bound  T2
 0.000000000000000      !3 nu
 2.28799205729843       !4 w1
 1.66984169151304       !5 w2
 765.000000000000       !6 tau1
 123.681096540395       !7 tau2
 0.435373658834304      !8 alpha
 -0.163432965           !9 beta-1
** Austenite-->Pearlite
 526.210                !1 Lower T Bound  T1
 753.00                 !2 Lower T Bound  T2
 0.000000000000000      !3 nu
 4.04607798880874       !4 w1
 0.684067807458189      !5 w2
 753.000000000000       !6 tau1
 102.904924592109       !7 tau2
 0.749159065188540      !8 alpha
 0.20088411402973       !9 beta-1
** Austenite-->Bainite
```

```
 400.0                !1  Lower T Bound
 450.0                !2  LB and UB Separation T
 560.0                !3  Upper T Bound
 0.000000000000000        !4  nu
 4.778339685511038E-002    !5  w1
 0.204945701044177        !6  w2
 560.000000000000         !7  tau1
 50.0000000000000         !8  tau2
 0.526200231609644        !9  alpha
 -0.827778478             !10 beta-1
 0.20000000               !11 epsilon
 1.00000000               !12 L1
 1.00000000               !13 L2
** Martensite-->Tempered Martensite
 100.0                !1  T1
 250.0                !2  T2
 0.002                !3  nu
 3.74405165079170         !4  w1
 2.96300858911378         !5  w2
 500.000000000000         !6  tau1
 200.000000000000         !7  tau2
 0.000000000000000        !8  alpha
 0.000000000000000        !9  beta-1
** Ferrite-->Austenite
 730.0                !1
 1400.0               !2
 3.32436450283705         !3
 1.05740096448232         !4
 15.9627678089941         !5
 1410.53454029999         !6
 378.873815742864         !7
 0.00000000000000         !8
 0.00000000000000         !9
** Pearlite-->Austenite
 730.0                !1
 1400.0               !2
 3.32436450283705         !3
 1.05740096448232         !4
 15.9627678089941         !5
 1410.53454029999         !6
 378.873815742864         !7
 0.00000000000000         !8
 0.00000000000000         !9
** Upper Bainite-->Austenite
 730.0                !1
 1400.0               !2
```

```
 3.32436450283705          !3
 1.05740096448232          !4
 15.9627678089941          !5
 1410.53454029999          !6
 378.873815742864          !7
 0.00000000000000          !8
 0.00000000000000          !9
** Lower Bainite-->Austenite
 730.0                     !1
 1400.0                    !2
 3.32436450283705          !3
 1.05740096448232          !4
 15.9627678089941          !5
 1410.53454029999          !6
 378.873815742864          !7
 0.00000000000000          !8
 0.00000000000000          !9
** Martensite-->Austenite
 730.0                     !1
 1400.0                    !2
 3.32436450283705          !3
 1.05740096448232          !4
 15.9627678089941          !5
 1410.53454029999          !6
 378.873815742864          !7
 0.00000000000000          !8
 0.00000000000000          !9
** Tempered Martensite-->Austenite
 730.0                     !1
 1400.0                    !2
 3.32436450283705          !3
 1.05740096448232          !4
 15.9627678089941          !5
 1410.53454029999          !6
 378.873815742864          !7
 0.00000000000000          !8
 0.00000000000000          !9
# Chemical composition of data set NO. 2  (0.3%)
#  G.S.    Carb.   Mn.     Si.     Ni.     Cr.     Mo.     ...
   0.70E+1  0.30E+0  0.83E+0  0.22E+0  0.15E+0  0.80E+0  0.40E-1

…

# Chemical composition of data set NO. 3  (0.8%C)
#  G.S.    Carb.   Mn.     Si.     Ni.     Cr.     Mo.     ...
   0.70E+1  0.80E+0  0.83E+0  0.22E+0  0.15E+0  0.80E+0  0.40E-1
```

```
** Austenite-->Martensite
 1.350000E+02                  !Ms     0.850000E+02
 2.702764760427735E-002          !mobility
 0.323846251334467               !alpha
  0.25311900028855               !beta
 2.000000E-01                   !epsilon_m
** Austenite-->Ferrite
 0.548580E+03            !1 Lower T Bound  T1
 0.765000E+03            !2 Upper T Bound  T2
 0.000000000000000        !3 nu
 2.36710940295634         !4 w1
 1.68351590999636         !5 w2
 765.000000000000         !6 tau1
 127.500832667570         !7 tau2
 0.513957742221075        !8 alpha
 0.15455779300            !9 beta-1
** Austenite-->Pearlite
 0.529440E+03             !1 Lower T Bound  T1
 0.753000E+03             !2 Lower T Bound  T2
 0.000000000000000        !3 nu
 4.38598912866095         !4 w1
 0.692781433211479        !5 w2
 753.000000000000         !6 tau1
 116.520899031273         !7 tau2
 0.716838655802562        !8 alpha
 0.19270897580435         !9 beta-1
** Austenite-->Bainite
 200.0                  !1  Lower T Bound
 450.0                  !2  LB and UB Separation T
 560.0                  !3  Upper T Bound
 0.000000000000000         !4  nu
 1.60447203997923          !5  w1
 8.746126066099634E-002    !6  w2
 560.000000000000          !7  tau1
 79.2906904544637          !8  tau2
 0.783026410692588         !9  alpha
 0.694609156              !10 beta-1
 0.2                   !11 epsilon
 1.00000000000000          !12 L1
 1.00000000000000          !13 L2
** Martensite-->Tempered Martensite
 100.0                  !31  T1
 250.0                  !32  T2
 0.002                  !33  nu
 3.74405165079170         !34  w1
 2.96300858911378         !35  w2
```

```
 500.000000000000          !36  tau1
 200.000000000000          !37  tau2
 0.000000000000000         !38  alpha
 0.000000000000000         !39  beta-1
** Ferrite-->Austenite
 730.0                     !1
 1400.0                    !2
 3.32436450283705          !3
 1.05740096448232          !4
 15.9627678089941          !5
 1410.53454029999          !6
 378.873815742864          !7
 0.00000000000000          !8
 0.00000000000000          !9
** Pearlite-->Austenite
 730.0                     !1
 1400.0                    !2
 3.32436450283705          !3
 1.05740096448232          !4
 15.9627678089941          !5
 1410.53454029999          !6
 378.873815742864          !7
 0.00000000000000          !8
 0.00000000000000          !9
** Upper Bainite-->Austenite
 730.0                     !1
 1400.0                    !2
 3.32436450283705          !3
 1.05740096448232          !4
 15.9627678089941          !5
 1410.53454029999          !6
 378.873815742864          !7
 0.00000000000000          !8
 0.00000000000000          !9
** Lower Bainite-->Austenite
 730.0                     !1
 1400.0                    !2
 3.32436450283705          !3
 1.05740096448232          !4
 15.9627678089941          !5
 1410.53454029999          !6
 378.873815742864          !7
 0.00000000000000          !8
 0.00000000000000          !9
** Martensite-->Austenite
 730.0                     !1
```

```
 1400.0                !2
 3.32436450283705      !3
 1.05740096448232      !4
 15.9627678089941      !5
 1410.53454029999      !6
 378.873815742864      !7
 0.00000000000000      !8
 0.00000000000000      !9
** Tempered Martensite-->Austenite
 730.0                 !1
 1400.0                !2
 3.32436450283705      !3
 1.05740096448232      !4
 15.9627678089941      !5
 1410.53454029999      !6
 378.873815742864      !7
 0.00000000000000      !8
 0.00000000000000      !9
****************** END OF FILE ******************
```

Pyrowear 53 Phase property data:

```
**------------------------------------------------------      line 1
**    DDDDDD          A           NN    N  TTTTTTT  EEEEEEE        line 2
**    D       D      A  A         N N   N     T     E              line 3
**    D       D     A    A        N  N  N     T     EEEEEEE        line 4
**    D       D    AAAAAAA       N   N N     T     E              line 5
**    DDDDDD   A          A      N    NN     T     EEEEEEE        line 6
**                                                    line 7
**              Version 3_3                           line 8
**------------------------------------------------------      line 9
**    Deformation Control Technology, Inc.                  line 10
**         All rights reserved                              line 11
**                                                         line 12
**    Latest modification: 01/25/2005                       line 13
**    Modified by: DCT                                      line 14
**    IMPORTANT: The file format is fixed                   line 15
** ----------------------------------------------------     line 16
**    Mechanical Data starts from here                      line 17
MAR2007      ! DATA version control  UPPERCASE              line 18
SPYRO        ! matnam must be UPPERCASE                     line 19
** ----------------------------------------------------     line 20
** 27 plastic parameters for each phase                     line 21
** Aust.   Ferr.     Pear.     U_Bain.   L_Bain.   Mart.    T_Mart.   line 22
1.9480E+01, 8.9825E+00, 8.9825E+00, 6.1036E+01, 6.1036E+01, 6.4000E+01,
6.1036E+01  line 23 V
```

6.0299E+02, 1.9072E+03, 1.9072E+03, 8.2421E+02, 8.2421E+02, 5.1370E+02, 8.2421E+02 line 24 V
3.4589E+01, 2.5848E-03, 2.5848E-03, 2.4035E+01, 2.4035E+01, 1.0520E+03, 2.4035E+01 line 25 Y
3.4751E+03, 1.3108E+04, 1.3108E+04, 4.3888E+03, 4.3888E+03, 1.4800E+01, 4.3888E+03 line 26 Y
9.8205E-01, 0.0000E+00, 0.0000E+00, 1.0524E-05, 1.0524E-05, 9.1480E-08, 1.0524E-05 line 27 f
2.5940E+03, 8.7441E-03, 8.7441E-03, 1.5024E+03, 1.5024E+03, 6.2330E+01, 1.5024E+03 line 28 f
4.2004E+04, 3.8417E+00, 3.8417E+00, 3.1270E+00, 3.1270E+00, 1.5254E-01, 3.1270E+00 line 29 rd1
9.5318E+03, 2.2139E+01, 2.2139E+01, 1.4009E+02, 1.4009E+02, 3.6607E+02, 1.4009E+02 line 30 rd1
2.2354E+03, 2.0341E+05, 2.0341E+05, 1.6270E+05, 1.6270E+05, 7.7360E+04, 1.6270E+05 line 31 h1
1.9844E-01, 9.0201E+01, 9.0201E+01, 1.7081E+02, 1.7081E+02, 2.6500E+00, 1.7081E+02 line 32 h1
1.1000E-04, 4.3240E+05, 4.3240E+05, 4.4897E+01, 4.4897E+01, 1.0000E+01, 4.4897E+01 line 33 rs1
5.8832E+02, 1.0325E+04, 1.0325E+04, 8.8757E+07, 8.8757E+07, 5.3336E+03, 8.8757E+07 line 34 rs1
2.1503E+04, 1.4973E+02, 1.4973E+02, 7.4089E+02, 7.4089E+02, 6.4728E-06, 7.4089E+02 line 35 Rd2
1.2944E+04, 6.7300E+03, 6.7300E+03, 8.4830E+05, 8.4830E+05, 8.3886E+02, 8.4830E+05 line 36 Rd2
1.6173E+03, 2.3086E+03, 2.3086E+03, 3.6682E+03, 3.6682E+03, 3.0740E+03, 3.6682E+03 line 37 H2
4.0556E-01, 0.0000E+00, 0.0000E+00, 4.8027E-01, 4.8027E-01,-8.2460E-01, 4.8027E-01 line 38 H2
3.3010E+01, 7.6012E+01, 7.6012E+01, 7.7570E+04, 7.7570E+04, 1.7566E+00, 7.7570E+04 line 39 Rs2
9.2921E+03, 7.9349E+06, 7.9349E+06, 3.4162E+04, 3.4162E+04, 3.9541E+04, 3.4162E+04 line 40 Rs2
2.1240E-03, 5.8469E-03, 5.8469E-03, 1.0085E-02, 1.0085E-02, 1.1600E-02, 1.0085E-02 line 41 Y
7.7193E+02, 8.9511E+02, 8.9511E+02, 7.6417E+02, 7.6417E+02, 5.7940E+02, 7.6417E+02 line 42 Y
1.1767E-01, 5.6585E-06, 5.6585E-06, 4.7763E-02, 4.7763E-02, 9.3420E-02, 4.7763E-02 line 43 Y
3.6844E+06, 1.2000E+08, 1.2000E+08, 2.6033E+05, 2.6033E+05, 4.1180E+07, 2.6033E+05 line 44 h1
2.9727E+03, 1.0678E+05, 1.0678E+05, 0.0000E+00, 0.0000E+00, 4.2059E+04, 0.0000E+00 line 45 h1
1.6964E+06,-2.2074E+05,-2.2074E+05, 4.7209E+05, 4.7209E+05, 9.4670E+07, 4.7209E+05 line 46 H2

```
1.7718E+03,-7.6867E+02,-7.6867E+02, 0.0000E+00, 0.0000E+00,-2.4821E+07,
0.0000E+00  line 47 H2
5.0301E+02, 4.5353E-02, 4.5353E-02, 4.3378E+03, 4.3378E+03, 3.0000E+03,
4.3378E+03  line 48 Y
1.6001E+02, 9.8003E+01, 9.8003E+01, 4.7838E+05, 4.7838E+05, 4.0375E+03,
4.7838E+05  line 49 Y
** ----------------------------------------------------      line 50
**  Young's Modulus:  E0 + E1*T + E2*T^2 + E3*T^3                line 51
**     E0          E1          E2          E3                  line 52
  2.0650E+05, -3.8000E+01, -9.1500E-02, -2.7500E-06            line 53
**  Poisson's Ratio:  nu0 + nu1*T                               line 54
**   nu0         nu1                                           line 55
  2.82E-1,   3.0000E-05                                        line 56
** ----------------------------------------------------        line 57
**  Trip parameters:    1.382599528,  2.08E-03,   186.165048,  2.141388508        line 58
**  paramA1  paramA2    param_b   param_m (old parameter, new model by charlie)
line 59
   1.10,  1.28E-03,   186.165048,  2.141388508                 line 60
** ----------------------------------------------------        line 61
**  Latent Heat of the individual transformations               line 62
** A-->F  A-->P  A-->UB  A-->LB  A-->M  M-->TM                  line 63
  0.59,  0.59,  0.59,   0.59,   0.64,  0.00                    line 64
** ----------------------------------------------------        line 65
**  Specific Heat of all the 7 phases  (2nd term is linear temperature dependent)   line 66
**  Austenite                                                   line 67
  365.0,  0.2938                                               line 68
**  Ferrite                                                     line 69
  450.0,  0.3875                                               line 70
**  Pearlite                                                    line 71
  450.0,  0.3875                                               line 72
**  Upper Bainite                                               line 73
  450.0,  0.3875                                               line 74
**  Lower Bainite                                               line 75
  450.0,  0.3875                                               line 76
**  Martensite                                                  line 77
  450.0,  0.3875                                               line 78
**  Tempered Martensite                                         line 79
  450.0,  0.3875                                               line 80
** ----------------------------------------------------        line 81
**  Thermal Conductivity (2nd term is linear temperature dependent)        line 82
**  Austenite                                                   line 83
  0.016,  1.3e-5                                               line 84
**  Ferrite                                                     line 85
  0.059,  -2.25e-5                                             line 86
**  Pearlite                                                    line 87
  0.043,  -1.9e-5                                              line 88
```

```
**  Upper Bainite                                                    line 89
 0.040,  -2.3e-5                                                   line 90
**  Lower Bainite                                                   line 91
 0.040,  -2.3e-5                                                   line 92
**  Martensite                                                     line 93
 0.025,  3.0e-6                                                    line 94
**  Tempered Martensite                                              line 95
 0.025,  3.0e-6                                                    line 96
** ------------------------------------------------------          line 97
**  CTE and Transformation Strain                                    line 98
**--Austenite:  a1+a2*C+a3*T                                       line 99
**    a1       a2        a3                                       line 100
 -0.0229, 0.01237, 2.267e-05                                       line 101
**--Ferrite:   m1+m2*C+m3*T+m4*C*T+m5*T^2+m6*C*T^2                 (A<-->F)
line 102
**    m1       m2        m3        m4        m5        m6          line 103
 -0.012572, 0.0090506, 1.146e-5, 2.2117656e-6, 3.55e-9, -4.97342e-10      line 104
**--Pearlite:  m1+m2*C+m3*T+m4*C*T+m5*T^2+m6*C*T^2                 (A<-->P)
line 105
**    m1       m2        m3        m4        m5        m6          line 106
 -0.012572, 0.0090506, 1.146e-5, 2.2117656e-6, 3.55e-9, -4.97342e-10      line 107
**--Upper Bainite:  m1+m2*C+m3*T+m4*C*T+m5*T^2+m6*C*T^2            (A<--
>UB)    line 108
**    m1       m2        m3        m4        m5        m6          line 109
 -0.012572, 0.0090506, 1.146e-5, 2.2117656e-6, 3.55e-9, -4.97342e-10      line 110
**--Lower Bainite:  m1+m2*C+m3*T+m4*C*T+m5*T^2+m6*C*T^2            (A<--
>LB)    line 111
**    m1       m2        m3        m4        m5        m6          line 112
 -0.012572, 0.0090506, 1.146e-5, 2.2117656e-6, 3.55e-9, -4.97342e-10      line 113
**--Martensite:  m1+m2*C+m3*C^2+m4*T+m5*C*T+m6*T^2+m7*C*T^2+m8*T^3
(A<-->M)     line 114
**    m1        m2        m3      m4      m5      m6      m7      m8          line 115
 -0.009882, -0.0003061, 0.01430, 1.3e-5, -4.3e-6, 2.9e-9, 1.4e-9, 1.091e-12       line 116
**--Tempered Mart.:
m1+m2*C+m3*C^2+m4*T+m5*C*T+m6*T^2+m7*C*T^2+m8*T^3  (M<-->TM)   line
117
**    m1       m2        m3        m4        m5        m6          line 118
 -0.009882, -0.0003061, 0.01430, 1.3e-5, -4.3e-6, 2.9e-9, 1.4e-9, 1.091e-12       line 119
** ------------------------------------------------------          line 120
**  Equilibrium Heat up (Austenization) kinetics:  3 kinetics parameters          line 121
**  explanations                                                   line 122
 760.0, 901.767, 203.0                                             line 123
** ------------------------------------------------------          line 124
**  Hardness Data:  Updated for Feb UMAT on 9/12/2006                line 125
**  ncl = number of carbon levels                                  line 126
 4                                                                 line 127
```

```
** Individual Phase Hardness(HRC) at Room Temperature for Each Carbon Levels
line 128
**  Carbon level vpc(i): 0.2% ----------------------------------  line 129
 0.2                                                          line 130
** HRC-AUST--HRC-FERR--HRC-PEAR--HRC-MART                                line
131
  20.0      20.0     25.0     46.0                              line 132
** Bs--and--Ms(C)                                               line 133
  600.0    400.0                                             line 134
**  Carbon level vpc(i): 0.4% ----------------------------------  line 135
 0.4                                                          line 136

** HRC-AUST--HRC-FERR--HRC-PEAR--HRC-MART                                line
137
  22.0      22.0     27.0     48.0                              line 138
** Bs--and--Ms(C)                                               line 139
  600.0    330.0                                             line 140
**  Carbon level vpc(i): 0.6% ----------------------------------
 0.6
** HRC-AUST--HRC-FERR--HRC-PEAR--HRC-MART
  25.0      25.0     30.0     55.0
** Bs--and--Ms(C)
  600.0    270.0
**  Carbon level vpc(i): 0.8% ----------------------------------
 0.8
** HRC-AUST--HRC-FERR--HRC-PEAR--HRC-MART
  28.0      28.0     35.0     60.0
** Bs--and--Ms(C)
  600.0    200.0
* --------------------------- END OF FILE -------------------------
```

Appendix 2: Carburizing Simulation File

Quarter tooth 3D carburizing input file, carb3d46.inp:

```
*Heading
** Job name: carb3d46 Model name: carb3d43
*Preprint, echo=NO, model=NO, history=NO, contact=NO
**
** PARTS
**
*Part, name=PART-1
*Node
      1,   -4.6511035,   258.062195, -0.719272971
      2,  -3.75551462,   258.062531, -0.719274044
      3,  -4.65176582,   258.171661, -0.750257552
      4,  -3.75619125,   258.171112,  -0.75068891
      5,   -4.6511035,   258.062317, -0.675595582
      6,  -3.75551462,   258.062622, -0.675596595
      7,  -4.65175343,   258.171814, -0.704724967
      8,  -3.75621176,   258.171234, -0.705127954
      9,   -4.6511035,   258.062469, -0.610079527
     10,  -3.75551462,   258.062775, -0.610080481
     11,  -4.65173531,   258.172089, -0.636419713
     12,  -3.75624251,   258.171417, -0.636780679
     13,   -4.6511035,   258.062683,  -0.52292192
     14,  -3.75551462,   258.062988, -0.522922814
     15,  -4.65171146,   258.172424, -0.545539796

…

  54364,   26.6544209,   275.462677, -0.398691267
  54365,   26.6543961,   271.342804, 2.48397537e-05
  54366,   26.6543961,   271.857819, 2.48869001e-05
  54367,   26.6543961,   272.372864, 2.49340483e-05
  54368,   26.6543961,   272.887878, 2.49811947e-05
  54369,   26.6543961,   273.402893, 2.5028341e-05
  54370,   26.6543961,   273.917908, 2.50754892e-05
  54371,   26.6543961,   274.432953, 2.51226356e-05
  54372,   26.6543961,   274.947968, 2.51697838e-05
  54373,   26.6543961,   275.462982, 2.52169302e-05
*Element, type=DC3D8
    1,     1,     2,     4,     3,     5,     6,     8,     7
    2,     5,     6,     8,     7,     9,    10,    12,    11
```

```
   3,    9,   10,   12,   11,   13,   14,   16,   15
   4,   13,   14,   16,   15,   17,   18,   20,   19
   5,   17,   18,   20,   19,   21,   22,   24,   23
   6,   21,   22,   24,   23,   25,   26,   28,   27

…

48344, 54359, 54278, 54287, 54368, 54360, 54279, 54288, 54369
48345, 54360, 54279, 54288, 54369, 54361, 54280, 54289, 54370
48346, 54361, 54280, 54289, 54370, 54362, 54281, 54290, 54371
48347, 54362, 54281, 54290, 54371, 54363, 54282, 54291, 54372
48348, 54363, 54282, 54291, 54372, 54364, 54283, 54292, 54373
*Elset, elset=_PICKEDSET2, internal, generate
    1,  48348,      1
** Section: Section-1-_PICKEDSET2
*Solid Section, elset=_PICKEDSET2, material=SPYRO
1.,
*End Part
**
**
** ASSEMBLY
**
*Assembly, name=Assembly
**
*Instance, name=PART-1-1, part=PART-1
*End Instance
**
*Nset, nset=ALL, instance=PART-1-1, generate
    1,  54373,      1
*Nset, nset=SOLID_NSET, instance=PART-1-1, generate
    1,  54373,      1
*Nset, nset=MONITOR, instance=PART-1-1
 10767,
*Nset, nset=_PICKEDSET7, internal, instance=PART-1-1
 13918,
*Nset, nset=ALLNODES, instance=PART-1-1, generate
    1,  54373,      1
*Nset, nset=_PICKEDSET10, internal, instance=PART-1-1, generate
    1,  54373,      1
*Elset, elset=__PICKEDSURF9_S2, internal, instance=PART-1-1
  3663,  3672,  3681,  3690,  3699,  3708,  3717,  3726,  3735,  3744,  3753,  3762,  3771,
3780,  3789,  3798
  3807,  3816,  3825,  3834,  3843,  3852,  3861,  3870,  3879,  3888,  3897,  3906,  3915,
3924,  3933,  3942
  3951,  3960,  3969,  3978,  3987,  3996,  4005,  4014,  4023,  4032,  4041,  4050,  4059,
4068,  4077,  4086
```

…

38907, 38916, 38925, 38934, 38943, 38952, 38961, 38970, 38979, 38988, 38997, 39006, 39015, 39024, 39033, 39042
39051, 39060, 39069, 39078, 39087, 39096
*Surface, type=ELEMENT, name=_PICKEDSURF9, internal
__PICKEDSURF9_S2_1, S2
*Elset, elset=_DISTFLUX-1_S2, internal, instance=PART-1-1
3663, 3672, 3681, 3690, 3699, 3708, 3717, 3726, 3735, 3744, 3753, 3762, 3771, 3780, 3789, 3798
3807, 3816, 3825, 3834, 3843, 3852, 3861, 3870, 3879, 3888, 3897, 3906, 3915, 3924, 3933, 3942
3951, 3960, 3969, 3978, 3987, 3996, 4005, 4014, 4023, 4032, 4041, 4050, 4059, 4068, 4077, 4086

…

38763, 38772, 38781, 38790, 38799, 38808, 38817, 38826, 38835, 38844, 38853, 38862, 38871, 38880, 38889, 38898
38907, 38916, 38925, 38934, 38943, 38952, 38961, 38970, 38979, 38988, 38997, 39006, 39015, 39024, 39033, 39042
39051, 39060, 39069, 39078, 39087, 39096
*Surface, type=ELEMENT, name=DISTFLUX-1
_DISTFLUX-1_S2, S2
*Elset, elset=_DISTFLUX-2_S2, internal, instance=PART-1-1
3663, 3672, 3681, 3690, 3699, 3708, 3717, 3726, 3735, 3744, 3753, 3762, 3771, 3780, 3789, 3798
3807, 3816, 3825, 3834, 3843, 3852, 3861, 3870, 3879, 3888, 3897, 3906, 3915, 3924, 3933, 3942
3951, 3960, 3969, 3978, 3987, 3996, 4005, 4014, 4023, 4032, 4041, 4050, 4059, 4068, 4077, 4086

…

38763, 38772, 38781, 38790, 38799, 38808, 38817, 38826, 38835, 38844, 38853, 38862, 38871, 38880, 38889, 38898
38907, 38916, 38925, 38934, 38943, 38952, 38961, 38970, 38979, 38988, 38997, 39006, 39015, 39024, 39033, 39042
39051, 39060, 39069, 39078, 39087, 39096
*Surface, type=ELEMENT, name=DISTFLUX-2
_DISTFLUX-2_S2, S2
*Elset, elset=__PickedSurf14_S2, internal, instance=PART-1-1
3663, 3672, 3681, 3690, 3699, 3708, 3717, 3726, 3735, 3744, 3753, 3762, 3771, 3780, 3789, 3798

```
 3807, 3816, 3825, 3834, 3843, 3852, 3861, 3870, 3879, 3888, 3897, 3906, 3915,
3924, 3933, 3942
 3951, 3960, 3969, 3978, 3987, 3996, 4005, 4014, 4023, 4032, 4041, 4050, 4059,
4068, 4077, 4086

…

 46413, 46422, 46431, 46440, 46449, 46458, 46467, 46476, 46485, 46494, 46503, 46512,
46521, 46530, 46539, 46548
 46557, 46566, 46575, 46584, 46593, 46602, 46611, 46620, 46629, 46638, 46647, 46656,
46665, 46674, 46683, 46692
 46701, 46710, 46719, 46728
*Surface, type=ELEMENT, name=_PickedSurf14, internal
__PickedSurf14_S2, S2
*End Assembly
**
** MATERIALS
**
*Material, name=SPYRO
*Density
 7.91e-06,
*Depvar
    100,
*Diffusivity
 1.52398e-06,  0.002,   788.
 1.64519e-06, 0.0025,   788.
 1.77604e-06,  0.003,   788.
  1.9173e-06, 0.0035,   788.
 2.06979e-06,  0.004,   788.

…

0.000107427,  0.007,  1100.
 0.000111919, 0.0075,  1100.
 0.000116598,  0.008,  1100.
 0.000121474, 0.0085,  1100.
*Solubility
1.,
**
** PREDEFINED FIELDS
**
** Name: Field-1   Type: Temperature
*Initial Conditions, type=TEMPERATURE
_PICKEDSET10, 1038.
*Initial Conditions, type=CONCENTRATION
_PickedSet10, 9.71e-09
```

```
** ----------------------------------------------------------------
**
** STEP: carburizing
**
*Step, name=carburizing, inc=2000
carburize 32 minutes in vaccum
*Mass Diffusion, end=PERIOD, dcmax=0.002
1., 1920., 0.001, 10.,
**
** LOADS
**
** Name: DISTFLUX-1   Type: Surface concentration flux
*Dflux
__PickedSurf14_S2, S2, 2.5e-11
**
** OUTPUT REQUESTS
**
*Restart, write, frequency=100
*Monitor, dof=11, node=_PICKEDSET7, frequency=100
**
** FIELD OUTPUT: F-Output-1
**
*Output, field, variable=PRESELECT
**
** FIELD OUTPUT: F-Output-3
**
*Output, field, frequency=100
*Element Output, directions=YES
CONC,
**
** FIELD OUTPUT: F-Output-2
**
*Node Output
NNC,
**
** HISTORY OUTPUT: H-Output-1
**
*Output, history, variable=PRESELECT
**
** HISTORY OUTPUT: H-Output-2
**
*Output, history, frequency=100
*Element Output
SOL,
*End Step
** ----------------------------------------------------------------
```

```
**
** STEP: diffuse
**
*Step, name=diffuse, inc=2000
diffuse 38 minutes in vaccum
*Mass Diffusion, end=PERIOD, dcmax=0.002
1., 2280., 0.001, 10.,
**
** LOADS
**
** Name: DISTFLUX-2   Type: Surface concentration flux
*Dflux
__PickedSurf14_S2, S2, 0
**
** OUTPUT REQUESTS
**
*Restart, write, frequency=100
*Monitor, dof=11, node=_PICKEDSET7, frequency=100
**
** FIELD OUTPUT: F-Output-4
**
*Output, field, variable=PRESELECT
**
** FIELD OUTPUT: F-Output-6
**
*Output, field, frequency=100
*Element Output, directions=YES
CONC,
**
** FIELD OUTPUT: F-Output-5
**
*Node Output
NNC,
**
** HISTORY OUTPUT: H-Output-3
**
*Output, history, variable=PRESELECT
**
** HISTORY OUTPUT: H-Output-4
**
*Output, history, frequency=100
*Element Output
SOL,
*End Step
```

Appendix 3: Heat Transfer File

```
*Heading
** Job name: quench3d47 Model name: carb3d43
*Preprint, echo=NO, model=NO, history=NO, contact=NO
**
** PARTS
**
*Part, name=PART-1
*Node
      1,   -4.6511035,   258.062195, -0.719272971
      2,  -3.75551462,   258.062531, -0.719274044
      3,  -4.65176582,   258.171661, -0.750257552

…

  54371,   26.6543961,   274.432953, 2.51226356e-05
  54372,   26.6543961,   274.947968, 2.51697838e-05
  54373,   26.6543961,   275.462982, 2.52169302e-05
*Element, type=DC3D8
    1,     1,     2,     4,     3,     5,     6,     8,     7
    2,     5,     6,     8,     7,     9,    10,    12,    11
    3,     9,    10,    12,    11,    13,    14,    16,    15
    4,    13,    14,    16,    15,    17,    18,    20,    19
    5,    17,    18,    20,    19,    21,    22,    24,    23

…

48345, 54360, 54279, 54288, 54369, 54361, 54280, 54289, 54370
48346, 54361, 54280, 54289, 54370, 54362, 54281, 54290, 54371
48347, 54362, 54281, 54290, 54371, 54363, 54282, 54291, 54372
48348, 54363, 54282, 54291, 54372, 54364, 54283, 54292, 54373
*Elset, elset=_PICKEDSET2, internal, generate
     1,  48348,      1
** Section: Section-1-_PICKEDSET2
*Solid Section, elset=_PICKEDSET2, material=SPYRO
1.,
*End Part
**
**
** ASSEMBLY
**
*Assembly, name=Assembly
```

```
**
*Instance, name=PART-1-1, part=PART-1
*End Instance
**
*Nset, nset=ALL, instance=PART-1-1, generate
    1,  54373,      1
*Nset, nset=SOLID_NSET, instance=PART-1-1, generate
    1,  54373,      1
*Nset, nset=MONITOR, instance=PART-1-1
 10767,
*Nset, nset=_PICKEDSET7, internal, instance=PART-1-1
 13918,
*Nset, nset=ALLNODES, instance=PART-1-1, generate
    1,  54373,      1
*Nset, nset=_PICKEDSET10, internal, instance=PART-1-1, generate
    1,  54373,      1
*Elset, elset=__PICKEDSURF9_S2, internal, instance=PART-1-1
  3663,  3672,  3681,  3690,  3699,  3708,  3717,  3726,  3735,  3744,  3753,  3762,  3771,
3780,  3789,  3798
  3807,  3816,  3825,  3834,  3843,  3852,  3861,  3870,  3879,  3888,  3897,  3906,  3915,
3924,  3933,  3942
  3951,  3960,  3969,  3978,  3987,  3996,  4005,  4014,  4023,  4032,  4041,  4050,  4059,
4068,  4077,  4086

…

 38763, 38772, 38781, 38790, 38799, 38808, 38817, 38826, 38835, 38844, 38853, 38862,
38871, 38880, 38889, 38898
 38907, 38916, 38925, 38934, 38943, 38952, 38961, 38970, 38979, 38988, 38997, 39006,
39015, 39024, 39033, 39042
 39051, 39060, 39069, 39078, 39087, 39096
*Nset, nset=_PickedSet20, internal, instance=PART-1-1
 11511,
*Elset, elset=__PICKEDSURF9_S2_1, internal, instance=PART-1-1
  3663,  3672,  3681,  3690,  3699,  3708,  3717,  3726,  3735,  3744,  3753,  3762,  3771,
3780,  3789,  3798
  3807,  3816,  3825,  3834,  3843,  3852,  3861,  3870,  3879,  3888,  3897,  3906,  3915,
3924,  3933,  3942

…

 38907, 38916, 38925, 38934, 38943, 38952, 38961, 38970, 38979, 38988, 38997, 39006,
39015, 39024, 39033, 39042
 39051, 39060, 39069, 39078, 39087, 39096
*Surface, type=ELEMENT, name=_PICKEDSURF9, internal
__PICKEDSURF9_S2_1, S2
```

*Elset, elset=_DISTFLUX-1_S2, internal, instance=PART-1-1
3663, 3672, 3681, 3690, 3699, 3708, 3717, 3726, 3735, 3744, 3753, 3762, 3771, 3780, 3789, 3798
3807, 3816, 3825, 3834, 3843, 3852, 3861, 3870, 3879, 3888, 3897, 3906, 3915, 3924, 3933, 3942

…

38907, 38916, 38925, 38934, 38943, 38952, 38961, 38970, 38979, 38988, 38997, 39006, 39015, 39024, 39033, 39042
39051, 39060, 39069, 39078, 39087, 39096
*Surface, type=ELEMENT, name=DISTFLUX-1
_DISTFLUX-1_S2, S2
*Elset, elset=_DISTFLUX-2_S2, internal, instance=PART-1-1
3663, 3672, 3681, 3690, 3699, 3708, 3717, 3726, 3735, 3744, 3753, 3762, 3771, 3780, 3789, 3798
3807, 3816, 3825, 3834, 3843, 3852, 3861, 3870, 3879, 3888, 3897, 3906, 3915, 3924, 3933, 3942

…

38907, 38916, 38925, 38934, 38943, 38952, 38961, 38970, 38979, 38988, 38997, 39006, 39015, 39024, 39033, 39042
39051, 39060, 39069, 39078, 39087, 39096
*Surface, type=ELEMENT, name=DISTFLUX-2
_DISTFLUX-2_S2, S2
*Elset, elset=__PickedSurf15_S2, internal, instance=PART-1-1
3663, 3672, 3681, 3690, 3699, 3708, 3717, 3726, 3735, 3744, 3753, 3762, 3771, 3780, 3789, 3798
3807, 3816, 3825, 3834, 3843, 3852, 3861, 3870, 3879, 3888, 3897, 3906, 3915, 3924, 3933, 3942

…

48195, 48204, 48213, 48222, 48231, 48240, 48249, 48258, 48267, 48276, 48285, 48294, 48303, 48312, 48321, 48330
48339, 48348
*Elset, elset=__PickedSurf15_S3, internal, instance=PART-1-1
1, 2, 3, 4, 5, 6, 7, 8, 9, 262, 263, 264, 265, 266, 267, 268
269, 270, 523, 524, 525, 526, 527, 528, 529, 530, 531, 784, 785, 786, 787, 788
789, 790, 791, 792, 1045, 1046, 1047, 1048, 1049, 1050, 1051, 1052, 1053, 1306, 1307, 1308

…

45288, 45541, 45542, 45543, 45544, 45545, 45546, 45547, 45548, 45549, 45802, 45803, 45804, 45805, 45806, 45807
45808, 45809, 45810, 46063, 46064, 46065, 46066, 46067, 46068, 46069, 46070, 46071
*Elset, elset=__PickedSurf15_S4, internal, instance=PART-1-1
21808, 21809, 21810, 21811, 21812, 21813, 21814, 21815, 21816, 21817, 21818, 21819, 21820, 21821, 21822, 21823
21824, 21825, 21826, 21827, 21828, 21829, 21830, 21831, 21832, 21833, 21834, 21835, 21836, 21837, 21838, 21839

…

47513, 47514, 47515, 47516, 47517, 47518, 47519, 47520, 47521, 47522, 47523, 47524, 47525, 47526, 47527, 47528
47529, 47530, 47531, 47532, 47533, 47534, 47535, 47536, 47537, 47538
*Elset, elset=__PickedSurf15_S6, internal, instance=PART-1-1
18730, 18731, 18732, 18733, 18734, 18735, 18736, 18737, 18738, 18739, 18740, 18741, 18742, 18743, 18744, 18745
18746, 18747, 18748, 18749, 18750, 18751, 18752, 18753, 18754, 18755, 18756, 18757, 18758, 18759, 18760, 18761

…

48324, 48325, 48326, 48327, 48328, 48329, 48330, 48331, 48332, 48333, 48334, 48335, 48336, 48337, 48338, 48339
48340, 48341, 48342, 48343, 48344, 48345, 48346, 48347, 48348
*Surface, type=ELEMENT, name=_PickedSurf15, internal
__PickedSurf15_S2, S2
__PickedSurf15_S3, S3
__PickedSurf15_S4, S4
__PickedSurf15_S6, S6
*Elset, elset=__PickedSurf16_S2, internal, instance=PART-1-1
17685, 17694, 17703, 17712, 17721, 17730, 17739, 17748, 17757, 17766, 17775, 17784, 17793, 17802, 17811, 17820
17829, 17838, 17847, 17856, 17865, 17874, 17883, 17892, 17901, 17910, 17919, 17928, 17937, 17946, 17955, 17964

…

24723, 24732, 24741, 24750, 24759, 24768, 24777, 24786, 24795, 24804, 24813, 24822, 24831, 24840, 24849, 24858
24867, 24876, 24885, 24894, 24903, 24912, 24921, 24930, 24939, 24948, 24957, 24966
*Elset, elset=__PickedSurf16_S4, internal, instance=PART-1-1
21808, 21809, 21810, 21811, 21812, 21813, 21814, 21815, 21816, 21817, 21818, 21819, 21820, 21821, 21822, 21823
21824, 21825, 21826, 21827, 21828, 21829, 21830, 21831, 21832, 21833, 21834, 21835, 21836, 21837, 21838, 21839

…

26083, 26084, 26085, 26086, 26087, 26088, 26089, 26090, 26091, 26092, 26093, 26094, 26095, 26096, 26097, 26098
26099, 26100
*Elset, elset=__PickedSurf16_S6, internal, instance=PART-1-1
18730, 18731, 18732, 18733, 18734, 18735, 18736, 18737, 18738, 18739, 18740, 18741, 18742, 18743, 18744, 18745
18746, 18747, 18748, 18749, 18750, 18751, 18752, 18753, 18754, 18755, 18756, 18757, 18758, 18759, 18760, 18761

…

22989, 22990, 22991, 22992, 22993, 22994, 22995, 22996, 22997, 22998, 22999, 23000, 23001, 23002, 23003, 23004
23005, 23006, 23007, 23008, 23009, 23010, 23011, 23012, 23013, 23014, 23015, 23016, 23017, 23018, 23019, 23020
23021, 23022
*Surface, type=ELEMENT, name=_PickedSurf16, internal
__PickedSurf16_S2, S2
__PickedSurf16_S4, S4
__PickedSurf16_S6, S6
*Elset, elset=__PickedSurf17_S2, internal, instance=PART-1-1
10719, 10728, 10737, 10746, 10755, 10764, 10773, 10782, 10791, 10800, 10809, 10818, 10827, 10836, 10845, 10854
10863, 10872, 10881, 10890, 10899, 10908, 10917, 10926, 10935, 10944, 10953, 10962, 10971, 10980, 10989, 10998

…

48195, 48204, 48213, 48222, 48231, 48240, 48249, 48258, 48267, 48276, 48285, 48294, 48303, 48312, 48321, 48330
48339, 48348
*Surface, type=ELEMENT, name=_PickedSurf17, internal
__PickedSurf17_S2, S2
*Elset, elset=__PickedSurf18_S2, internal, instance=PART-1-1
3663, 3672, 3681, 3690, 3699, 3708, 3717, 3726, 3735, 3744, 3753, 3762, 3771, 3780, 3789, 3798
3807, 3816, 3825, 3834, 3843, 3852, 3861, 3870, 3879, 3888, 3897, 3906, 3915, 3924, 3933, 3942

…

46449, 46458, 46467, 46476, 46485, 46494, 46503, 46512, 46521, 46530, 46539, 46548, 46557, 46566, 46575, 46584

46593, 46602, 46611, 46620, 46629, 46638, 46647, 46656, 46665, 46674, 46683, 46692, 46701, 46710, 46719, 46728
*Elset, elset=__PickedSurf18_S4, internal, instance=PART-1-1
20674, 20675, 20676, 20677, 20678, 20679, 20680, 20681, 20682, 20683, 20684, 20685, 20686, 20687, 20688, 20689
20690, 20691, 20692, 20693, 20694, 20695, 20696, 20697, 20698, 20699, 20700, 20701, 20702, 20703, 20704, 20705

…

47511, 47512, 47513, 47514, 47515, 47516, 47517, 47518, 47519, 47520, 47521, 47522, 47523, 47524, 47525, 47526
47527, 47528, 47529, 47530, 47531, 47532, 47533, 47534, 47535, 47536, 47537, 47538
*Elset, elset=__PickedSurf18_S6, internal, instance=PART-1-1
18730, 18731, 18732, 18733, 18734, 18735, 18736, 18737, 18738, 18739, 18740, 18741, 18742, 18743, 18744, 18745
18746, 18747, 18748, 18749, 18750, 18751, 18752, 18753, 18754, 18755, 18756, 18757, 18758, 18759, 18760, 18761

…

48324, 48325, 48326, 48327, 48328, 48329, 48330, 48331, 48332, 48333, 48334, 48335, 48336, 48337, 48338, 48339
48340, 48341, 48342, 48343, 48344, 48345, 48346, 48347, 48348
*Surface, type=ELEMENT, name=_PickedSurf18, internal
__PickedSurf18_S2, S2
__PickedSurf18_S4, S4
__PickedSurf18_S6, S6
*Elset, elset=__PickedSurf19_S2, internal, instance=PART-1-1
3663, 3672, 3681, 3690, 3699, 3708, 3717, 3726, 3735, 3744, 3753, 3762, 3771, 3780, 3789, 3798
3807, 3816, 3825, 3834, 3843, 3852, 3861, 3870, 3879, 3888, 3897, 3906, 3915, 3924, 3933, 3942

…

48195, 48204, 48213, 48222, 48231, 48240, 48249, 48258, 48267, 48276, 48285, 48294, 48303, 48312, 48321, 48330
48339, 48348
*Elset, elset=__PickedSurf19_S4, internal, instance=PART-1-1
20674, 20675, 20676, 20677, 20678, 20679, 20680, 20681, 20682, 20683, 20684, 20685, 20686, 20687, 20688, 20689
20690, 20691, 20692, 20693, 20694, 20695, 20696, 20697, 20698, 20699, 20700, 20701, 20702, 20703, 20704, 20705

…

```
 47511, 47512, 47513, 47514, 47515, 47516, 47517, 47518, 47519, 47520, 47521, 47522,
47523, 47524, 47525, 47526
 47527, 47528, 47529, 47530, 47531, 47532, 47533, 47534, 47535, 47536, 47537, 47538
*Elset, elset=__PickedSurf19_S6, internal, instance=PART-1-1
 18730, 18731, 18732, 18733, 18734, 18735, 18736, 18737, 18738, 18739, 18740, 18741,
18742, 18743, 18744, 18745

…

 48324, 48325, 48326, 48327, 48328, 48329, 48330, 48331, 48332, 48333, 48334, 48335,
48336, 48337, 48338, 48339
 48340, 48341, 48342, 48343, 48344, 48345, 48346, 48347, 48348
*Surface, type=ELEMENT, name=_PickedSurf19, internal
__PickedSurf19_S2, S2
__PickedSurf19_S4, S4
__PickedSurf19_S6, S6
*End Assembly
**
** MATERIALS
**
*Material, name=SPYRO
*Density
 7.91e-06,
*Depvar
    100,
*User Material, constants=8, type=THERMAL
 7.91e-06,  0., 0.5, 0.5,  0.,  0.,  0.,  0.
**
** INTERACTION PROPERTIES
**
*Film Property, name=heat
.0002, 20
.000237, 231.
.000283, 287.
.000335, 343.
.0001, 400.
.0001, 500.
9e-05, 565.
8e-05, 620.
8e-05, 850.
0.00008, 1000.
*Film Property, name=oil
0.0005,          20.
0.0025,          150.
0.0075,          300.
```

0.01, 400.
0.01875, 450.
0.025, 500.
0.025, 550.
0.02375, 600.
0.015, 650.
0.01, 700.
0.0075, 750.
0.0065, 800.
*Film Property, name=oil4percent
0.000018, 20.
0.00009, 150.
0.00027, 300.
0.00036, 400.
0.000675, 450.
0.0009, 500.
0.0009, 550.
0.000855, 600.
0.00054, 650.
0.00036, 700.
0.00027, 750.
0.000234, 800.
*Film Property, name=oil3
0.00002, 20.
0.0001, 150.
0.0003, 300.
0.0004, 400.
0.00075, 450.
0.001, 500.
0.001, 550.
0.00095, 600.
0.0006, 650.
0.0004, 700.
0.0003, 750.
0.00026, 800.
*Film Property, name=coldair
0.00009, -80.
0.00011, 37.
0.000129, 65.
0.000143, 93.
0.000162, 120.
0.000178, 148.
0.000197, 176.
0.000237, 231.
0.000283, 287.
0.000335, 343.

```
0.000393,       398.
0.000458,       454.
0.000533,       509.
0.000616,       565.
0.000708,       620.
0.000811,       676.
*Surface Interaction, name=shims
1.,
*Surface Behavior, pressure-overclosure=HARD
*Gap Conductance
 0.002,0.
   0.,1.
**
** PREDEFINED FIELDS
**
** Name: Field-1   Type: Temperature
*Initial Conditions, type=TEMPERATURE
_PICKEDSET10, 20.
*Initial Conditions, type=FIELD, VAR=1, input=quartertooth1130.nod
*Initial Conditions, type=FIELD, VAR=2
_PickedSet10, 2.0
** ----------------------------------------------------------------
**
** STEP: heat
**
*Step, name=heat, inc=2000
austenize
*Heat Transfer, end=PERIOD, deltmx=15.
1., 5000., 0.001, 100.,
**
** INTERACTIONS
**
** Interaction: heat
*Sfilm
_PickedSurf15, F, 913., heat
**
** OUTPUT REQUESTS
**
*Restart, write, frequency=1000
*Monitor, dof=11, node=_PickedSet20, frequency=1000
**
** FIELD OUTPUT: F-Output-1
**
*Output, field, variable=PRESELECT, frequency=100
**
** FIELD OUTPUT: everything
```

```
**
*Output, field, frequency=1000
*Node Output
NT,
*Element Output, directions=YES
SDV,
**
** HISTORY OUTPUT: H-Output-1
**
*Output, history, variable=PRESELECT, frequency=100
*El Print, freq=999999
*Node Print, freq=999999
*Node File, freq=1000
NT,
*End Step
** ----------------------------------------------------------------
**
** STEP: transfer
**
*Step, name=transfer, inc=1000
transfer
*Heat Transfer, end=PERIOD, deltmx=15.
0.1, 60., 0.0001, 10.,
**
*FIELD, OP=NEW, VAR=1
*FIELD, OP=NEW, VAR=2
_PickedSet10, -2.0
** INTERACTIONS
**
** Interaction: transfer
*Sfilm
_PickedSurf16, F, 20., coldair
**
** OUTPUT REQUESTS
**
*Restart, write, frequency=1000
**
** FIELD OUTPUT: F-Output-1
**
*Output, field, variable=PRESELECT, frequency=100
**
** FIELD OUTPUT: everything
**
*Output, field, frequency=1000
*Node Output
NT,
```

```
*Element Output, directions=YES
SDV,
**
** HISTORY OUTPUT: H-Output-1
**
*Output, history, variable=PRESELECT, frequency=100
*El Print, freq=999999
*Node Print, freq=999999
*Node File, freq=1000
NT,
*End Step
** ----------------------------------------------------------------
** STEP: quench1
**
*Step, name=quench1, inc=2000
quench 10s 620 gal/min
*Heat Transfer, end=PERIOD, deltmx=20.
0.01, 10., 0.0001, 0.1,
**
** INTERACTIONS
**
** Interaction: quench1
*Sfilm, OP=NEW
_PickedSurf17, F, 38., oil4percent
** Interaction: quench1fast
*Sfilm, OP=NEW
_PickedSurf18, F, 38., oil
**
** OUTPUT REQUESTS
**
*Restart, write, frequency=1000
**
** FIELD OUTPUT: F-Output-1
**
*Output, field, variable=PRESELECT, frequency=50
**
** FIELD OUTPUT: everything
**
*Output, field, frequency=1000
*Node Output
NT,
*Element Output, directions=YES
SDV,
**
** HISTORY OUTPUT: H-Output-1
**
```

```
*Output, history, variable=PRESELECT, frequency=50
*El Print, freq=999999
*Node Print, freq=999999
*Node File, freq=1000
NT,
*End Step
** ----------------------------------------------------------------
**
** STEP: quench2
**
*Step, name=quench2, inc=2000
quench 130 gal/min 4 min
*Heat Transfer, end=PERIOD, deltmx=25.
0.01, 240., 0.0001, 10.,
**
** INTERACTIONS
**
** Interaction: quenchslow
*Sfilm, OP=NEW
_PickedSurf19, F, 38., oil4percent
**
** OUTPUT REQUESTS
**
*Restart, write, frequency=1000
**
** FIELD OUTPUT: F-Output-1
**
*Output, field, variable=PRESELECT, frequency=50
**
** FIELD OUTPUT: everything
**
*Output, field, frequency=1000
*Node Output
NT,
*Element Output, directions=YES
SDV,
**
** HISTORY OUTPUT: H-Output-1
**
*Output, history, variable=PRESELECT, frequency=50
*El Print, freq=999999
*Node Print, freq=999999
*Node File, freq=1000
NT,
*End Step
** ----------------------------------------------------------------
```

```
**
** STEP: quench3
**
*Step, name=quench3, inc=2000
8 min 620 gal/min
*Heat Transfer, end=PERIOD, deltmx=25
1., 480., 0.0001, 15.,
**
** Interaction: quench1
*Sfilm, OP=NEW
_PickedSurf17, F, 38., oil4percent
** Interaction: quench1fast
*Sfilm, OP=NEW
_PickedSurf18, F, 38., oil3
** OUTPUT REQUESTS
**
*Restart, write, frequency=1000
**
** FIELD OUTPUT: F-Output-1
**
*Output, field, variable=PRESELECT, frequency=50
**
** FIELD OUTPUT: everything
**
*Output, field, frequency=1000
*Node Output
NT,
*Element Output, directions=YES
SDV,
**
** HISTORY OUTPUT: H-Output-1
**
*Output, history, variable=PRESELECT, frequency=50
*El Print, freq=999999
*Node Print, freq=999999
*Node File, freq=1000
NT,
*End Step
** STEP: measure
**
*Step, name=measure, inc=2000
measure
*Heat Transfer, end=PERIOD, deltmx=20
1., 1800., 0.001, 50.,
**
** Interaction: quench1
```

```
*Sfilm, OP=NEW
_PickedSurf17, F, 38., coldair
** Interaction: quench1fast
*Sfilm, OP=NEW
_PickedSurf18, F, 38., coldair
** OUTPUT REQUESTS
**
*Restart, write, frequency=1000
**
** FIELD OUTPUT: F-Output-1
**
*Output, field, variable=PRESELECT, frequency=50
**
** FIELD OUTPUT: everything
**
*Output, field, frequency=1000
*Node Output
NT,
*Element Output, directions=YES
SDV,
**
** HISTORY OUTPUT: H-Output-1
**
*Output, history, variable=PRESELECT, frequency=50
*El Print, freq=999999
*Node Print, freq=999999
*Node File, freq=1000
NT,
*End Step
** STEP: freeze
**
*Step, name=freeze, inc=2000
freeze
*Heat Transfer, end=PERIOD, deltmx=20
1., 3600., 0.01, 50.,
**
** Interaction: quench1
*Sfilm, OP=NEW
_PickedSurf17, F, -80., coldair
** Interaction: quench1fast
*Sfilm, OP=NEW
_PickedSurf18, F, -80., coldair
** OUTPUT REQUESTS
**
*Restart, write, frequency=1000
**
```

```
** FIELD OUTPUT: F-Output-1
**
*Output, field, variable=PRESELECT, frequency=50
**
** FIELD OUTPUT: everything
**
*Output, field, frequency=1000
*Node Output
NT,
*Element Output, directions=YES
SDV,
**
** HISTORY OUTPUT: H-Output-1
**
*Output, history, variable=PRESELECT, frequency=50
*El Print, freq=999999
*Node Print, freq=999999
*Node File, freq=1000
NT,
*End Step
```

Appendix 4: Stress Simulation File

High Pressure Gas Quenching Simulation Input File

```
*Heading
** Job name: evenquench2 Model name: Model-1
*Preprint, echo=NO, model=NO, history=NO, contact=NO
**
** PARTS
**
*Part, name="sikorsky complete simple"
*Node
      1, -0.649962068,  -223.069565,  -223.069565
      2, -0.649962068,  -196.218597,  -196.218597
      3,   26.6550388,  -194.781754,  -194.781754

…

  52329,  -17.6309128,  -4.23327971,  -267.532501
  52330,  -21.2823315,  -4.23270845,   -267.59494
*Element, type=C3D8
   1,    81,    69,    46,    47, 12525, 12513, 12490, 12491
   2,    69,    22,     8,    46, 12513, 12489, 12475, 12490
   3,    14,    70,   122,     1, 12481, 12514, 12566,   627

…

29085, 42301,  2311, 42357, 42353,  7873,   361,  7929,  7925
29086,  9971,  9970, 42355, 42356,  1790,  1791,  7927,  7928
29087, 42293, 42355, 42354, 42294,  7865,  7927,  7926,  7866
29088, 42363, 42338, 42323, 42321,  7935,  7910,  7895,  7893
*Nset, nset=_PickedSet60, internal, generate
    1,  52330,      1
*Elset, elset=_PickedSet60, internal, generate
    1,  38784,      1
*Nset, nset=partset, generate
    1,  52330,      1
*Elset, elset=partset, generate
    1,  38784,      1
*Elset, elset=_partsurf_S4, internal
    5,    10,    16,    19,    21,    27,    34,    35,    59,    63,    70,   106,   111,   117,   120,
122
   128,   135,   136,   160,   164,   171,   207,   212,   218,   221,   223,   229,   236,   237,
261,   265
```

…

38491, 38497, 38500, 38502, 38508, 38515, 38516, 38540, 38544, 38551, 38587, 38592, 38598, 38601, 38603, 38609
38616, 38617, 38641, 38645, 38652, 38688, 38693, 38699, 38702, 38704, 38710, 38717, 38718, 38742, 38746, 38753
*Elset, elset=_partsurf_S6, internal
12, 28, 32, 38, 41, 43, 48, 51, 52, 54, 55, 99, 113, 129, 133, 139
142, 144, 149, 152, 153, 155, 156, 200, 214, 230, 234, 240, 243, 245, 250, 253

…

38522, 38524, 38529, 38532, 38533, 38535, 38536, 38580, 38594, 38610, 38614, 38620, 38623, 38625, 38630, 38633
38634, 38636, 38637, 38681, 38695, 38711, 38715, 38721, 38724, 38726, 38731, 38734, 38735, 38737, 38738, 38782
*Elset, elset=_partsurf_S5, internal
30, 131, 232, 333, 434, 535, 636, 737, 838, 939, 1040, 1141, 1242, 1343, 1444, 1545
1646, 1747, 1848, 1949, 2050, 2151, 2252, 2353, 2454, 2555, 2656, 2757, 2858, 2959, 3060, 3161

…

35582, 35683, 35784, 35885, 35986, 36087, 36188, 36289, 36390, 36491, 36592, 36693, 36794, 36895, 36996, 37097
37198, 37299, 37400, 37501, 37602, 37703, 37804, 37905, 38006, 38107, 38208, 38309, 38410, 38511, 38612, 38713
*Elset, elset=_partsurf_S3, internal
35, 60, 64, 136, 161, 165, 237, 262, 266, 338, 363, 367, 439, 464, 468, 540
565, 569, 641, 666, 670, 742, 767, 771, 843, 868, 872, 944, 969, 973, 1045, 1070

…

37733, 37737, 37809, 37834, 37838, 37910, 37935, 37939, 38011, 38036, 38040, 38112, 38137, 38141, 38213, 38238
38242, 38314, 38339, 38343, 38415, 38440, 38444, 38516, 38541, 38545, 38617, 38642, 38646, 38718, 38743, 38747
*Surface, type=ELEMENT, name=partsurf
_partsurf_S4, S4
_partsurf_S6, S6

```
_partsurf_S5, S5
_partsurf_S3, S3
** Section: Section-1
*Solid Section, elset=_PickedSet60, material=SPYRO
1.,
*End Part
**
**
** ASSEMBLY
**
*Assembly, name=Assembly
**
*Instance, name="sikorsky complete simple-1", part="sikorsky complete simple"
*End Instance
**
*Nset, nset=_PickedSet4, internal, instance="sikorsky complete simple-1"
 160,
*Nset, nset=_PickedSetX, internal, instance="sikorsky complete simple-1"
 160,
 *Nset, nset=_PickedSetY, internal, instance="sikorsky complete simple-1"
 176
 *Nset, nset=_PickedSetZ, internal, instance="sikorsky complete simple-1"
366
*Nset, nset=surface, instance="sikorsky complete simple-1", generate
     1,  52330,      1
*Elset, elset=surface, instance="sikorsky complete simple-1", generate
     1,  38784,      1
*Nset, nset=_PickedSet12, internal, instance="sikorsky complete simple-1", generate
     1,  52330,      1
*Elset, elset=_PickedSet12, internal, instance="sikorsky complete simple-1", generate
     1,  38784,      1
*Elset, elset=_mesh_S4, internal, instance="sikorsky complete simple-1"
     5,    10,    16,    19,    21,    27,    34,    35,    59,    63,    70,   106,   111,   117,   120,
122
   128,   135,   136,   160,   164,   171,   207,   212,   218,   221,   223,   229,   236,   237,
261,   265

…

 38491, 38497, 38500, 38502, 38508, 38515, 38516, 38540, 38544, 38551, 38587, 38592,
38598, 38601, 38603, 38609
 38616, 38617, 38641, 38645, 38652, 38688, 38693, 38699, 38702, 38704, 38710, 38717,
38718, 38742, 38746, 38753
*Elset, elset=_mesh_S6, internal, instance="sikorsky complete simple-1"
    12,    28,    32,    38,    41,    43,    48,    51,    52,    54,    55,    99,   113,   129,   133,
139
```

142, 144, 149, 152, 153, 155, 156, 200, 214, 230, 234, 240, 243, 245, 250, 253

…

38522, 38524, 38529, 38532, 38533, 38535, 38536, 38580, 38594, 38610, 38614, 38620, 38623, 38625, 38630, 38633
38634, 38636, 38637, 38681, 38695, 38711, 38715, 38721, 38724, 38726, 38731, 38734, 38735, 38737, 38738, 38782
*Elset, elset=_mesh_S5, internal, instance="sikorsky complete simple-1"
30, 131, 232, 333, 434, 535, 636, 737, 838, 939, 1040, 1141, 1242, 1343, 1444, 1545
1646, 1747, 1848, 1949, 2050, 2151, 2252, 2353, 2454, 2555, 2656, 2757, 2858, 2959, 3060, 3161

…

35582, 35683, 35784, 35885, 35986, 36087, 36188, 36289, 36390, 36491, 36592, 36693, 36794, 36895, 36996, 37097
37198, 37299, 37400, 37501, 37602, 37703, 37804, 37905, 38006, 38107, 38208, 38309, 38410, 38511, 38612, 38713
*Elset, elset=_mesh_S3, internal, instance="sikorsky complete simple-1"
35, 60, 64, 136, 161, 165, 237, 262, 266, 338, 363, 367, 439, 464, 468, 540
565, 569, 641, 666, 670, 742, 767, 771, 843, 868, 872, 944, 969, 973, 1045, 1070

…

37733, 37737, 37809, 37834, 37838, 37910, 37935, 37939, 38011, 38036, 38040, 38112, 38137, 38141, 38213, 38238
38242, 38314, 38339, 38343, 38415, 38440, 38444, 38516, 38541, 38545, 38617, 38642, 38646, 38718, 38743, 38747
*Surface, type=ELEMENT, name=mesh
_mesh_S4, S4
_mesh_S6, S6
_mesh_S5, S5
_mesh_S3, S3
*Elset, elset="__T0_sikorsky complete simple-1_M_S2", internal, instance="sikorsky complete simple-1", generate
4748, 4848, 1
*Surface, type=ELEMENT, name=_T0_sikorsky complete simple-1_M, internal
"__T0_sikorsky complete simple-1_M_S2", S2
*Elset, elset="__T0_sikorsky complete simple-1_S_S2", internal, instance="sikorsky complete simple-1", generate
9596, 9696, 1

```
*Surface, type=ELEMENT, name=_T0_sikorsky complete simple-1_S, internal
"__T0_sikorsky complete simple-1_S_S2", S2
*Tie, name="_T0_sikorsky complete simple-1", position tolerance=116.973
_T0_sikorsky complete simple-1_S, _T0_sikorsky complete simple-1_M
*Elset, elset="__T1_sikorsky complete simple-1_M_S1", internal, instance="sikorsky
complete simple-1", generate
 4849,  4949,     1
*Surface, type=ELEMENT, name=_T1_sikorsky complete simple-1_M, internal
"__T1_sikorsky complete simple-1_M_S1", S1
*Elset, elset="__T1_sikorsky complete simple-1_S_S2", internal, instance="sikorsky
complete simple-1", generate
 14444,  14544,     1
*Surface, type=ELEMENT, name=_T1_sikorsky complete simple-1_S, internal
"__T1_sikorsky complete simple-1_S_S2", S2
*Tie, name="_T1_sikorsky complete simple-1", position tolerance=116.973
_T1_sikorsky complete simple-1_S, _T1_sikorsky complete simple-1_M
*Elset, elset="__T2_sikorsky complete simple-1_M_S1", internal, instance="sikorsky
complete simple-1", generate
 14545,  14645,     1
*Surface, type=ELEMENT, name=_T2_sikorsky complete simple-1_M, internal
"__T2_sikorsky complete simple-1_M_S1", S1
*Elset, elset="__T2_sikorsky complete simple-1_S_S2", internal, instance="sikorsky
complete simple-1", generate
 24140,  24240,     1
*Surface, type=ELEMENT, name=_T2_sikorsky complete simple-1_S, internal
"__T2_sikorsky complete simple-1_S_S2", S2
*Tie, name="_T2_sikorsky complete simple-1", position tolerance=116.973
_T2_sikorsky complete simple-1_S, _T2_sikorsky complete simple-1_M
*Elset, elset="__T3_sikorsky complete simple-1_M_S1", internal, instance="sikorsky
complete simple-1", generate
 19393,  19493,     1
*Surface, type=ELEMENT, name=_T3_sikorsky complete simple-1_M, internal
"__T3_sikorsky complete simple-1_M_S1", S1
*Elset, elset="__T3_sikorsky complete simple-1_S_S2", internal, instance="sikorsky
complete simple-1", generate
 28988,  29088,     1
*Surface, type=ELEMENT, name=_T3_sikorsky complete simple-1_S, internal
"__T3_sikorsky complete simple-1_S_S2", S2
*Tie, name="_T3_sikorsky complete simple-1", position tolerance=116.973
_T3_sikorsky complete simple-1_S, _T3_sikorsky complete simple-1_M
*Elset, elset="__T4_sikorsky complete simple-1_M_S1", internal, instance="sikorsky
complete simple-1", generate
 24241,  24341,     1
*Surface, type=ELEMENT, name=_T4_sikorsky complete simple-1_M, internal
"__T4_sikorsky complete simple-1_M_S1", S1
```

```
*Elset, elset="__T4_sikorsky complete simple-1_S_S2", internal, instance="sikorsky
complete simple-1", generate
 33836,  33936,      1
*Surface, type=ELEMENT, name=_T4_sikorsky complete simple-1_S, internal
"__T4_sikorsky complete simple-1_S_S2", S2
*Tie, name="_T4_sikorsky complete simple-1", position tolerance=116.973
_T4_sikorsky complete simple-1_S, _T4_sikorsky complete simple-1_M
*End Assembly
**
**
** BOUNDARY CONDITIONS
**
** Name: BC-1 Type: Displacement/Rotation
*Boundary
_PickedSetX, encastre
** Name: 1 Type: Displacement/Rotation
*Boundary
_PickedSetZ, 3, 3
** Name: BC-3 Type: Displacement/Rotation
*Boundary
_PickedSetY, 2, 2
_PickedSetY, 3, 3
**
** MATERIALS
**
*Material, name=SPYRO
** Pyrowear 53
*Density
 7.91e-06,
*Depvar
    100,
*User Material, constants=8, type=mechanical
 7.91e-06,  0., 0.5, 0.5,  0.,  0.,  0.,  0.
**
** INTERACTION PROPERTIES
**
*Film Property, name=heat
.0002, 20
.000237, 231.
.000283, 287.
.000335, 343.
.0001, 400.
.0001, 500.
9e-05, 565.
8e-05, 620.
8e-05, 850.
```

0.00008, 1000.
*Film Property, name=oil
0.0005, 20.
0.0025, 150.
0.0075, 300.
0.01, 400.
0.01875, 450.
0.025, 500.
0.025, 550.
0.02375, 600.
0.015, 650.
0.01, 700.
0.0075, 750.
0.0065, 800.
*Film Property, name=oil4percent
0.000018, 20.
0.00009, 150.
0.00027, 300.
0.00036, 400.
0.000675, 450.
0.0009, 500.
0.0009, 550.
0.000855, 600.
0.00054, 650.
0.00036, 700.
0.00027, 750.
0.000234, 800.
*Film Property, name=oil3
0.00002, 20.
0.0001, 150.
0.0003, 300.
0.0004, 400.
0.00075, 450.
0.001, 500.
0.001, 550.
0.00095, 600.
0.0006, 650.
0.0004, 700.
0.0003, 750.
0.00026, 800.
*Film Property, name=coldair
0.00009, -80.
0.00011, 37.
0.000129, 65.
0.000143, 93.
0.000162, 120.

```
0.000178,       148.
0.000197,       176.
0.000237,       231.
0.000283,       287.
0.000335,       343.
0.000393,       398.
0.000458,       454.
0.000533,       509.
0.000616,       565.
0.000708,       620.
0.000811,       676.
*Film Property, name=nitrogen_quench
0.0001, 20.
0.000208387, 90.3846
0.000208387,    96.1538

…

0.000448387,    373.077
0.000432903,    834.615
0.000425162,    848.077
0.000425, 900
**
** PREDEFINED FIELDS
**
** Name: temp   Type: Temperature
*Initial Conditions, type=TEMPERATURE
_PickedSet12, 20.
*Initial Conditions, type=FIELD, VAR=1
_pickedset12, .001
*Initial Conditions, type=FIELD, VAR=2
_pickedset12, 2.0
** ----------------------------------------------------------------
**
** STEP: Step-1
**
*Step, name=Step-1, inc=2000
heat up
*static
5., 5000., 0.001, 100.,
**
** INTERACTIONS
**
*TEMPERATURE, FILE=evenquenchgas, Bstep=1
** OUTPUT REQUESTS
**
```

```
*Restart, write, frequency=50
**
** FIELD OUTPUT: F-Output-1
**
*Output, field, frequency=50
*Node Output
NT, U
*Element Output, directions=YES
SDV, S
*Output, history, frequency=50
*End Step
** ----------------------------------------------------------------
** STEP: transfer
**
*Step, name=transfer, inc=1000
quench
*static
1., 60., 0.01, 10.,
**
** INTERACTIONS
**
*TEMPERATURE, FILE=evenquenchgas, Bstep=2
**
** OUTPUT REQUESTS
**
*Restart, write, frequency=50
**
** FIELD OUTPUT: F-Output-1
**
*Output, field, frequency=50
*Node Output
NT, U
*Element Output, directions=YES
SDV, S
*Output, history, frequency=50
*End Step
** ----------------------------------------------------------------
**
** STEP: quench1
**
*Step, name=quench1, inc=3000
quench
*STATIC
0.1, 10., 0.0001, 1.,
**
*FIELD, OP=NEW, VAR=1
```

```
*FIELD, OP=NEW, VAR=2
_PickedSet12, -2.0
** INTERACTIONS
**
*TEMPERATURE, FILE=evenquenchgas, Bstep=3
** OUTPUT REQUESTS
**
*Restart, write, frequency=50
**
** FIELD OUTPUT: F-Output-1
**
*Output, field, frequency=50
*Node Output
NT, U
*Element Output, directions=YES
SDV, S
*Output, history, frequency=50
*End Step
** ----------------------------------------------------------------
** STEP: quench2
**
*Step, name=quench2, inc=3000
quench
*STATIC
0.1, 240., 0.0001, 10.,
**
** INTERACTIONS
*TEMPERATURE, FILE=evenquenchgas, Bstep=4
** OUTPUT REQUESTS
**
*Restart, write, frequency=50
**
** FIELD OUTPUT: F-Output-1
**
*Output, field, frequency=50
*Node Output
NT, U
*Element Output, directions=YES
SDV, S
*Output, history, frequency=50
*End Step
** ----------------------------------------------------------------
** STEP: quench3
**
*Step, name=quench3, inc=3000
quench
```

```
*STATIC
0.1, 480., 0.0001, 10.,
**
** INTERACTIONS
**
*TEMPERATURE, FILE=evenquenchgas, Bstep=5
** OUTPUT REQUESTS
**
*Restart, write, frequency=50
**
** FIELD OUTPUT: F-Output-1
**
*Output, field, frequency=50
*Node Output
NT, U
*Element Output, directions=YES
SDV, S
*Output, history, frequency=50
*End Step
** ----------------------------------------------------------------
** STEP: measure
**
*Step, name=measure, inc=1000
quench
*STATIC
1., 1800., 0.01, 100.,
**
** INTERACTIONS
**
*TEMPERATURE, FILE=evenquenchgas, Bstep=6
**
** OUTPUT REQUESTS
**
*Restart, write, frequency=50
**
** FIELD OUTPUT: F-Output-1
**
*Output, field, frequency=50
*Node Output
NT, U
*Element Output, directions=YES
SDV, S
*Output, history, frequency=50
*End Step
** ----------------------------------------------------------------
** STEP: freeze
```

```
**
*Step, name=freeze, inc=1000
quench
*STATIC
1., 3600., 0.01, 150.,
**
** INTERACTIONS
**
*TEMPERATURE, FILE=evenquenchgas, Bstep=7
**
** OUTPUT REQUESTS
**
*Restart, write, frequency=50
**
** FIELD OUTPUT: F-Output-1
**
*Output, field, frequency=50
*Node Output
NT, U
*Element Output, directions=YES
SDV, S
*Output, history, frequency=50
*End Step
```

Appendix 5: Physically Measured Distortion

Measured Distortion Values Before Heat Treating

	S/N 178	S/N 179	S/N 180	S/N 181
I.D.	20.2910	20.2910	20.2915	20.2910
Root				
	S/N 178	**S/N 179**	**S/N 180**	**S/N 181**
	20.9010	20.9000	20.9010	20.8970
	20.9020	20.9000	20.9000	20.8980
	20.9000	20.9000	20.9020	20.8980
	20.9010	20.9000	20.9010	20.8970
	20.9010	20.8995	20.9020	20.8960
	20.9000	20.8990	20.9020	20.8970
	20.9010	20.8990	20.9020	20.8980
	20.9020	20.8990	20.9020	20.8970
	20.8990	20.8995	20.9020	20.8970
	20.9000	20.9000	20.9020	20.8980
	20.9010	20.9000	20.9015	20.8970
	20.9020	20.9000	20.9010	20.8970
	20.9010	20.9000	20.9020	20.8970
	20.9010	20.9000	20.9000	20.8980
	20.9010	20.9010	20.9010	20.8960
	20.9000	20.9000	20.9010	20.8970
	20.9000	20.9000	20.9000	20.8980
	20.9010	20.9000	20.9010	20.8980
	20.9010	20.9000	20.9000	20.8970
	20.9010	20.9000	20.9010	20.8970
	20.9010	20.9000	20.9020	20.8980
Out of Round	**.003**	**.001**	**.002**	**.002**
Wire	**S/N 178**	**S/N 179**	**S/N 180**	**S/N 181**
	20.266	20.268	20.270	20.264
	20.266	20.267	20.270	20.263
	20.265	20.267	20.269	20.263
	20.265	20.267	20.269	20.263
	20.266	20.267	20.269	20.264
	20.266	20.266	20.269	20.263
	20.267	20.266	20.269	20.262
	20.267	20.267	20.268	20.263
	20.267	20.267	20.268	20.263
	20.267	20.268	20.270	20.264

20.266	20.268	20.270	20.263
20.266	20.268	20.269	20.265
20.266	20.267	20.269	20.264
20.266	20.267	20.268	20.264
20.265	20.267	20.268	20.263
20.265	20.268	20.690	20.264
20.265	20.267	20.268	20.263
20.264	20.267	20.269	20.263
20.264	20.267	20.269	20.264
20.265	20.268	20.270	20.264
20.265	20.267	20.269	20.264

Measured Distortion Values After Carburizing

Root Diameter	Master Diameter =20.930"	all dimensions in inches					
	S/N 178		**S/N 179**		**S/N 180**		**S/N 181**
-0.072	20.858	-0.075	20.855	-0.066	20.864	-0.025	20.905
-0.075	20.855	-0.071	20.859	-0.06	20.87	-0.023	20.907
-0.072	20.858	-0.067	20.863	-0.05	20.88	-0.021	20.909
-0.063	20.867	-0.053	20.877	-0.035	20.895	-0.02	20.91
-0.044	20.886	-0.032	20.898	-0.018	20.912	-0.015	20.915
-0.023	20.907	-0.01	20.92	0	20.93	-0.013	20.917
-0.01	20.92	0.015	20.945	0.019	20.949	-0.015	20.915
0.015	20.945	0.025	20.955	0.022	20.952	-0.019	20.911
0.024	20.954	0.025	20.955	0.026	20.956	-0.024	20.906
0.025	20.955	0.03	20.96	0.022	20.952	-0.029	20.901
0.015	20.945	0.022	20.952	0.018	20.948	-0.031	20.899
0.007	20.937	0.005	20.935	0	20.93	-0.031	20.899
-0.014	20.916	-0.018	20.912	-0.005	20.925	-0.03	20.9
-0.033	20.897	-0.04	20.89	-0.028	20.902	-0.029	20.901
-0.051	20.879	-0.058	20.872	-0.046	20.884	-0.026	20.904
-0.065	20.865	-0.072	20.858	-0.059	20.871	-0.025	20.905
Out of Round	**0.1**		**0.105**		**0.92**		**0.018**

Measured Values after Quench, Freeze and Temper

(dimensions in inches) **Root Diameter Master = 20.930"**

S/N 181	S/N 178	S/N 179	S/N 180
-0.002	-0.011	-0.010	-0.012
-0.003	-0.011	0.000	-0.012
-0.004	-0.010	-0.001	-0.011
-0.005	-0.009	-0.002	-0.011
-0.005	-0.009	-0.002	-0.011
-0.005	-0.007	-0.002	-0.011
-0.007	-0.005	-0.003	-0.010
-0.010	-0.004	-0.003	-0.010
-0.011	-0.004	-0.004	-0.010
-0.011	-0.002	-0.004	-0.010
-0.013	-0.002	-0.005	-0.010
-0.012	-0.003	-0.005	-0.008

	-0.008	-0.003	-0.005	-0.008
	-0.007	-0.004	-0.004	-0.007
	-0.005	-0.005	-0.003	-0.008
	-0.003	-0.005	-0.003	-0.007
	-0.003	-0.006	-0.002	-0.007
	-0.001	-0.006	-0.002	-0.008
	-0.001	-0.008	-0.002	-0.008
	-0.001	-0.008	-0.002	-0.010
	-0.002	-0.010	-0.001	-0.011
Out of Round	**.012**	**.009**	**.005**	**.005**
TAPER	**0.019**	**0.024**	**0.021**	**0.012**

Taper Indicates increase in diameter from bottom to top

Dimension over wires Master = 20.298"

S/N 181	S/N 178	S/N 179	S/N 180
-0.005	-0.015	-0.014	-0.016
-0.007	-0.014	-0.013	-0.016
-0.008	-0.013	-0.012	-0.016
-0.008	-0.011	-0.012	-0.015
-0.008	-0.011	-0.012	-0.014
-0.008	-0.010	-0.010	-0.015
-0.012	-0.010	-0.010	-0.013
-0.014	-0.008	-0.010	-0.012
-0.015	-0.007	-0.009	-0.012
-0.015	-0.007	-0.008	-0.011
-0.015	-0.007	-0.008	-0.011
-0.016	-0.005	-0.009	-0.010
-0.014	-0.005	-0.009	-0.009
-0.012	-0.005	-0.010	-0.008
-0.010	-0.006	-0.010	-0.010
-0.010	-0.007	-0.011	-0.010
-0.009	-0.007	-0.013	-0.011
-0.009	-0.008	-0.013	-0.012
-0.008	-0.010	-0.012	-0.013
-0.007	-0.012	-0.013	-0.015
-0.005	-0.013	-0.014	-0.015
.011	**.010**	**.006**	**.008**

Out of Round